3-2022

Life Cycle Analysis of Hydrogen Fuel Derived from Aluminum Versus Diesel

Tyson S. Metlen

LIFE CYCLE ANALYSIS OF HYDROGEN FUEL DERIVED FROM ALUMINUM VERSUS DIESEL

THESIS

Tyson S. Metlen, Major, USMC

AFIT-ENV-MS-22-M-236

DEPARTMENT OF THE AIR FORCE
AIR UNIVERSITY

AIR FORCE INSTITUTE OF TECHNOLOGY

Wright-Patterson Air Force Base, Ohio

AFIT-ENV-MS-22-M-236

LIFE CYCLE ANALYSIS OF HYDROGEN FUEL DERIVED FROM ALUMINUM VERSUS DIESEL

THESIS

Presented to the Faculty

Department of Systems Engineering and Management

Graduate School of Engineering and Management

Air Force Institute of Technology

Air University

Air Education and Training Command

In Partial Fulfillment of the Requirements for the

Degree of Master of Science in Environmental Engineering

Tyson S. Metlen, MIE

Major, USMC

March 2022

AFIT-ENV-MS-22-M-236

LIFE CYCLE ANALYSIS OF HYDROGEN FUEL DERIVED FROM ALUMINUM VERSUS DIESEL

Tyson S. Metlen, MIE

Major, USMC

Committee Membership:

Dr. Eric G. Mbonimpa, PhD, PE
Chair

Lieutenant Colonel John E. Stubbs, PhD, USAF
Member

Major Trevor W. Sleight, PhD, USAF
Member

Abstract

The Department of Defense needs energy sources beyond petroleum products to effectively combat area denial strategies employed by its adversaries. Petroleum fuels are expensive, they have deleterious environmental impacts, and most of the world's oil reservoirs are in volatile countries. A proposed alternative energy carrier is reacting aluminum with water to produce hydrogen and using the hydrogen as a fuel source. Normally aluminum forms a protective oxide layer that prevents continuous reaction but if aluminum is mixed with a 3.5% by weight gallium-indium eutectic, the oxide layer cannot form, and the reaction is sustainable. This study conducts a life cycle assessment, economic analysis, and discusses logistical considerations to compare using diesel to hydrogen derived from the aluminum-water reaction in a Western Pacific theater. The life cycle assessment uses Sphera's GaBi software and life cycle impact assessment tool TRACI 2.1, to characterize and compare the environmental impacts of diesel and aluminum. Every category of environmental impact is monetized and combined with the economic analysis to provide a single score for comparison. The result is that aluminum, even with the best-case scenario of 90% scrap aluminum and 95% eutectic recovery, is more environmentally harmful and economically expensive than diesel.

Acknowledgments

First and foremost, I want to convey my deep appreciation to my wife for supporting my efforts and patience with time commitments. I would also like to express my sincere appreciation to my faculty advisor, Dr. Eric Mbonimpa, for his guidance and support throughout the course of this thesis effort. The insight and experience was certainly appreciated. To Major Stone, my sponsor from the Marine Corps Expeditionary Energy Office, thank you for the thesis idea, support, and latitude provided to me in this endeavor.

Tyson S. Metlen

Table of Contents

Page

Abstract iv
Table of Contents vi
List of Figures ix
List of Tables ix
List of Equations x
I. Introduction 1
Background 1
Problem Statement 4
Research Objectives 4
Methodology 5
Assumptions/Limitations 6
Implications or Expected Contributions 6
Summary 6
II. Literature Review 8
Chapter Overview 8
Life Cycle Assessment 8
Hydrogen 15
Activated Aluminum 27
Military Fuel 37
Summary 43
III. Methodology 44
Chapter Overview 44

Overview of Research Methodology....44
Diesel Fuel Consumption and Pricing....45
Hydrogen Consumption....50
Activated Aluminum Hydrogen Production and Pricing....54
LCA and GaBi Modeling....58
Summary....66
IV. Analysis and Results....67
Chapter Overview....67
Diesel Results....67
Hydrogen Fuel Cell Results....70
Activated Aluminum Results....72
Economic Analysis and Comparison....75
Logistical Comparison....78
Potential Areas of Improvement....81
Summary....82
V. Conclusions and Recommendations....83
Overview....83
Summary of Research Question....83
Limitations and Assumptions....84
Future Research....86
Significance of Research....86
Appendix A: DLA Diesel Price Compilation....88
Appendix B: Metal Prices....89
Appendix C: GaBi Activated Aluminum Plan....91

Appendix D: GaBi Diesel Plan 92
Appendix E: Monte Carlo Convergence Analyses 93
Appendix F: SimaPro Results 97
Bibliography 98

List of Figures

Page

Figure 1: Life Cycle of a Metal 9

Figure 2: ReCiPe2016 Midpoint to Endpoint Relationships 12

Figure 3: Fuel Cell Schematic 25

Figure 4: The Bayer Cycle 32

Figure 5: Diesel Life Cycle 42

Figure 6: Argonne National Laboratory Toyota Mirai Efficiency 51

Figure 7: Gallium Price ($/kg) 56

Figure 8: Aluminum Price Histogram 57

Figure 9: Activated Aluminum System Boundary 60

Figure 10: Diesel kg/kWh Histogram 68

Figure 11: Diesel Engine kg/kWh versus rpm 69

Figure 12: Fuel Cell kg/kWh Histogram 71

Figure 13: Activated Aluminum USD/kWh Histogram 73

Figure 14: Activated Aluminum g/kWh Histogram 73

Figure 15: Economic and Environmental Impact Summation 77

List of Tables

Page

Table 1: TRACI 2.1 Categories and Units 12

Table 2: Midpoint Level Environmental Prices 14

Table 3: Hydrogen Production LCA 18

Table 4: Literature PEMFC Efficiencies 27

Table 5: World Aluminum Smelter Production and Capacity 30

Table 6: World Alumina Refinery and Bauxite Mine Production and Reserves 31

Table 7: Aluminum Production CO_2 Emissions 33

Table 8: Gallium World Production 35

Table 9: Indium World Production 37

Table 10: Literature Diesel Engine Efficiencies 41

Table 11: Literature Diesel Well-to-Combustion GWP 43

Table 12: Cummins Maritime Performance Curve 46

Table 13: Diesel kg/kWh 47

Table 14: Fuel Cell kg/kWh 52

Table 15: Activated Aluminum Recycled Content Scenarios 59

Table 16: GaBi Model User Created Processes 62

Table 17: Environmental Category Prices 65

Table 18: Diesel kg/kWh and $/kWh Results 69

Table 19: Diesel LCA and LCIA Results 70

Table 20: Hydrogen and Activated Aluminum kg/kWh and $/kWh Results 72

Table 21: Activated Aluminum LCA and LCIA Results 75

Table 22: Economic and Environmental Impact Summation 76

List of Equations

Page

Equation 1 3

Equation 2 16

Equation 3 16

Equation 4 17

Equation 5 21

Equation 6 23

Equation 7 48

Equation 8 49

Equation 9 50

Equation 10 53

Equation 11 54

Equation 12 58

LIFE CYCLE ASSESSMENT OF HYDROGEN FUEL DERIVED FROM ALUMINUM VERSUS DIESEL

I. Introduction

Background

As anthropogenic emissions and their impacts on climate change have become irrefutable, the need for alternative, low emission energy sources and carriers is undeniable. In addition to environmental pressures requiring a shift from petroleum-based fuels, geopolitical and economic concerns all point to the United States not only needing energy independence, but needing the ability to fuel the military in new ways (Samaras et al., 2019). The United States Marine Corps' Force Design 2030 (Berger, 2020) outlines how Distributed Maritime Operations (DMO) and Expeditionary Advanced Base Operations (EABO) are ways to combat rising anti-access and area denial strategies developed by our adversaries. Unfortunately, while these methods increase survivability, decrease detection, and decrease vulnerability to high value assets, they also complicate the logistical problem set. This is an issue as the United States Navy's Merchant Marine fleet is aging and already overtaxed providing for current operations (Wakim, 2019). To answer the need to shift from petroleum-based fuels and meet the needs of the military, a power source or energy carrier needs to be economically and environmentally sustainable, while conserving weight, volume, and EABO longevity.

Hydrogen is one potential energy carrier that could enable minimal impacts on the biosphere and is anticipated to be part of the global energy system over the next decade (Ratnakar et al., 2021). Based on the International Energy Agency's Net Zero

Emissions by 2050 scenario, annual global demand of hydrogen needs to be 530 Mt, compared to the 2020 demand of 90 Mt. However, based on expected growth and announced governmental pledges, the anticipated annual global demand will be 250 Mt by 2050 ((International Energy Agency), 2021). If strategically sound, the military could significantly contribute to the global shift towards hydrogen and away from petroleum-based fuels.

While hydrogen is extremely abundant within bonds in water and hydrocarbons, it does not naturally occur in a gaseous form. Consequently, processes are needed to release and capture the hydrogen, some of which are significant carbon sources while others could have minimal emissions. Existing and potential production methods are thermochemical, electrolytic, direct solar water splitting, and biological processes ((EERE), 2020). However, the global demand of 90 Mt of hydrogen is met primarily through the fossil fuel based thermochemical processes of steam-methane reforming (59% global production), a byproduct of naphtha refineries (21% global production), and coal gasification (19% global production). While these methods are relatively inexpensive at less than \$2/kg-H_2, they still have a significant environmental impact with 900 Mt of direct CO_2 emissions produced in 2020, resulting in 10 Mt-CO_2/Mt-H_2 ((International Energy Agency), 2021).

Hydrogen has a low energy barrier for combustion in air, a low normal boiling point (20.4 K), a large liquid to vapor volume expansion (860 times at ambient conditions), can leak through many materials due to its molecular size, causes hydrogen embrittlement in many materials, and has a very low volumetric energy density of 8 MJ/L, as opposed to diesel at 36 MJ/L. All these characteristics require special

considerations and equipment to effectively transport or store hydrogen, which would further complicate any logistical supply chain of hydrogen gas (Ratnakar et al., 2021). Potential alternatives to fielding a supply chain that can support hydrogen compression or liquefaction are physical or chemical binding. Examples of chemical binding are in the form of ammonia, ethanol, or methane, but require dehydrogenation methods that are not suitable for DMO applications. Physical binding involves absorption into other materials, such as metal, to form metal hydrides. However, these methods have issues with accessing the hydrogen when needed and require precious metals such as lithium or magnesium (Ratnakar et al., 2021).

An alternative method of generating hydrogen is through processing aluminum with a small amount of gallium and indium, which bypasses the naturally occurring oxide layer on aluminum, and allows for a reaction with water to create hydrogen. This reaction is shown in Equation 1 and, due to the normally inert nature of aluminum, would allow for long term energy storage and hydrogen production on site, minimizing the issues with a gaseous or liquified hydrogen logistics train (Slocum et al., 2020).

$$2Al + 6H_2O \rightarrow 2Al(OH)_3 + 3H_2 + Q$$ (Slocum, 2018)

Equation 1

The purpose of this thesis is to determine if deriving hydrogen from activated aluminum is an economically, strategically, or environmentally viable alternative to diesel while operating in a contested DMO environment by using a life cycle assessment (LCA).

Problem Statement

In 2011 the Commandant of the Marine Corps issued the Expeditionary Energy Strategy and Implementation Plan with the intent of increasing energy efficiency across the spectrum of military operations, particularly a 50% increase in operational energy efficiency on the battlefield. The purpose was to make the Marine Corps more capable in austere and expeditionary environments, which requires a "decreased demand for logistics support" (E2O, 2011). Additionally, as the Department of Defense (DoD) is the single largest producer of greenhouse gasses in the world and global warming is the most certain of threats that the United States faces in the coming decades, a reduction in emissions is imperative (Crawford, 2019). Activated aluminum is a fuel source that the Expeditionary Energy Office (E2O) has identified with the potential for supplementing liquid fuel but has not had the opportunity to conduct an analysis on the economic, strategic, or environmental impact that would have. This thesis provides decision makers and researchers the ability to make an informed decision when comparing fuels.

Research Objectives

This thesis explores the viability of using hydrogen derived from activated aluminum in a DMO environment, specifically in a Western Pacific theater and as a replacement for diesel in the Long Range Unmanned Surface Vessel (LRUSV). Additionally, the thesis explores using newly sourced versus recycled aluminum, recovering used eutectic, and the resulting differences in financial and environmental costs. The alternative paths; newly sourced, recycled, or diesel, are compared via a "well-to-wake" LCA (Comer & Osipova, 2021). This means accounting for all environmental

impacts associated with extraction of the material from the earth, processing to a usable product, associated transportation impacts, and emissions when converted to energy. The specific questions that this thesis explores are how this fuel compares environmentally, using a life cycle impact assessment (LCIA) methodology; economically, using market value pricing; and logistically to diesel.

Methodology

This thesis follows ISO 14040 and ISO 14044 to conduct a LCA to compare the environmental impacts of diesel and activated aluminum. The LCA was primarily conducted using GaBi, a LCA software by Sphera, and verified using Simapro, another LCA software. In both software applications, the environmental outputs of both fuels are modeled from the anticipated LRUSV operational profile. Fuel consumption for diesel was based off the power curves for the currently planned LRUSV Cummins diesel engine. Fuel consumption for hydrogen was based off the proton-exchange membrane fuel cell (PEMFC) used in a 2017 Toyota Mirai. The life cycle of each fuel is modeled from base material extraction to emissions from fuel consumption with the functional unit being 1 kWh of energy. Then, using the automated outputs of the software, the environmental impacts of each fuel are compared by monetizing and summing the environmental categories from the Environmental Protection Agency's (EPA) Tool for Reduction and Assessment of Chemicals and Other Environmental Impacts (TRACI).

The economic comparison of the two fuels was conducted using historical market values for the materials needed for activated aluminum and historical bulk diesel prices

for the DoD. The respective masses needed to generate 1 kWh were multiplied by the cost per mass, allowing for a direct comparison of the functional unit.

The logistical comparison of the two fuels is based primarily on physical and chemical properties and material availability. Specifically, power density, density, storage, survivability, and global production locations.

Assumptions/Limitations

This thesis and LCA is limited only to the fuels, not the life cycles of the vehicles, engines, or fuel cell systems. This simplifies the model and allows for a more versatile comparison as most sources of electricity used by the military are diesel powered internal combustion engines (ICE) (E2O, 2011). Additionally, it is assumed that the systems and logistical support will be in the Western Pacific in line with the shift in military doctrine to near-peer competition. Current allies, such as Australia and Japan, are assumed to remain strategic sources of material, logistical support, and logistical hubs.

Implications or Expected Contributions

This thesis was conducted to fulfill requirements for a graduate degree in Environmental Engineering at the Air Force Institute of Technology and on behalf of the USMC E2O. This research was intended to assist in decision making, allocation of funds, and topics for further research and acquisitions. To the author's knowledge, all comparative assertions will be disclosed to the public.

Summary

This thesis contains a total of five chapters that contain the introduction, literature review, methodology, results and analysis, and conclusions and recommendations.

Chapter 2 is the literature review and provides the background for conducting a LCA, hydrogen production, hydrogen as an energy carrier, activated aluminum, and the DoD's need for alternative fuels. Chapter 3 is the methodology and describes how the LCA and economic analysis were completed and how their inputs were determined. Chapter 4 is the analysis and results and provides the results of the LCA, economic analysis, discusses logistical considerations for both fuels, and potential areas of improvement for activated aluminum. Chapter 5 covers conclusions and recommendations, providing final synthesis for the results and recommendations for future research and decision makers.

II. Literature Review

Chapter Overview

This chapter discusses the purpose of a LCA, how a LCA is conducted, and how two different products with a similar purpose can be compared. Then, the chapter provides the background behind using hydrogen as a fuel source, the current challenges associated with hydrogen, and how activated aluminum could be a part of a hydrogen logistics system. Associated with activated aluminum, the chapter covers background on activated aluminum's constituents, production, reaction to create hydrogen, and current research. Finally, to support the need for the thesis, there is a short discussion on current USMC policies, directives, and paradigm shifts with a focus on energy. Specifically, diesel and its use in the military; how energy intensive military operations have become with an associated increase in environmental, logistical, and economic burdens; and how DMO requires different energy solutions.

Life Cycle Assessment

As a generalization, the LCA process consists of developing a model that considers the environmental impacts of a product's entire life, from material extraction to disposal and reuse. Figure 1 shows a simplistic life cycle of a recyclable metal. Not included, but what is considered in a life cycle, is transportation throughout the cycle, energy requirements such as fuel or electricity, packaging, materials used for manufacturing such as lime, specialized equipment, etc. To maintain the value of a LCA, the process is guided by the International Organization for Standardization with their 14044 and 14040 publications (ISO, 2006b, 2006a).

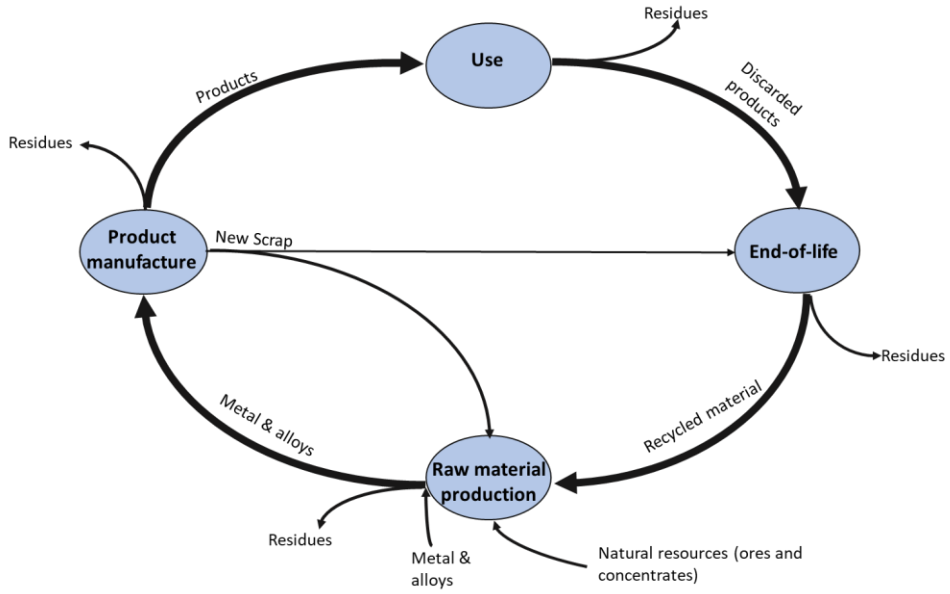

Figure 1: Life Cycle of a Metal

(Reproduced using (Graedal et al., 2011))

A LCA can be used to "identify opportunities to improve the environmental performance of products at various points in their life cycle or inform decision-makers…for the purpose of strategic planning, priority setting, product or process design" (ISO, 2006a). The LCA process consists of four phases: "the goal and scope definition phase, the inventory analysis phase, the impact assessment phase, and the interpretation phase" (ISO, 2006a). This type of analysis can be conducted on a single product, but for the purpose of this thesis, boils down to conducting a cost-benefit-analysis when comparing two products that serve the same purpose (Arendt et al., 2020). For instance, in a business model, when comparing proposed projects, the criteria for project selection could be financial benefit, risk, or how the project aligns with company goals. Then, each of those criteria are weighted differently based on the preferences of the decision maker (Nicholas & Steyn, 2017). A LCA provides another criterion to

consider and, for the military, weigh against financial costs, strategic impacts, tactical considerations, etc.

The goal and scope definition phase defines the purpose behind conducting the LCA and what does or does not pertain. The goal of an LCA is the reason behind conducting an LCA in the first place (ISO, 2006b). The scope sets the system boundary for what or what will not be considered during the assessment, the functional unit, the LCIA methodology used, and any assumptions or limitations in the assessment (ISO, 2006b).

The functional unit is the reference that sets the common basis for different systems being compared (ISO, 2006a). For instance, a LCA that compared a biodiesel blend to low sulfur diesel had a functional unit of 1 kWh produced from combustion in a 30 kW generator. Due to the properties of the fuel, each had a different consumption rate to produce 1 kWh. Based on that consumption, the impacts of each fuels' lifecycle could be compared (Viornery-Portillo et al., 2020).

The system boundary determines the extent of what is considered during the analysis. Ideally all inputs and outputs of the system are "material or energy" that come directly "from the environment without previous human transformation", or elementary flows. Identifying these flows is the inventory analysis phase. However, depending on the system, certain flows could have a negligible effect on the overall analysis compared to the effort to include the flow (ISO, 2006a). An example is allocating the fuel used for transportation but not the life cycle of the actual vehicle. The fraction of a vehicle's lifespan used to transport a small product does "not significantly change the overall conclusions of the study" and the effort required to model the life cycle of every vehicle

used throughout the product's life is not justifiable. The system boundary also helps inventory all the systems inputs and outputs, with both the boundary and life cycle inventory analysis being an iterative process as more is learned (ISO, 2006a).

The impact assessment and interpretation phases require determining which LCIA methodology to use and how to communicate the results. With the complexity associated with determining environmental impacts, there are many different methodologies. These methodologies, such as CML, EDIP, EcoIndicator, TRACI, EPFL 2002+, UseTox, and ReCiPe, vary based on geographic location, categories of interest, type of output, etc. (Bare, 2012; PE International AG, 2012). The purpose of the LCA, as well as the intended audience, influences the best method to choose and how to communicate the results. For instance, TRACI 2.1 uses the output of an LCA, such as chemical emissions or fossil fuel use, to provide an estimated quantification for the separate environmental impact categories of ozone depletion, global warming, acidification, eutrophication, smog formation, human health from particulate matter, human cancerous effects, human noncancerous effects, ecotoxicity, and fossil fuel use. It is up to the user to determine the importance of each category and how to characterize the impacts of each one (Bare, 2012). Alternatively, ReCiPe2016 has similar impact categories, plus an additional seven, which are labeled as midpoint impact categories. The methodology then estimates the damage pathways, such as how cancerous toxicity creates an increase in cancers, and conglomerates the total damage pathways to an endpoint area, in this case damage to human health. Due to the nature of risk characterization, which accounts for variations in human and ecosystem reactions to chemicals, each level from midpoint to endpoint

increases the uncertainty (EPA, 2004; Huijbregts et al., 2017). A diagram of the relationships used in ReCiPe2016 is shown in Figure 2.

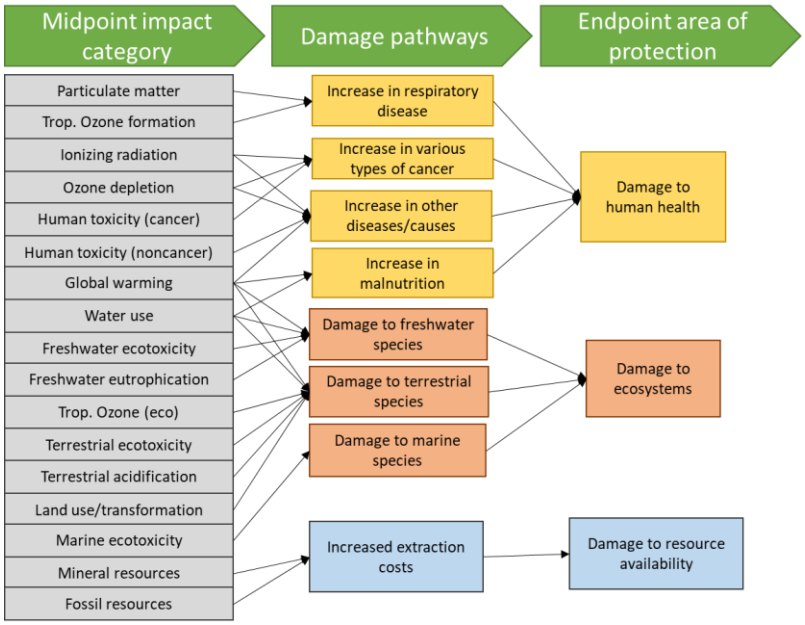

Figure 2: ReCiPe2016 Midpoint to Endpoint Relationships

(Reproduced using (Huijbregts et al., 2017))

While comparing two different products, the results of these categories can give decision makers a general idea of which product is worse but can lack reference. Particularly when trying to determine which category has the most severe impacts (Arendt et al., 2020). For instance, the units used for each category with TRACI 2.1 are shown in Table 1, but without context do not provide much information.

Table 1: TRACI 2.1 Categories and Units

Category	**Unit**	**Meaning**
Ozone Depletion	kg CFC-11 eq/kg substance	Chlorofluorocarbons and substances linked to decreasing the stratospheric ozone level
Global Warming	kg CO_2-eq/kg substance	Global warming potential of greenhouse gases (i.e. methane) relative to CO_2 with 100-year time horizons
Acidification	kg SO_2-eq/kg	Increasing concentration of the hydrogen ion

	substance	potential in a local environment from acids
Eutrophication	kg N-eq/kg substance	Enrichment of the aquatic environment with nutrients that accelerate algal biomass
Human Health Particulate Matter	$PM_{2.5}$-eq/kg substance	All inhalable coarse particles between 2.5-10 μm in diameter with health impacts characterized with $PM_{2.5}$ as the reference
Human Health Cancerous	CTUh (Comparative Toxic Unit)	From USEtox 2.0, characterizes human toxicity impacts at the midpoint level to provide the estimated increase in morbidity in the total human population. CTUh/kg substance = disease cases/kg substance (Fantke et al., 2017)
Human Health Noncancerous	CTUh	
Ecotoxicity	CTUe	From USEtox 2.0 and estimates "potentially affected fraction of species (PAF) integrated over time and volume per unit mass of chemical emitted". CTUe/kg substance = PAF m^3day/kg substance (Fantke et al., 2017)
Resource Depletion (fossil fuel)	MJ	Resource depletion. How much excess fuel is consumed
Smog Formation	kg O_3-eq/kg substance	Ground level ozone from the reaction between nitrogen oxide and volatile organic compounds in sunlight. Has detrimental human health and ecological impacts. Based on Maximum Incremental Reactivity values

(Adapted from (Bare, 2012). Sections pulled from other sources are cited.)

During the interpretation phase, one solution to the ambiguity of the results is to convert them to monetary units. For example, determining what 1 kg CO_2-eq released into the atmosphere costs society due to global warming (Arendt et al., 2020). Unfortunately, there are wide variations in estimates for the social cost of any substance. These variations stem from differences in opinions on discount rates, the impact of the damage, politics, etc. The best documented social cost is for carbon and climate change, with values differing by one to two orders of magnitude (Arendt et al., 2020; EPA, 2016). The most succinct valuation for most categories was found in the European Union Environmental Prices Handbook, shown in Table 2. These prices would then be

multiplied by the categorical quantities determined by the LCA. The result provides a decision maker values that can be contrasted against each other, to determine the greatest environmental impact, and as a whole against an economic product comparison (Arendt et al., 2020; de Bruyn et al., 2018).

Table 2: Midpoint Level Environmental Prices

Theme	Unit	External Cost	Weighting factor
Climate Change	$/kg CO_2-eq	$0.073	$0.073
Ozone depletion	$/kg CFC-eq	$38.993	$157.767
Human toxicity	$/kg 1,4 DB-eq	$0.127	$0.115
Photochemical oxidant formation	$/kg NMVOC-eq	$1.475	$1.475
Particulate matter formation	$/kg PM_{10}-eq	$50.280	$50.280
Ionizing radiation	$/kg kBq U235-eq	$0.059	$0.059
Acidification	$/kg SO_2-eq	$6.375	$9.594
Freshwater eutrophication	$/kg P-eq	$2.386	$6.234
Marine eutrophication	$/kg N	$3.989	$3.989
Terrestrial Ecotoxicity	$/kg 1,4 DB-eq	$11.146	$11.146
Freshwater ecotoxicity	$/kg 1,4 DB-eq	$0.046	$0.046
Marine ecotoxicity	$/kg 1,4 DB-eq	$0.009	$0.009
Land use	$/$m^2$ year	$0.108	$0.162

(Adapted from (de Bruyn et al., 2018) with 2015 Euro converted to 2021 USD with a 2015 currency conversion of €1 to $1.087 and 18% inflation from 2015 to 2021 ((US Bureau of Labor), 2021; Reserve, 2021))

Life Cycle Assessment Software

As discussed previously, LCAs are complicated and require access to information that is not readily available to a researcher. Such as the amount of emissions associated with using a MJ of electricity from the Australian electric grid. To assist the public and private sector in conducting LCAs, organizations, such as Ecoinvent, have created databases that contain the inputs and outputs for thousands of materials and processes

(Frischknecht & Rebitzer, 2005). However, while informative, building a LCA from such databases would be labor intensive, which resulted in software packages being developed for LCAs. While each software is different, they provide a user interface to model a life cycle, access to life cycle databases, automate LCIA methodologies, and provide statistical tools for analysis (Goedkoop et al., 2016; PE International AG, 2012). The two leading software programs are SimaPro and GaBi with their own database sets and access to the Ecoinvent database. When several products had their life cycles modeled on both programs, most of the results were the same. However, in some instances there were large enough differences, particularly during impact assessment, that could "influence the conclusions drawn from an LCA study." That stated, no clear preference between the two software programs was found (Herrmann & Moltesen, 2015).

Hydrogen

Hydrogen has been used as a fuel source for decades, particularly as rocket propellant, and its place in both mobile and stationary power applications has been growing. For mobile applications, it has been used as a fuel in ICEs, gas turbine engines, or converted to energy in fuel cells. For stationary applications it can be used in hydrogen-oxygen steam generators or in gas turbines (Ratnakar et al., 2021). However, hydrogen as a fuel source is uncommon and the current demand for hydrogen, 90 Mt annually, comes as feedstock for ammonia and methanol production (45 Mt H_2), feedstock and reagents for refineries (40 Mt H_2), and for the direct reduced iron process for steelmaking (5 Mt H_2). Annual hydrogen demand in transportation is 20 kt-H_2, 0.02% of the total annual demand ((International Energy Agency), 2021). While not applicable

in a DMO environment, hydrogen pipelines are the most cost efficient method of hydrogen transportation that is currently used, with approximately 5,000 km of hydrogen pipelines concentrated near petroleum refineries and chemical plants ((International Energy Agency), 2021). However, as previously mentioned, the requirements and infrastructure necessary to deliver and store hydrogen at distributed, end-use locations present significant obstacles to full scale development.

Hydrogen Production

The predominate hydrogen production method is steam-methane reforming at 59% global production ((International Energy Agency), 2021). This method is produced from mixing natural gas with steam at high temperatures to produce hydrogen and carbon monoxide, in accordance with Equation 2. Additional steam is added to gain more hydrogen and to convert the CO to CO_2, in accordance with Equation 3 (Al-Qahtani et al., 2021).

$$CH_4 + H_2O \rightarrow CO + 3H_2$$ (Al-Qahtani et al., 2021)

Equation 2

$$CO + H_2O \rightarrow CO_2 + H_2$$ (Al-Qahtani et al., 2021)

Equation 3

With 21% of the global hydrogen production, naphtha refineries are substantial hydrogen producers but this production is not the reason for their operation ((International Energy Agency), 2021). Naphtha refineries increase the octane and decrease the sulfur of heavy naphtha, which is blended with gasoline to reduce knocking in engines. The increase in octane is obtained through dehydrogenation of naphthenes to aromatics and other chemical reactions. An example is converting cyclohexane to

benzene with the byproduct of $3H_2$. However, this requires substantial energy and precious metals as catalysts (Eser, 2020). Consequently, if the need for high octane fuel decreases, then this production method would decrease, as well.

Coal gasification occurs when coal is heated to 800-1300 °C and pressurized to 30-70 bar to create a syngas mixture of CO, H_2, CO_2, and CH_4. Then, much like steam-methane reforming, steam is added to gain hydrogen gas (Al-Qahtani et al., 2021). The specific reaction, coupled with Equation 2 and 3, is shown in Equation 4..

$$C + 2H_2O \rightarrow CO_2 + 2H_2 \qquad \text{(Al-Qahtani et al., 2021)}$$

Equation 4

The primary alternative low-carbon hydrogen production methods are natural gas steam-methane reforming with carbon capture, utilization, and storage (CCUS) (0.7 Mt, 0.7% global production) and electrolytic from low-carbon energy sources (30 kt, 0.03% global production). Based on current and planned projects, by 2030 the capacity for CCUS is expected to grow to 9 Mt and electrolytic hydrogen could expand to 8 Mt ((International Energy Agency), 2021). CCUS are employed by directing flue gases through an amine solvent to capture the CO_2 then thermally desorbing and compressing the CO_2 for storage. The downsides are additional energy is required to regenerate the amine solvent and to compress the CO_2; then determining how and where to dispose of the captured CO_2 (Al-Qahtani et al., 2021).

Using Table 3 to examine a LCA of the primary hydrogen production methods, it is clear steam methane reforming with CCS has the lowest combined environmental and levelized cost; while electrolysis, using nuclear or wind, has the lowest environmental

impact (Al-Qahtani et al., 2021). Hydrogen produced in naphtha refineries is not included as it is a byproduct of an existing process.

Table 3: Hydrogen Production LCA

	USD2019/kgH2			
H2 Production	**Total Cost**	**Levelized Cost**	**Environmental Impact**	**$kgCO_2$-eq/kgH_2**
Steam Methane Reforming + CCS	4.6	1.9	2.7	5
Methane Pyrolysis	4.9	1.9	3	6
Steam Methane Reforming	5.5	1.4	4.1	11.2
Nuclear Electrolysis	5.7	4.9	0.8	0.67
Wind Electrolysis	6.5	5.5	1	0.86
Coal Gasification + CCS	10.6	2.4	8.2	10
Biomass Gasification + CCS	11.7	3.9	7.8	-13.1
Solar PV Electrolysis	12.5	9.7	2.8	3.1
Biomass Gasification	12.5	2.5	10	0.65
Coal Gasification	12.9	1.7	11.2	25.2

Reproduced using (Al-Qahtani et al., 2021)

Hydrogen Transportation and Storage

The United States Department of Energy (DOE) has an ultimate hydrogen production and delivery cost goal of less than \$4/kg-H_2 and storage systems with 2.2 kWh/kg and 1.7 kWh/L gravimetric and volumetric energy densities, respectively. The 2025 goals are to achieve 1.8 kWh/kg and 1.3 kWh/L for gravimetric and volumetric energy densities, respectively, at a cost of \$9/kWh (Department of Energy, 2020). For reference, diesel has gravimetric and volumetric energy densities at 9.7 kWh/kg and 10.8 kWh/L, respectively (Slocum, 2018). For a volumetric comparison, at standard ambient conditions (25 degrees Celsius and 1 atmosphere) 1 kg-H_2 fills 11.9 cubic meters. With a density of 845 kg/m^3, this same volume would hold 10 tonnes of diesel (Viornery-Portillo et al., 2020). Consequently, to make transporting and storing hydrogen cost effective, it must be compressed, liquefied, transported in another form, produced on site, or

produced as required. For passenger vehicles, current hydrogen tank operating pressures range between 350 to 700 bar, with these compression pressures taking 1.7 to 6.4 kWh/kg-H_2. Alternatively, energy requirements to liquefy hydrogen are typically 10-13 kWh/kg-LH_2 (DOE, 2009). Using a 57% efficient fuel cell system and the lower heating value (LHV) of hydrogen as 33.32 kWh/kg, 1 kg-H_2 provides approximately 19 kWh of energy (Lohse-Busch et al., 2018). Consequently, when transporting hydrogen, compression takes 9-34% of the useful energy while liquefication takes 52-68% of the useful energy. For an additional comparison, using the ideal gas law, 1 kg-H_2 at standard temperature and 500 bar fills about 0.025 m^3 while 1 kg of liquified hydrogen (LH_2) fills about 0.014 m^3, nearly halving the required volume (Ratnakar et al., 2021).

Besides the energy used to compress hydrogen, which lowers overall efficiency, there are several other challenges associated with compression. The first and foremost, as described above, is that obtaining a volumetric energy density on par with other fuels requires significant and unrealistic pressures for common use. Secondary issues are high compressor maintenance costs, acoustic pollution, and low efficiencies for mechanical compressors and high material costs, water entrainment, sealing, and back diffusion for electrochemical compressors (Ratnakar et al., 2021). Due to the conglomerate of disadvantages associated with compressed hydrogen, particularly volumetric needs, most of the literature agrees that compressed hydrogen used for mobile applications in a low carbon economy is practical for long range and heavy duty vehicles, but not for regular passenger cars (Department of Energy, 2020; Ratnakar et al., 2021; Volkswagen, 2019).

For transporting liquified hydrogen, another difficulty is that it must be maintained at 20 K or lower, significantly lower than the 110 K required for liquified

natural gas. Even with excellent insulation, current holding tanks at NASA result in 0.03-0.05% boil off losses per day and require integrated refrigeration and storage to counter these losses. Boil off also decreases the safety of the system as it is a fire hazard (Ratnakar et al., 2021). Additionally, current insulation techniques require two concentric tanks with the space between the inner and outer tanks maintained as at least a partial vacuum and filled with an insulation material. This technique is cost prohibitive and challenges construction practices when scaling to larger tank sizes, such as those that have enabled establishing the transportation and storage economy of liquified natural gas (Ratnakar et al., 2021). Due to these difficulties, the viability of transporting large quantities of liquified hydrogen is still in the development stage with the world's first liquefied hydrogen carrier ship only launching in 2019 and its maiden voyage with cargo still delayed until at least mid-2022 (Collins, 2021). The ship itself is designed to carry 1,250 m^3, or 75 tonnes of liquified hydrogen, well below the 20,000-40,000 m^3 capacities used with liquified natural gas (Ratnakar et al., 2021).

Alternative Hydrogen Storage and Transportation

To avoid the issues involved with compressed or liquified hydrogen, the literature has a wide spectrum of material-based hydrogen storage that involves adsorption, bulk absorption, or chemical interactions. The primary intent of the research is to achieve high energy storage and ease of transportation that would make a hydrogen economy more practical.

Adsorption involves hydrogen absorbing to the surfaces of carbon-based material, which requires significant surface area, such as powdered activated carbon (Department of Energy, 2020; Ratnakar et al., 2021). While these methods can achieve high

gravimetric densities, the corresponding volumetric densities are nearly inversed, with low volumetric densities continuing to be a barrier for economically transporting hydrogen (Department of Energy, 2020).

For absorption, hydrogen can absorb into the metal crystal lattice structure of metal hydrides such as nickel, lithium, magnesium, boron, or aluminum (Ratnakar et al., 2021). The reversible interaction for metal hydrides is shown in Equation 5, with A_yB_z indicating an intermetallic alloy such as sodium borohydride, sodium aluminum hydride, lanthanum nickel hydride, etc. (Lototskyy et al., 2017; Slocum, 2018).

$$A_yB_z + xH_2 \underset{\rightarrow}{\leftarrow} A_yB_zH_{2x} + \Delta Q$$ (Lototskyy et al., 2017)

Equation 5

The primary considerations with metal hydrides are the pressure, temperature, and concentration of hydrogen. The higher the temperature, the more pressure is needed to achieve the same concentration levels. Consequently, heat is required to release the hydrogen from the hydride; if those temperature requirements are higher than the byproduct of the energy generation system, the entire system loses efficiency (Lototskyy et al., 2017). Additionally, while metal hydride technology is improving, they still have issues with low storage capacities by weight, slow kinetics, and low reversibility (Rusman & Dahari, 2016).

As previously mentioned, chemical storage is possible with chemicals such as ammonia, or hydrocarbons, such as ethanol, and provides higher storage density and performance at lower pressures and higher temperatures. However, these methods require hydrogen regeneration via pyrolysis or other dehydrogenation practices, which is not

suitable for DMO operations. Additionally, these methods require pollution controls for CO_2 with hydrocarbons and NO_x for ammonia (Ratnakar et al., 2021).

Hydrogen Energy Conversion and Fuel Cells

As a fuel, hydrogen can be converted to usable energy through combustion in ICEs, or gas turbines, or the electrochemical reaction in fuel cells. However, before further discussion, it is imperative to discuss how to compare efficiencies and emissions of different fuel to power conversion methods. Specifically, there is a difference between power that can be gained from combusting material and the obtainable power from the reaction in an electrochemical cell.

Heat of combustion, or heating value, is "the amount of heat released when 1 gram molecular weight of a substance is burned in oxygen" (Harrison et al., 2010). This measurement can either include the latent heat required to condense water, known as the higher heating value (HHV), or water vapor is allowed to escape and not included in the heating value. This latter condition is known as the lower heating value (LHV). In most practical instances of combustion, water vapor escapes with the exhaust stream and the LHV accurately depicts the heating value. Additionally, the heating value changes according to environmental conditions, so values are generally reported for 25 °C and 1 atmosphere, standard conditions (Harrison et al., 2010). For hydrogen combustion, the HHV is 141.8 MJ/kg while the LHV is 119.45 MJ/kg (Balli et al., 2021; Harrison et al., 2010).

In an electrochemical reaction, the reaction that occurs in fuel cells, both electricity and heat are produced. The amount of electrical energy, or the energy used to do work, is determined by the Gibbs free energy value. The remaining heat produced by

the reaction is the difference between the heating value and the Gibbs free energy. For example, for hydrogen, Gibbs free energy is 117.67 MJ/kg (Harrison et al., 2010). There is a 1.78 MJ/kg difference between this value and the LHV. For an ideal electrochemical reaction and no losses, the reaction would provide 117.67 MJ/kg of electricity and 1.78 MJ/kg of heat (Harrison et al., 2010).

The efficiency of a fuel to power system is calculated by Equation 6 (Harrison et al., 2010). Of note, the reference used the HHV, the standard for most United States ICE ratings, but this paper uses the LHV, which is more common for European ratings, United States high-temperature fuel cell developers, and other reviewed literature (Balli et al., 2021; Harrison et al., 2010).

$$Electrical\ Efficiency\ (LHV) = \frac{Electricity\ Produced}{LHV\ of\ Fuel\ Used}$$ (Harrison et al., 2010)

Equation 6

Using Equation 6, it is clear that an ideal electrochemical reaction will not result in 100% efficiency as the Gibbs free energy/LHV (117.67/119.95) MJ/kg results in only 98.1% (Harrison et al., 2010). To emphasize, this thesis focuses on the efficiency of the fuel cell system, rather than the fuel cell stack. The reason for this is that the system includes all the other necessary components for operation such as humidifiers, power conditioners, etc. (Harrison et al., 2010). This provides a more useful comparison of fuel consumption for a life cycle assessment.

Hydrogen can be used as the only fuel in an ICE or blended with petroleum fuels as an energy booster. When hydrogen is the sole fuel used in an ICE, the engine requires specialization. Specifically, the hydrogen is ported into the cylinders at high pressure as a gas, the engine requires enhanced fuel control, the engine needs enhanced thermal

management and materials due to the high temperature exhaust gases, and a smaller spark plug gap and lower ignition energy due to hydrogen's low and quick combustion rate. An ICE that solely uses hydrogen has some efficiency increases, with efficiencies reported around 35-45%, and decreased emissions, but produces 50-80% of the power produced by a gasoline engine. When hydrogen is blended with petroleum fuels there is an increase in efficiencies and decrease in most emissions except NO_x. However, blended systems are uncommon due to increased complication of the system, discussed issues with supporting a hydrogen economy, and increased costs (Shinde & K., 2021).

In a thermodynamic comparison of hydrogen used in a gas turbine engine instead of kerosene, there was a 10% decrease in power, a decrease in efficiency of about 0.8% (from 37.01% to 36.73%), and an increase in nitrogen emissions. The tradeoff is that there was about a 60% decrease in specific fuel consumption and a decrease in carbon emissions. Additionally, with the cost of hydrogen in the study at $4.94/kg and for kerosene at $0.459/kg, there was an increase in cost from $0.66 per second to $2.58 per second (Balli et al., 2021). With the current cost of hydrogen, low carbon emission penalties, and high carbon production methods of hydrogen, there are few instances of hydrogen fueled turbines. However, there are instances of sustained gas turbine operation with hydrogen-enriched fuel, with enrichment ranging from 12-60%. Projections for power production using hydrogen in gas turbine engines are highly dependent on CO_2 emission caps but show usage is unlikely as it is inefficient to use renewable energy to create hydrogen just to convert it back to electricity (Öberg et al., 2022).

Fuel cells consist of an anode and cathode, separated by an electrolyte, and flow channels that allow the reactants into the fuel cell. They operate by pumping the fuel

source, such as hydrogen, to the anode while simultaneously pumping oxygen (or ambient air) to the cathode. For low temperature fuel cells, a catalyst is placed at the anode to convert fuel molecules to protons and electrons, an unnecessary step for high temperature fuel cells. Then the electrons travel from the anode to the cathode along a separate circuit, creating an electric current, while the positive ions travel through the electrolyte to the cathode (Abdelkareem et al., 2021). Figure 3 shows a simplified diagram of a hydrogen fuel cell. The result of the reaction for hydrogen fuel cells is electricity, water, and heat (Montero-Sousa et al., 2020).

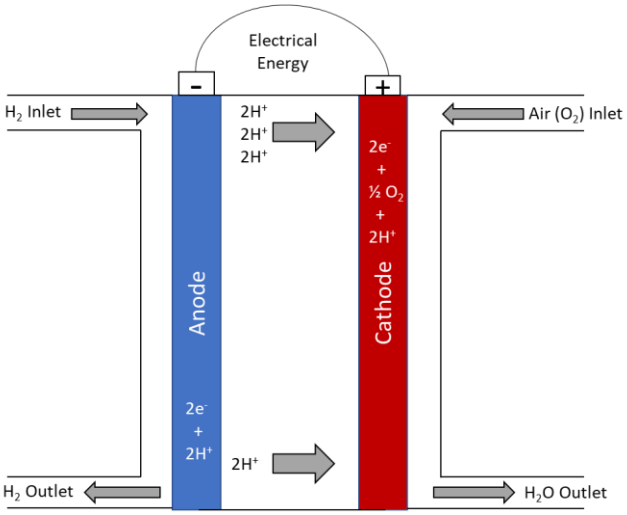

Figure 3: Fuel Cell Schematic

(Reproduced using (Montero-Sousa et al., 2020))

Fuel cells come in many different types and are generally defined by the fuel type, electrolyte, and operating temperature. Some of the potential fuels that can be used in a fuel cell are hydrogen, methanol, ethanol, carbon monoxide, etc. Each fuel has its advantages and disadvantages. Methanol for instance, has high energy density and no carbon emissions, but current technology struggles with the fuel crossing from the anode

to the cathode, resulting in low efficiencies and cathode poisoning (Abdelkareem et al., 2021).

Some of the primary electrolytes used in fuel cells are Nafion (Sulfonated Polytetrafluorethylene), alkaline, phosphoric acid, and molten carbonate. Of primary interest in this thesis is the Nafion, which is the primary electrolyte used in PEMFCs as it operates at the relatively low temperature of 80 °C, has a power range from 1W-500kW, can start and stop quickly (Abdelkareem et al., 2021), and is the type used in commercially available vehicles (Lohse-Busch et al., 2018). Selecting this type of fuel cell for this thesis allowed for a comparison of efficiencies in the literature and deriving a realistic average and associated error for a PEMFC system that is commercially viable. The downside of PEMFCs is that platinum is needed as a catalyst, for efficiency, which significantly increases the cost of the system. Consequently, there is deep interest in reducing the amount of platinum via platinum alloys, nano structures, and alternatives, such as Fe-N-C catalysts. Indicative of this interest, the DOE's fuel cell research and development subprogram devoted 30% of its 2019 budget to catalysts and electrode improvement (Department of Energy, 2020).

The literature shows a significant range of PEMFC fuel cell system efficiencies with Table 4 showing ranges or the average. Of particular interest, the efficiency of a fuel cell system generally decreases as the load increases, with most efficient operation at low load demands (Lohse-Busch et al., 2018).

Table 4: Literature PEMFC Efficiencies

Source	(Lohse-Busch et al., 2018)	(Abdelkareem et al., 2021)	(Kim & Kim, 2015)	(Montero-Sousa et al., 2020)	(Özçelep et al., 2020)	(Department of Energy, 2020)
Efficiency Range %	40-63.7	40-50	40	40	45-54	58
Max output kW	114	500	0.1	5	0.005	0.00055/cm^2

Activated Aluminum

An alternative method of obtaining hydrogen is by reacting aluminum with water in accordance with Equation 1. While aluminum usually forms a protective aluminum oxide layer that prevents continuous reaction, there are several ways to prevent or remove this layer. These methods include mechanical scraping, thermal removal, corrosion via alkaline or acidic solutions, mixing aluminum powder with inorganic salts, or liquid metal embrittlement. While effective, some methods require high energy, such as thermal or mechanical, while others use caustic liquids and produce toxic products (Slocum, 2018). Liquid metal embrittlement does not have the same issues but, the most effective metals used for embrittlement, gallium and indium, are expensive, requiring a method that minimalizes their use while maximizing the total hydrogen yield (Slocum, 2018).

Research conducted by Johnathan Slocum for his PhD at the Massachusetts Institute of Technology, showed that soaking 6 mm (0.3 g) aluminum spheres in a gallium-indium eutectic bath for 120 minutes at 120°C, resulted in 3.55% gallium-indium weight by mass and a 88.7% yield of hydrogen when reacted with water (Slocum, 2018). Variations in soak time, temperature, and the eutectic composition showed that the above metrics, with the eutectic composition 80% gallium and 20% indium by weight, provided the best yield. After soaking, the aluminum spheres were centrifuged to remove the

excess eutectic and hermetically sealed “for one week to facilitate the diffusion of the eutectic into the grain boundaries” (Slocum, 2018). When each 6 mm sphere was reacted with 5 mL of water, the outputs were heat, hydrogen, and aluminum hydroxide (Slocum, 2018). With a potential energy of 31 MJ/kg, if 1 kg-Al perfectly reacted with water, it would result in 0.112 kg-H_2 and 15.1 MJ of heat energy (Slocum, 2018).

Once the reaction is complete, it is possible to recover and reuse the gallium-indium eutectic. This is because the eutectic interrupts the formation of the oxide layer and does not participate in the reaction. Previous research found that gravity settling, solids collection, washing with 50°C water, and settling again resulted in almost complete recovery of gallium in a pure gallium-aluminum mixture (Tekade et al., 2020). Another reference estimates 95% recovery rates of the eutectic (Godart et al., 2021). Additionally, the aluminum hydroxide byproduct can be fed back into aluminum production, sold as pharmaceuticals, or used in flame retardants (Slocum, 2018).

As proof of concept, a couple of fuel cell power systems have been developed to operate from activated aluminum. The first system was a 3 kW generator where the activated aluminum was fed into a reaction chamber, hydrogen produced, conditioned, and consumed by a PEMFC. Due to PEMFC hydrogen requirements, the hydrogen had to be cooled and separated from the water vapor that was produced with the reaction. The system was able to provide a stable 3 kW for one hour but refueling required opening the reaction chamber, removing the aluminum hydroxide, and reloading with activated aluminum. The overall efficiency of the system was 20% due to waste heat from the reaction, a 40% efficient fuel cell, energy needed to pump water into the chamber, the cooling system, and other electronics (Godart et al., 2021). The second system was a

converted BMW i3 vehicle where a 10 kW fuel cell, powered by hydrogen from activated aluminum, charged the vehicle's battery. Due to the heat from the reaction and from fuel cell operation, extensive modification to the vehicle's heat radiation system had to be conducted, but ultimately the system provided stable power (Godart et al., 2021).

Other potential uses of activated aluminum referenced in the literature are directly fueling a converted ICE, which could obtain 35% efficiency; a 20W emergency powerpack that can attach to a canteen; and a reverse osmosis system that is driven entirely by the activated aluminum reaction with water (Godart & Hart, 2020). Additionally, while scrap aluminum can be used to fuel the reaction, different aluminum alloys have different reaction characteristics and hydrogen production. An alloy with 0.6% by weight silicon resulted in an increase in hydrogen yield, increase in reaction temperature, and a sharper flow rate with an associated decrease in overall reaction time, when compared to pure aluminum. Conversely, an alloy with 1% by weight magnesium resulted in a decrease in hydrogen yield, decrease in reaction temperature, and a decreased flow rate with an associated increase in overall reaction time. An alloy with 0.6% silicon and 1% magnesium resulted in a reaction that performed more unpredictably, but had results that were somewhat in between the silicon and magnesium alloys (Meroueh et al., 2020).

Aluminum

Aluminum is one of the most abundant metals in Earth's crust and is used throughout society for construction, transportation, electrical conductors, packaging, etc. Its production also increased by 52% from 2010 to 2018 with a 2020 production rate of 65.2 million tonnes (Saevarsdottir et al., 2020; USGS, 2021a). The largest producer is

China, with 37 million tonnes annual production, followed by India and Russia, each with 3.6 million tonnes annual production. Aluminum production rates and capacities throughout the world are shown in Table 5. Note that China produces more than half of the world's aluminum, which could complicate an aluminum fuel supply chain if the United States is involved in an armed conflict with them or their allies.

Table 5: World Aluminum Smelter Production and Capacity

	Production		Yearend capacity	
	2019	2020[e]	2019	2020[e]
United States	1,093	1,000	1,790	1,790
Australia	1,570	1,600	1,720	1,720
Bahrain	1,370	1,500	1,540	1,540
Canada	2,850	3,100	3,270	3,270
China	35,000	37,000	41,300	43,000
Iceland	845	840	890	890
India	3,640	3,600	4,060	4,060
Norway	1,400	1,400	1,430	1,430
Russia	3,640	3,600	4,020	4,020
United Arab Emirates	2,600	2,600	2,700	2,700
Other countries	9,200	9,000	12,200	12,300
World total (rounded)	63,200	65,200	74,900	76,700

(Data in thousand metric tons. From (USGS, 2021a))

While aluminum is abundant, it is only found as an oxide ore, with bauxite the most widely distributed ore used in its production. Economically viable bauxite "typically contains 30-50% of extractable alumina" which are in the form of gibbsite, also known as aluminum hydroxide ($Al(OH)_3$), boehmite, and diaspore (Bagshaw, 2017). To get from bauxite to aluminum, the ore is mined, generally from surface deposits, converted to alumina with the Bayer Process, and the alumina is smelted into aluminum ingots via electrolysis (Saevarsdottir et al., 2020). Table 6 shows the global bauxite reserves, production, and alumina production. Of note, Australia has significant bauxite and alumina production, 30% and 15% of the global production, respectively. Depending on aluminum production and economics, an aluminum fuel supply chain supporting

operations in the Western Pacific would be significantly shortened if provided from Australia.

Table 6: World Alumina Refinery and Bauxite Mine Production and Reserves

	Mine production				Bauxite reserves[6]
	Alumina[5]		Bauxite		
	2019	2020[e]	2019	2020[e]	
United States	1,410	1,300	W	W	20,000
Australia	20,200	21,000	105,000	110,000	[7]5,100,000
Brazil	8,700	9,600	34,000	35,000	2,700,000
Canada	1,520	1,500	—	—	—
China	72,500	74,000	70,000	60,000	1,000,000
Guinea	368	460	67,000	82,000	7,400,000
India	6,690	6,700	23,000	22,000	660,000
Indonesia	1,000	1,000	17,000	23,000	1,200,000
Jamaica	2,170	1,700	9,020	7,700	2,000,000
Kazakhstan	1,500	1,500	5,800	5,800	160,000
Malaysia	—	—	900	500	170,000
Russia	2,760	2,800	5,570	6,100	500,000
Saudi Arabia	1,840	1,800	4,050	4,000	190,000
Vietnam	1,370	1,400	4,000	4,000	3,700,000
Other countries	10,900	12,000	12,000	11,000	4,900,000
World total (rounded)	133,000	136,000	[8]358,000	[8]371,000	30,000,000

(Data in thousand metric dry tons. From (USGS, 2021b))

For every tonne of alumina produced, the Bayer Process, shown in Figure 4, consumes 100 kg of hot caustic soda (sodium hydroxide solution), to dissolve the ground bauxite into aluminate ions, and consumes 50 kg of lime, to make the process more efficient by counteracting the effects of biological matter. In the precipitation portion of Figure 4, the aluminate ions are crystallized into aluminum hydroxide, which is then screened out and washed with water to remove the caustic soda liquor (Bagshaw, 2017). Then, in the calcination section, the aluminum hydroxide is heated to remove the water and obtain alumina (Al_2O_3). Depending on the quality of ore, the process produces 2-3 tonnes of waste, known as red mud, for every tonne of alumina. This waste is caustic, fine grained (20-45 μm), and while it contains many elements, particularly iron and

silicon, extraction of those elements is challenging. The waste also remains hazardous to the environment for hundreds of years (Bagshaw, 2017).

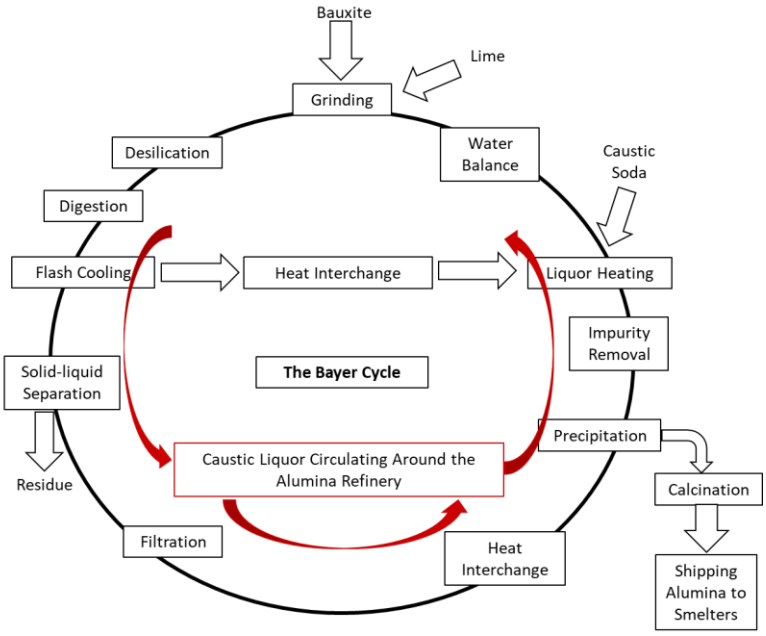

Figure 4: The Bayer Cycle

(Reproduced using (Bagshaw, 2017))

To produce aluminum, alumina is "dissolved in a sodium-aluminum-fluoride molten salt mixture" to provide the electrolyte medium between a carbon anode and cathode (Saevarsdottir et al., 2020). This causes an electrochemical reduction of the alumina to aluminum metal, electrochemical oxidation of the oxides to form carbon monoxide and dioxide, and liquifies the metal for collection at the bottom of the electrolysis cell. One tonne of aluminum requires two tonnes of alumina, 45,000-57,600 MJ, and 0.40-0.46 tonnes of carbon anode (Saevarsdottir et al., 2020).

In China, with its high usage of coal for electricity generation, one tonne of primary aluminum requires 144,612 MJ of life-cycle energy and produces 14.77 tonnes of CO_2-eq, with the electrolysis stage producing 70-77.2% of the total. Conversely, each

ton of recycled aluminum requires a life-cycle energy of 9,207 MJ, nearly a 95% reduction. A comparison of United States primary aluminum production found carbon emissions to be around half of China's, at 7.87 tonnes CO_2-eq per tonne of primary aluminum, primarily due to the different electricity generation mix (Peng et al., 2019; Wang, 2022). A different study, using SimaPro 8 linked to the Ecoinvent 2.2 database, found aluminum production to emit 8.2 tonnes CO_2-eq per tonne of aluminum (Nuss & Eckelman, 2014). Table 7, from a separate study, provides a comparison of each aluminum production step and associated CO_2 emissions between the global average and best available technology (BAT).

Table 7: Aluminum Production CO_2 Emissions

Processes	Global average CO_2 emissions (t CO_{2e}/t Al)	Global average emissions (%)	BAT emissions (t CO_{2e}/t Al)	BAT emissions (%)
Bauxite mining	0.03	0.2	.03	1
Alumina production	1.5	10.5	1.4	40
Calcined petroleum coke production	0.3	2.1	0.3	8.6
Carbon anode production	0.3	2.1	0.2	5.7
Cathode and spent potlining	0.03	0.2	0.03	1
Net cell carbon consumption	1.5	10.5	1.4	40
Perfluorocarbon emissions	0.2	1.4	0.02	0.6
Ingot casting fuel combustion	0.3	2.1	0.1	3
Electricity (world average)	10.2	70.6	0.01	0.3
Total	**14.4**	**100**	**3.5**	**100**

(Reproduced using (Saevarsdottir et al., 2020)

Aluminum recycling is a complicated process that requires effort from product designers to end users and policy makers. It is also usually a byproduct of a different process, such as auto repair, construction, demolition, etc. Once the waste is collected, it must be sorted into different alloy forms, removed from different materials, cleaned, and

machined into an appropriate state for secondary aluminum production, such as grinding or chipping (Wang, 2022). This process is simplified when scrap aluminum is collected from industrial level operations but significantly more challenging with post-consumer collections. The difficulty arises from consumer awareness and convenience, insufficient collection systems, the aluminum is connected to different material and difficult to remove, and scrap is mixed with different alloys, resulting in downcycling (Reuter et al., 2013; Wang, 2022).

Reports for current aluminum recycling rates vary, with significant differences between usage sectors (transportation, construction, packaging, etc.) (Wang, 2022). A 2011 global estimate is that 42-70% of aluminum is recycled at its end of life, with the remainder being landfilled, and aluminum production has 34-36% of recycled content (Graedal et al., 2011). With industry low-carbon targets, increasing demand for aluminum, and projected production capacity limits, the demand for scrap aluminum is projected to rise. The assumption is that secondary aluminum production will need "to grow by a compound annual growth rate of 5.8% in the next five years, faster than for primary" aluminum (Taylor, 2021).

Consequently, due to the production process and associated high energy requirements, aluminum production and its environmental impacts is highly dependent on the amount of recycled aluminum content and the energy generation mix used to power the process. Additionally, while the ore is abundant, refined aluminum is in high demand.

Gallium

Gallium's demand continues to increase as it is used in circuits, optoelectronic devices, light-emitting diodes, photodetectors, solar cells, defense applications, cable

television, wireless infrastructure, and satellites, among numerous other technological sectors. Gallium's semiconductor properties make it well suited for these applications, and in some cases, does not have any effective substitutes (de Oliveira et al., 2021; Jaskula, 2021).

Gallium is extracted primarily from bauxite and zinc ore deposits with concentrations ranging from "<10 to 812 parts per million (ppm), with an average of 57 ppm" (Schulte & Foley, 2014). With its concentrations in bauxite, gallium is primarily a byproduct of aluminum production with the aluminum "Bayer liquors containing 70-150 mg-Ga/L". Extraction from the Bayer liquors is conducted with "fractional precipitation, electrolytic processes, and with chelating agents" (de Oliveira et al., 2021). Due to its low concentrations, low recycling rates, and demand in the expanding technological sector, gallium is considered a critical material with a recoverable global supply at 1.6×10^6 tonnes (de Oliveira et al., 2021; Reuter et al., 2013). Table 8 provides 2019 and 2020 global production rates. Note that China and Russia produce 98% of the global supply.

Table 8: Gallium World Production

World Production and Reserves:

	Primary production	
	2019	2020[e]
United States	—	—
China	338,000	290,000
Japan	3,000	3,000
Korea, Republic of	2,000	3,000
Russia	8,000	4,000
Ukraine	—	—
World total (rounded)	351,000	300,000

(Data in kilograms. From (Jaskula, 2021))

Recycling gallium is difficult as it is nearly always alloyed and the separation techniques require variations on grinding, leaching with acids, precipitating and filtering

the metals, and separation via solvent extraction, similar to primary production from the Bayer liquor (de Oliveira et al., 2021; Fthenakis et al., 2009; Reuter et al., 2013). Reflecting the difficulty of recycling gallium from consumer products, end of life recycling for gallium is less than 1% of the amount landfilled. However, gallium production has 25-50% recycled content from scrap produced during manufacturing, such as broken gallium-arsenide wafers and sawdust (Graedal et al., 2011). Due to the production processes requiring further concentration of Bayer liquor and solvents, the global warming potential (GWP) for gallium is reported at 205 kg CO_2-eq per kg-Ga (Nuss & Eckelman, 2014).

Indium

Indium is primarily used in semiconductors (indium phosphide), solders (indium-lead), and flat-panel displays, particularly in liquid crystal displays as indium-tin oxide (ITO) (USGS, 2020). Production of indium is a byproduct of zinc production with concentrations of indium in zinc ore (sphalerite) at 1-100 ppm (Anderson, 2021). The acid leachate residues from zinc production contain about 0.2% indium. To obtain indium from the leachate, soda is added to precipitate the metal, the crystallized metal is filtered out, leached with sodium hydrochloric acid, and purified by cementation (Fthenakis et al., 2009). These extraction techniques lead to a GWP of 102 kg CO_2 -eq per kg-In (Nuss & Eckelman, 2014). Table 9 provides the global production quantities, again note that China provides over half of the global total.

Table 9: Indium World Production

World Refinery Production and Reserves:

	Refinery production 2019	2020[e]
United States	—	—
Belgium	20	20
Canada	61	50
China	535	500
France	40	50
Japan	70	65
Korea, Republic of	225	200
Peru	12	10
Russia	5	5
World total (rounded)	968	900

(Data in metric tons. From (Anderson, 2021))

Depending on the product, indium recycling can be lucrative, demonstrated by ITO alloy having approximately 1,200 tonnes a year reused for the reproduction of ITO (USGS, 2020). However, much like gallium, for consumer products containing indium, such as flat-panel displays, extraction is not lucrative because it is difficult and the indium quantities are so low (Reuter et al., 2013). Consequently, new indium can contain 25-50% recycled content from manufacturing processes, but end of life recycling is less than 1% of the amount landfilled (Graedal et al., 2011).

Military Fuel

The USMC, and the DoD in general, is highly interested in decreasing its energy usage and dependence on petroleum fuels. Several, but not all, of the reasons for these interests are intertwined and include a decrease in cost, an increase in mobility, enhanced expeditionary longevity, a decrease in environmental impacts, and energy independence.

With a DoD budget of over $700 billion per year, in 2017 $11.7 billion was spent on energy costs, $3.5 billion for installations and $8.2 billion to “power ships, aircraft, combat vehicles, and contingency bases”. Depending on fuel costs and operational

requirements, these numbers shift from year to year but require around 200 MJ per year for installations and at least 85 million barrels of fuel (Crawford, 2019). These budget requirements shift funding away from other priorities and "an increase in $10 per barrel for the DoD…is an increase equivalent to the entire Marine Corps' procurement budget." This leaves the DoD, and especially the Marine Corps with a smaller budget, vulnerable to energy price fluctuations (E2O, 2011). Any increase in energy efficiency allows for decreased spending and lessens the total fuel requirement, which drives the USMC's overarching goal of increasing "operational energy efficiency on the battlefield by 50 percent" (E2O, 2011).

The driving force behind the USMC's push for increased mobility and longevity is the "unrelenting increases in the range, accuracy, and lethality of modern weapons" with peer competitors and rogue regimes possessing "the technical acumen and economic heft" to directly challenge U.S. forces and imperil U.S. interests (Berger, 2020). To combat the proliferation of long-range fire and smart weapons that negate current Navy and Marine Corps amphibious capabilities, US forces must persist within range of enemy fires. EABO, DMO, and Littoral Operations in a Contested Environment (LOCE) are the naval operating concepts that are shaping the ability to respond to those threats (Berger, 2020). Within these concepts, contingency planning has shown that logistical support, and as a subset, energy demand, is a critical requirement and vulnerability (Berger, 2020; E2O, 2011). This vulnerability is compounded by the insufficient amount of supply vessels currently employed, US private shipping available for surge operations, and qualified mariners to crew ships if they were available (Wakim, 2019).

"Since the Vietnam conflict, there has been a 175% increase in gallons of fuel consumed per" service member per day. This is due to an increase in vehicle weight, number of vehicles, and electricity demand from computers and other command and control equipment. These fuel requirements result in vulnerable supply chains, from convoys to fuel depots, and limits "range and freedom of maneuver from the sea and on land" (E2O, 2011). If experience from the conflict in Afghanistan shows anything, it shows not only the economic cost of maintaining supply lines, but costs in operational capability and human life. Our adversaries observed the impacts of targeting fuel and water convoys and will continue to do so (E2O, 2011).

Littoral forces, or forces conducting LOCE, need mobility and persistence while maintaining a low signature. This means minimal infrastructure and the ability to be sustained in an austere environment. Consequently, logistical support must operate with reduced forward-located stockpiles, capable of readjusting supply missions on the fly, and integrate at the tactical level with local "micro-purchases of goods and services." A force multiplier in this effort is leveraging host nation support to reduce the force's signature (USMC, 2021). Consequently, increasing energy efficiency of equipment and obtaining local fuel or energy would have significant advantages.

The DoD has and continues to identify climate change as a national security risk by degrading installations and infrastructure, diverting training and operational forces in response to extreme weather events, and destabilizing entire geopolitical regions (Crawford, 2019; Department of Defense Office of the Undersecretary of Defense (Acquisition and Sustainment), 2021). With current energy usage, the DoD significantly contributes to global warming with estimates of 59 million metric tons of CO_2-eq emitted

in 2017 alone. This is greater than the emissions of entire countries such as Finland, Sweden, and Denmark (Crawford, 2019). At the local tactical level, being good stewards of the environment promote better relations with the host nation, which enables further support (USMC, 2021). Investments in, or adoptions of, technology that promote efficiency gains and decreased emissions support mitigating climate change and complying with executive orders (Department of Defense Office of the Undersecretary of Defense (Acquisition and Sustainment), 2021; E2O, 2011). Specifically Executive Order 14008, which makes climate considerations an "essential element of United States foreign policy and national security" (Department of Defense Office of the Undersecretary of Defense (Acquisition and Sustainment), 2021).

While in 2020 the US was a petroleum product exporter, this has not always been the case. With the Organization of Petroleum Exporting Countries (OPEC) controlling 75% of the world's known oil reserves, it is likely exports will eventually dwindle ((U.S. EIA), 2021; E2O, 2011). With the destabilizing impacts of climate change and with many OPEC countries already "unstable or prone to conflict," any dependence on petroleum products leaves the DoD vulnerable to fluctuations in supply and price (E2O, 2011). As a result of the issues with most of OPEC's primary producers, the US, partly through the DoD and partly through other national powers, spends significant resources on protecting global oil supplies and trade routes (Crawford, 2019).

All the above points lead to seeking innovative energy capabilities that can support the paradigm shift of combating near peer capabilities by conducting LOCE, EABO, and DMO while maintaining or decreasing economic and environmental impacts.

LRUSV and Diesel

The proposed LRUSV is an 11 meter autonomous surface vessel powered by two Cummins QSB 6.7 diesel inboards and propelled by Hamilton HTX30 water jets (*40 Defiant*, 2020). The operational concept for the LRUSV is to operate in groups to provide reconnaissance and firing capabilities for batteries located ashore. To prevent interference and prolong on-station time, each LRUSV would likely proceed to a designated sector and loiter until they needed to be refueled (USMC, 2021).

While jet fuel is the most widely used fuel in the DoD, that is primarily because aviation consumes around 70% of its operational energy. The next primary fuel is diesel at approximately 18% (Crawford, 2019). It is used in tactical vehicles, generators, and environmental control units (E2O, 2011). Table 10 shows a review of studies that used diesel engines and found efficiencies around 25-38%. Of note, peak efficiencies were usually around 75% load and at the rated speed. This is because diesel engine efficiencies vary depending on engine speed, load, and fuel type (Tabatabaei et al., 2019; Yesilyurt, 2020).

Table 10: Literature Diesel Engine Efficiencies

Source	(Hosseinzadeh-Bandbafha et al., 2021)	(Shi et al., 2009)	(Viornery-Portillo et al., 2020)	(Yesilyurt, 2020)	(Tabatabaei et al., 2019)
Efficiency Range %	18-25	18-35	37	15-37	23.7-38
Cylinders	6	9	4	1	4
Usage	Tractor	Maritime	Generator	Generator	Dynamometer

The life cycle of diesel involves crude oil extraction, crude oil storage and transportation, refining the crude into diesel and other petroleum products, transportation and storage of diesel, and consumption (Koroneos et al., 2005). As a co-product, all the

environmental impacts of diesel prior to the completion of refinement are shared with the other desirable products that are obtained from crude oil, such as kerosene and gasoline. Figure 5 shows a basic life cycle diagram of diesel.

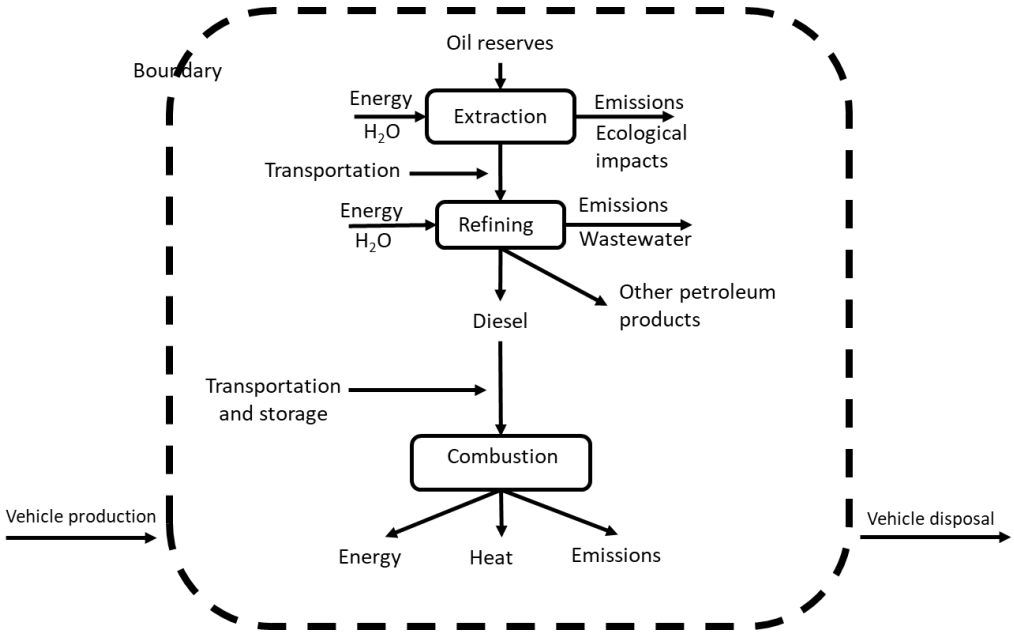

Figure 5: Diesel Life Cycle

(Reproduced using (Koroneos et al., 2005))

Emissions throughout the lifecycle vary depending on extraction method, such as fracking or drilling, transportation distances, and the engine. However, most literature agrees that the emissions from combustion are 81-85% of the total GWP of the life cycle (Comer & Osipova, 2021; Kinsel, 2010). Table 11 shows the GWP of diesel from different sources, adjusted to kg CO_2-eq/kWh. While other environmental impacts were reported in some of the literature, such as acidification, particulate matter, etc., they are not shown due to different methods of reporting based on the environmental assessment method used, as discussed previously.

Table 11: Literature Diesel Well-to-Combustion GWP

Source	(Hosseinzadeh-Bandbafha et al., 2021)	(US EPA, 2005)	(Smith et al., 2015)	(Comer & Osipova, 2021)	(Tabatabaei et al., 2019)	(Costa et al., 2021)
Combustion	0.524	0.703	0.76	-	0.67	-
Total Life Cycle	-	-	-	0.98	-	0.828
GWP units in kg-CO_2-eq per kWh						

Summary

This chapter discussed a hydrogen economy and the issues related to using hydrogen as a fuel source, activated aluminum, diesel, and why the military is searching for alternative fuels. The next chapter will discuss the methodology used to conduct the LCA, economic analysis, and how their respective inputs were determined.

III. Methodology

Chapter Overview

The purpose of this chapter is to discuss the methodology used to compare 1 kWh produced by combusting diesel in an internal combustion engine to 1 kWh produced from hydrogen, derived from reacting aluminum and water, in a fuel cell. First the methodology to determine diesel fuel consumption and prices is discussed. This is followed by determining hydrogen consumption in a fuel cell, how much hydrogen is produced from the reaction of activated aluminum and water, and the price of activated aluminum. Finally, the LCA methodology is explained.

Overview of Research Methodology

In order to compare the economic and environmental cost of energy that can be used for a specified purpose, e.g. providing power to a waterjet, it is necessary to analyze the fuel source used to provide that energy. This thesis explores the costs associated with obtaining 1 kWh from low-sulfur diesel to 1 kWh from hydrogen derived from the activated aluminum reaction. The economic analysis is a straight market value comparison between low sulfur diesel and the materials needed for activated aluminum. The environmental analysis uses GaBi, a LCA software produced by Sphera, to model the life cycle of diesel and hydrogen derived from activated aluminum. Then, using the LCIA method TRACI 2.1, environmental impact categories are monetized to provide an overall economic impact.

To compare two drastically different fuel sources, the functional unit must be equitable. In this case, 1 kWh of usable energy applied to the transmission prior to the

propulsion device of the LRUSV is the first equitable and comparable result of the fuel systems. From that equitable point, it is necessary to determine the amount of material used to create that energy, for this thesis, this is shown as kg/kWh. This quantity provides the ability to determine both the economic and environmental cost per kg and kWh. Of note, the unit kg/kWh was used in place of efficiency as that unit is easily input into GaBi without extra manipulation. Converting this unit to efficiency (%) is shown below, using Equation 6 (Harrison et al., 2010). The example calculation uses the LHV of diesel (ESSOM Co. LTD., 2019).

$$Electrical\ Efficiency\ (LHV) = \frac{\frac{1}{0.231\frac{kg}{kWh}}}{11.83\frac{kWh}{kg}} * 100 = 36.5\%$$

Within GaBi, there are multiple environmental impact assessment tools that convert the life cycle inputs into categorized environmental outputs. In this case, the TRACI 2.1 framework is used to compare the environmental impacts in eight different categories: global warming (kg-CO_2 eq), acidification (kg-SO_2 eq), ecotoxicity (CTUe), human health particulates (kg-PM 2.5 eq), human toxicity cancerous (CTUh), human toxicity noncancerous (CTUh), eutrophication (kg-N eq), and ozone depletion (kg-CFC 11 eq). TRACI 2.1 was used as it was developed and maintained by the EPA, provides consistent, comparable results, and is specific to North America and US policies (Bare, 2012).

Diesel Fuel Consumption and Pricing

Fuel consumption in combustion engines, as well as emissions, are highly dependent on the engine load, fuel properties, and engine specifications (Viornery-

Portillo et al., 2020). Consequently, to model fuel burn it was necessary to determine the operational profile of the LRUSV, the engine power output and associated fuel burn, and the power requirements of the LRUSV propulsion system. The operational profile was provided by the Marine Corps' LRUSV Capabilities Office and basically breaks down to 64% at idle range, 20% at cruise, and 16% at sprint or full throttle. This breakdown assumes a full mission profile. To determine the engine power output and associated fuel burn, linear interpolation was used with the Cummins engine performance chart in Table 12.

Table 12: Cummins Maritime Performance Curve

Speed	**Full Throttle**				**Propeller Demand**					
	Power		**Torque**		**Power**		**Torque**		**Fuel Consumption**	
rpm	kW	(hp)	N-m	(ft-lb)	kw	(hp)	N-m	(ft-lb)	L/hr	(gal/hr)
3375	404	542	1144	844						
3300	404	542	1170	863	404	542	1170	862.6	110.3	29.1
3200	404	542	1207	890	372	498.8	1110	818.6	98.4	26
3100	404	542	1245	918	341	457.8	1052	775.6	89.8	23.7
3000	404	542	1285	948	312	419	995	733.6	80.6	21.3
2900	404	542	1330	981	285	382.4	939	692.5	71.9	19
2800	402	540	1372	1012	259	347.8	885	652.4	65.4	17.3
2600	395	530	1452	1071	212	284.7	780	575.2	54.6	14.4
2400	385	517	1533	1131	171	229.4	681	502	43.8	11.6
2200	372	498	1613	1190	135	181.4	587	433	34.6	9.1
2000	355	476	1695	1250	105	140.2	499	368.2	27.4	7.2
1800	260	349	1382	1019	79	105.5	417	307.8	20.5	5.4
1600	167	224	995	734	57	76.8	342	252	15.1	4
1400	124	166	643	622	40	53.5	272	200.8	10.8	2.9
1200	92	124	733	541	26	35.3	209	154.5	7.6	2
1000	65	87	620	457	16	21.6	154	113.3	5.1	1.3
800	45	61	541	399	9	11.8	105	77.6	5	1.3
600	31	42	500	369	4	5.4	64	47.6	2.2	0.6

(Reproduced from (Cummins, 2013))

The provided propeller power demand and associated fuel burn, in L/hr, was used to determine the fuel consumption of the engine as it is loaded. The fuel consumption was

then divided by the power output and converted to kg of fuel to determine the kg/kWh.

An example calculation is shown below and the rest of the calculations are in Table 13.

Desired fuel burn engine power: 385 kW
Linear interpolation was used for finding the fuel burn between the propeller demand of 404 kW and 372 kW, with their respective fuel burns of 110.3 L/hr and 98.4 L/hr.

$$\frac{385-372}{404-372} * (110.3-98.4) + 98.4 = 103.234 \frac{L}{hr}$$

$$\frac{103.234 \frac{L}{hr}}{385\ kW} * \left(0.845 \frac{kg}{L}\right) = 0.227 \frac{kg}{kWh}$$

Table 13: Diesel kg/kWh

Propeller Demand			**Engine Speed and Power**				
Power (kW)	**Nm**	**Fuel**	**rpm**	**kw**	**L/hr**	**L/kWh**	**kg/kWh**
			3375	404			
404	1170	110.3	3300	404	110.3	0.273	0.231
372	1110	98.4	3200	404	110.3	0.273	0.231
341	1052	89.8	3100	404	110.3	0.273	0.231
312	995	80.6	3000	404	110.3	0.273	0.231
285	939	71.9	2900	404	110.3	0.273	0.231
259	885	65.4	2800	402	109.6	0.273	0.230
212	780	54.6	2600	395	107.0	0.271	0.229
171	681	43.8	2400	385	103.2	0.268	0.227
135	587	34.6	2200	372	98.4	0.265	0.224
105	499	27.4	2000	355	93.7	0.264	0.223
79	417	20.5	1800	260	65.7	0.253	0.213
57	342	15.1	1600	167	42.8	0.256	0.216
40	272	10.8	1400	124	32.0	0.258	0.218
26	209	7.6	1200	92	24.0	0.260	0.220
16	154	5.1	1000	65	17.1	0.263	0.222
9	105	5	800	45	12.1	0.268	0.227
4	64	2.2	700	37.5	10.2	0.273	0.230
			600	30	8.5	0.284	0.240

(Adapted from (Cummins, 2013))

To combine the operational profile with the engine's kg/kWh profile, a Monte Carlo simulation was used to determine the mean and standard deviation surrounding the

overall efficiency of the LRUSV when operated as predicted. This was necessary because the efficiency of internal combustion engines vary at different loads and speeds (Tabatabaei et al., 2019; Yesilyurt, 2020). In this case, with the operational profile requiring idling for 64% of the time, the average efficiency is decreased. Additionally, while the power charts give the fuel consumption based on propulsion requirements, the additional electrical load from accessories, such as radar, are unknown and beyond the scope of this thesis. Assuming different accessory operational times, a triangular distribution was simulated around idle efficiency, as the least efficient mode is at a no-load ground idle with increasing efficiency as the load increases, creating an upper limit. This was modeled in Excel using Equation 7 (Kotz & Rene van Dorp, 2004):

Where $a \leq m \leq b$, a is the left limit of the kg/kWh, b is the right limit, and y = a random number generator; rand() in Excel:

$$a + \sqrt{y(m-a)(b-a)}\ for\ 0 \leq y \leq \frac{m-a}{b-a}$$

$$b - \sqrt{(1-y)(b-m)(b-a)}\ for \frac{m-a}{b-a} \leq y \leq 1$$

Equation 7

(Adapted from (Kotz & Rene van Dorp, 2004))

A normal distribution was modeled around cruise as efficiency peaks around 2000-2200 rpm and quickly drops off either side. The model was created using a random number generator and normal distribution function in Excel with the mean and standard deviation taken from the efficiencies corresponding with the 1800 to 2600 rpm range. A normal distribution also assumes the LRUSV is governed by ground speed rather than rpm, which will make the efficiency and power setting variable based on currents and wind speed (Kragelund et al., 2013). Sprint, or full throttle, efficiency was taken as a point value due to the upper limit on fuel injection.

These distributions were combined with a Monte Carlo simulation that used random functions that fed into if, and, or functions in Excel that applied each distribution with the appropriate percentage of operation; 16% sprint, 20% cruise, and 64% idle. Equation 8 provides the logic with rand(1), rand(2) referencing separate random number generators:

For rand(1) ≤ 16%; Sprint point value
For 16% < rand(1) ≤ 80 %; Idle triangular distribution with a = 0.2266, m = 0.2395, b = 0.2398, y = rand(2)
For 80% < rand(1); Cruise normal distribution

Equation 8

This logic was applied for 20,000 iterations and an overall mean and standard deviation were determined using Excel functions. To verify the number of samples was sufficient, convergence was qualitatively determined by plotting a running average against a log n-axis, with n being the number of samples. The plot was visually confirmed to show convergence (Ballio & Guadagnini, 2004). The results were then used as the inputs for GaBi as the necessary amount of diesel to create 1 kWh.

Diesel Price

The cost of diesel was determined by compiling the Defense Logistics Agency's bulk fiscal year costs for ultra-low sulfur diesel 1 and 2 from 2009 to 2022, available in Appendix A. While commodity prices, in particular petroleum, show log-normal distributions, both a log-normal and normal distribution were used and resulted in similar results (OECD, 1993; Shih & Yu, 2010). Consequently, for simplicity, a normal distribution was assumed and the results were divided by 3.2 kg-diesel/gal to obtain a mean and variance for $/kg.

To determine the $/kWh of diesel, the calculated mean fuel efficiency in kg/kWh was multiplied by the mean $/kg and error was propagated with arithmetic calculations (Caldwell & Vahidsafa, 2020). Equation 9 shows the calculations used:

$$Mean: \frac{kg}{kWh} * \frac{\$}{kg} = \frac{\$}{kWh}$$

Standard deviation:

Where M = mean, V = Variance, and SD = Standard Deviation

$$SD_3 = M_3 * \sqrt{\left(\frac{SD_1}{M_1}\right)^2 + \left(\frac{SD_2}{M_2}\right)^2}$$ (Caldwell & Vahidsafa, 2020)

Equation 9

Hydrogen Consumption

To properly map the life cycle of obtaining 1 kWh from hydrogen derived from activated aluminum, it is necessary to determine how much energy is obtained from hydrogen and how much hydrogen is obtained from activated aluminum. Just like any fuel, each conversion from one state to another has its associated efficiencies.

Due to a lack of obtainable data from a hydrogen fuel cell system with an equivalent output necessary for the LRUSV, an Argonne National Laboratory study on a 2017 Toyota Mirai was used. The study was used in this thesis because the Toyota Mirai had a 90 kW capacity hydrogen fuel cell, the closest capacity to the LRUSV requirements found in the literature, the drivetrain is commercially available and could feasibly be applied to a marine application, and the study specifically tested the efficiency of the fuel cell system under various loads and environmental conditions (Lohse-Busch et al., 2018). The results of the study's efficiency to electrical output was adapted to Figure 6 (Lohse-Busch et al., 2018).

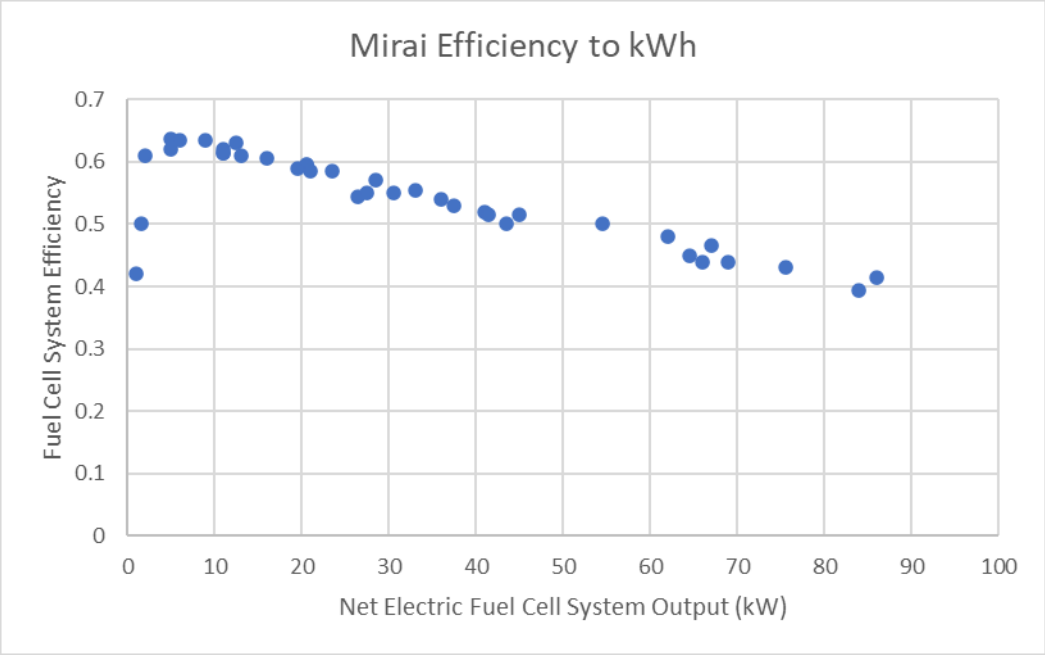

Figure 6: Argonne National Laboratory Toyota Mirai Efficiency
(Data obtained from (Lohse-Busch et al., 2018)**)**

To convert the efficiency to kg/kWh, the system output (kW) was divided by the efficiency to obtain the ideal output, or 100% efficiency. Then, using Equation 6 and the LHV of hydrogen, 33.32 kWh/kg, which was converted from 119.96 MJ/kg with 1 kWh equal to 3.6 MJ, the ideal output was divided by the LHV to obtain the kg of hydrogen used at each data point (Lohse-Busch et al., 2018). This amount was then divided by the system output to determine the final kg/kWh (Harrison et al., 2010). An example calculation is shown below with the compiled results in Table 14.

For a system output of 9 kW and the corresponding efficiency of 63.5%:

$$\frac{9\ kW}{0.635} = 14.17\ kW\ (ideal\ output)$$

$$\frac{14.17\ kW}{33.32\frac{kW}{kg}} = 0.425\ kgH_2\ (Mass\ H_2\ consumed\ to\ produce\ 9\ kW)$$

$$\frac{0.425\ kgH_2}{9\ kW} = 0.047\ \left(\frac{kgH_2}{kWh}\right)$$

Table 14: Fuel Cell kg/kWh

kW (system)	Efficiency	kW (potential)	kg-H2	kg / kWh
1	0.42	2.38	0.07	0.071
1.5	0.50	3.00	0.09	0.060
2	0.61	3.28	0.10	0.049
5	0.62	8.06	0.24	0.048
5	0.64	7.85	0.24	0.047
6	0.64	9.45	0.28	0.047
9	0.64	14.17	0.43	0.047
11	0.62	17.89	0.54	0.049
11	0.62	17.74	0.53	0.048
11	0.62	17.89	0.54	0.049
12.5	0.63	19.84	0.60	0.048
13	0.61	21.31	0.64	0.049
16	0.61	26.45	0.79	0.050
19.5	0.59	33.05	0.99	0.051
20.5	0.60	34.45	1.03	0.050
20.5	0.60	34.45	1.03	0.050
21	0.59	35.90	1.08	0.051
23.5	0.59	40.17	1.21	0.051
26.5	0.55	48.62	1.46	0.055
27.5	0.55	50.00	1.50	0.055
28.5	0.57	50.00	1.50	0.053
30.5	0.55	55.45	1.66	0.055
33	0.56	59.46	1.78	0.054
36	0.54	66.67	2.00	0.056
37.5	0.53	70.75	2.12	0.057
41	0.52	78.85	2.37	0.058
41.5	0.52	80.58	2.42	0.058
43.5	0.50	87.00	2.61	0.060
45	0.52	87.38	2.62	0.058
54.5	0.50	109.00	3.27	0.060
62	0.48	129.17	3.88	0.063
64.5	0.45	143.33	4.30	0.067
66	0.44	150.00	4.50	0.068
67	0.47	144.09	4.32	0.065
69	0.44	156.82	4.71	0.068
75.5	0.43	175.58	5.27	0.070
84	0.40	212.66	6.38	0.076
86	0.42	207.23	6.22	0.072

(Adapted from (Lohse-Busch et al., 2018))

Similar to the method used for diesel, the operational profile of the LRUSV was matched to the fuel cell efficiencies using a Monte Carlo simulation. However, unlike the simulation used for diesel, it was assumed that the efficiencies calculated for the power outputs that correspond to the operational profiles, such as idle, will stay relatively the same from the 90 kW fuel system to a 400 kW system. For instance, the cruise range for the 90 kW system provides 30 to 45 kW and the corresponding efficiencies are assumed to be similar for a 400 kW system operated at a mid-point power requirement. Then, based on the unknown power requirements of the accessory systems, a normal distribution was assumed around each operational point with their associated percentages. The normal distributions were modeled using the same normal distribution function in Excel used for the diesel cruise distribution. Equation 10 provides the logic for the simulation and the ranges of power outputs used to determine the means and standard deviations:

For rand(1) ≤ 16%; Sprint normal distribution (67-86 kW)
For 16% < rand(1) ≤ 80 %; Idle normal distribution (1.5-12.5 kW)
For 80% < rand(1); Cruise normal distribution (41.5-62 kW)

Equation 10

This logic was applied for 10,000 iterations then an overall mean and standard deviation was determined, using Excel functions. To verify the number of samples was sufficient, convergence was qualitatively determined the same way as diesel efficiency (Ballio & Guadagnini, 2004). The results were then used as the inputs for GaBi as the necessary amount of hydrogen to create 1 kWh.

Activated Aluminum Hydrogen Production and Pricing

To determine the amount of hydrogen derived from the activated aluminum, the data obtained from Johnathan Slocum's PhD study was used. Specifically, the mean and error around the mass of the spheres used in the reaction of activated aluminum and water, the mean percentage and error around the gallium-indium content in the spheres, and the mean and error around the yield of hydrogen from the reaction. Based on the study, activated aluminum yields 88.7% of the expected hydrogen from Equation 1, with a standard deviation of 1.8%. The spheres were 0.311g with a standard deviation of 0.003g and the percentage of mass of gallium-indium was an average of 3.55% with a standard deviation of 0.89% (Slocum, 2018; Slocum et al., 2020). All distributions were assumed to be normal and the resulting grams of hydrogen from each gram of activated aluminum were calculated in accordance with Equation 1 and the associated yield. Error was arithmetically propagated. The calculations follow the logic in Equation 11:

*Sphere mass * (1-GaIn%) = Aluminum Mass*
*Aluminum Mass * (mol-Al / 26.98 g-Al) = X mol-Al*
From Equation 1:
1 mol-Al = 3/2 mol-H_2
*X * (3/2) = Y mol-H_2 (ideal H_2 production)*
*Y mol-H_2 * (2.015 g-H_2 / mol-H_2) * (Average yield %) = g-H_2*
g-H_2 / g-sphere mass = g-H_2 / g-Activated Al

Equation 11

The resulting relationship between activated aluminum and hydrogen was used for inputs into GaBi as the quantity of hydrogen produced based on the amount of activated aluminum used in the reaction.

Hydrogen Price

The price of hydrogen derived from activated aluminum was calculated by combining the market costs of aluminum, gallium, and indium with the percentage by weight of the total mass to produce enough hydrogen for 1 kWh. The price of aluminum was obtained from St. Louis Federal Reserve Bank data that recorded the monthly price of aluminum per kg from the years 1990 to 2021. The prices of gallium and indium were obtained from the United States Geological Survey (USGS), which recorded the average annual cost of each element from the 1940's and 1930's to 2017, respectively. Additionally, for gallium and indium, the years of 2018 to 2021 were calculated from data obtained from www.tradingeconomics.com, which reported monthly averages for the mentioned years. Of note, the website only reported in Chinese Yuan (CNY) and was converted to dollars by the December 2021 exchange rate of 1 CNY to $0.16 (Reserve, 2021). Graphs showing the annual prices for each metal are available in Appendix B. Despite the availability of historical data, it was decided to only take pricing data from 2000 to 2021 for aluminum and 1990 to 2021 for gallium and indium. This was done to obtain a more current and accurate depiction of supply and demand and the associated variation in costs. An example is gallium with little production prior to its usefulness in electronics (Jaskula, 2021). Figure 7 shows the disparity in pricing from 1943 to 1990 and 1990 to present day (*Trading Econ.*, 2021; USGS et al., 2017).

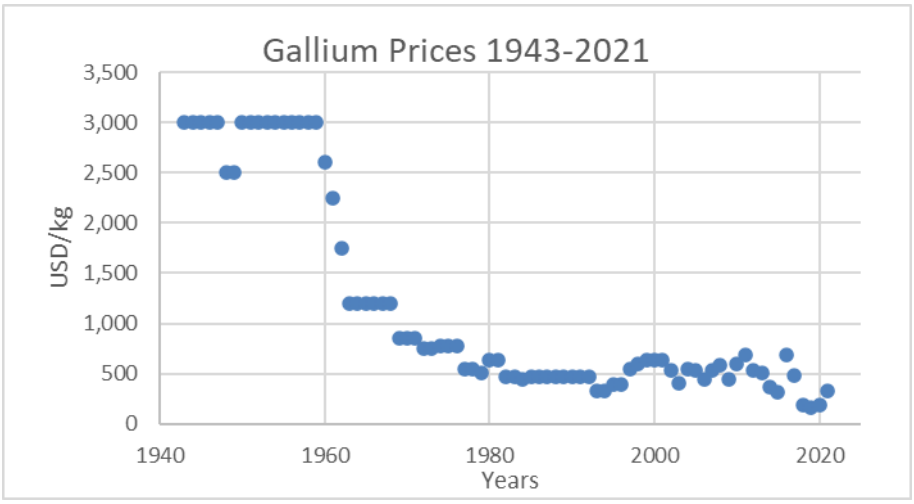

Figure 7: Gallium Price ($/kg)
(Data obtained from (*Trading Econ.*, 2021; USGS et al., 2017))

Based on the literature, commodity prices follow a log-normal distribution, so each element price distribution was assumed log-normal (OECD, 1993; Shih & Yu, 2010). This assumption seems validated as aluminum pricing has a skewness of 0.82 and the histogram seems to indicate a log-normal shape, seen in Figure 8 (Shih & Yu, 2010). Additionally, gallium and indium are right skewed with a skewness of 1.08 and 1.3, respectively. To obtain the log mean and standard deviation, the natural log of each data point was taken and the mean and standard deviation was calculated, using Excel functions. To calculate the cost of the activated aluminum and the $/kWh for this fuel, a Monte Carlo simulation was used to combine the log-normal distributions of the commodity prices and the normal distribution of activated aluminum mass and gallium-indium content.

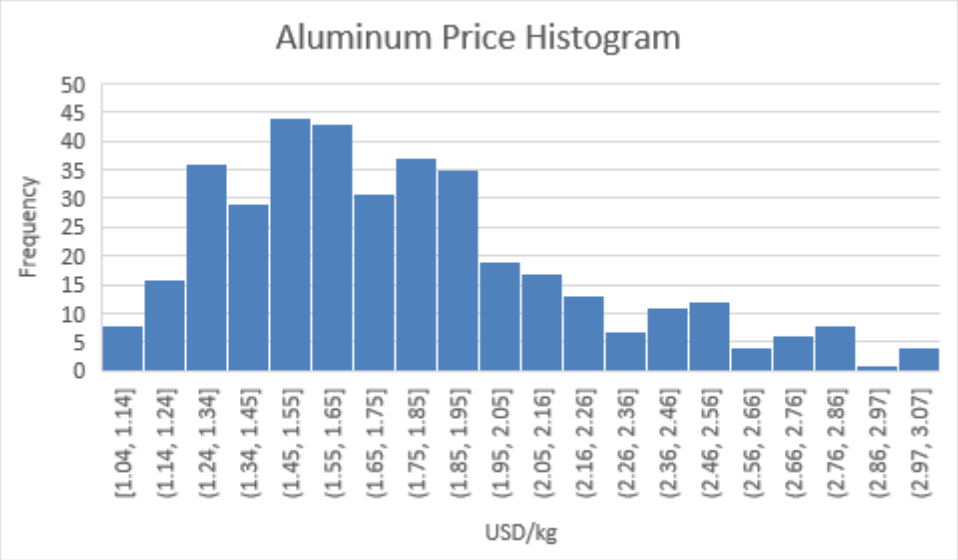

Figure 8: Aluminum Price Histogram
(Data obtained from (FRED, 2021))

The calculations, Excel functions, and logic used for the Monte Carlo simulation are shown in Equation 12 with the desired outputs in bold:

Total activated aluminum (ActAl) mass = Randomly generated number from a normal distribution using the mean and standard deviation of the mass of the ActAl sphere

*Al mass = ActAl mass *[1- (Randomly generated number from a normal distribution using the mean and standard deviation of the Ga-In content%)]*

*Ga mass = (ActAl mass – Al mass) * 0.8*

*In mass = (ActAl mass – Al mass) * 0.2*

*ActAl Price = (Randomly generated number from a log-normal distribution using the mean and standard deviation of the Al price) * Al mass + (Randomly generated number from a log-normal distribution using the mean and standard deviation of the Ga price) * Ga mass + (Randomly generated number from a log-normal distribution using the mean and standard deviation of the In price) * In mass*

*g-H_2 = (Al mass / 26.98 g/mol) * 3/2 * 2.0158 g/mol * (Randomly generated number from a normal distribution using the mean and standard deviation of the ActAl H_2 yield)*

kWh = g-H_2 / (Randomly generated number from a log-normal distribution using the mean and standard deviation of the Fuel Cell Efficiency)

$/kWh *= ActAl Price / kWh*
g-ActAl / kWh *= ActAl mass / kWh*

Equation 12

This logic was applied for 10,000 iterations and the mean and standard deviation were calculated using Excel functions. Convergence was again qualitatively determined by plotting a running average against a log n-axis for $/kWh (Ballio & Guadagnini, 2004). Additionally, the g-ActAl / kWh mean and standard deviation were used as an input for Gabi as the amount of activated aluminum needed to generate enough hydrogen for 1 kWh.

LCA and GaBi Modeling

In keeping with the ISO 14040 standards, the study consisted of defining the goal and scope of the assessment, conducting the inventory analysis, assessing the environmental impacts, and interpreting the impact of each category (ISO, 2006a). The inventory analysis and environmental impact assessment were conducted via GaBi, the Ecoinvent database, and TRACI 2.1 LCIA methodology that is integrated into GaBi. Interpretation of the results was conducted by monetizing each environmental impact category and determining which scenario had the least impact.

As previously stated, the goal of this LCA is to compare the environmental impacts of using diesel fuel, as opposed to hydrogen derived from the reaction of aluminum and water, to support military operations in the Western Pacific. The overarching purpose of the study is to provide researchers and decision makers the ability to make informed choices about investments and further research. Other than diesel usage, several activated aluminum scenarios are compared, shown in Table 15, with each

scenario showing the impacts of different recycled content used for aluminum, gallium, or indium. Scenario 1 is the most likely, based on global aluminum recycling and eutectic recovery rates, Scenario 2 is ideal, Scenario 3 is worst case, Scenario 4 shows mid-range, and Scenario 5 shows normal aluminum recycling and best case eutectic recovery (Godart & Hart, 2020; Graedal et al., 2011).

With aluminum hydroxide's molecular weight of 78 g/mol, the spent fuel is heavier than activated aluminum, at 28.8 g/mol. Using Equation 1, and a perfect reaction, 1 kg of aluminum becomes 1.4 kg of aluminum hydroxide. With this, considering the actions necessary to separate the eutectic from the aluminum hydroxide after the reaction is complete, and the logistical cost of removing material from a contested area, recovering the eutectic seems impractical. This logic leads to Scenario 1 as the most likely.

Table 15: Activated Aluminum Recycled Content Scenarios

	Recycled Content Scenarios				
Metal	1	2	3	4	5
Aluminum	35%	90%	10%	50%	35%
Gallium	1%	95%	1%	50%	95%
Indium	1%	95%	1%	50%	95%

The scope for both fuels encompasses the environmental impacts from raw material extraction to energy conversion or combustion. Due to a lack of data on a system that can continuously run from activated aluminum, the vehicles and engines that use the fuel are not considered; nor is packaging or unique transportation considerations. Specifically, activated aluminum's need to be sealed as it is reactive with water (Slocum, 2018). Figure 9 shows the system boundary for activated aluminum, with all major processes and materials. Anything with a dashed line, such as zinc smelting, is outside of

consideration. Not shown, for simplicity, are all the other inputs and outputs for each process such as energy, transportation, emissions, or waste products, other than the final reaction and energy conversion stage. Figure 5 shows the same for diesel. Appendix C and Appendix D show the activated aluminum and diesel plans, respectively, with all processes, transportation, and steps that were used to create the respective models in GaBi.

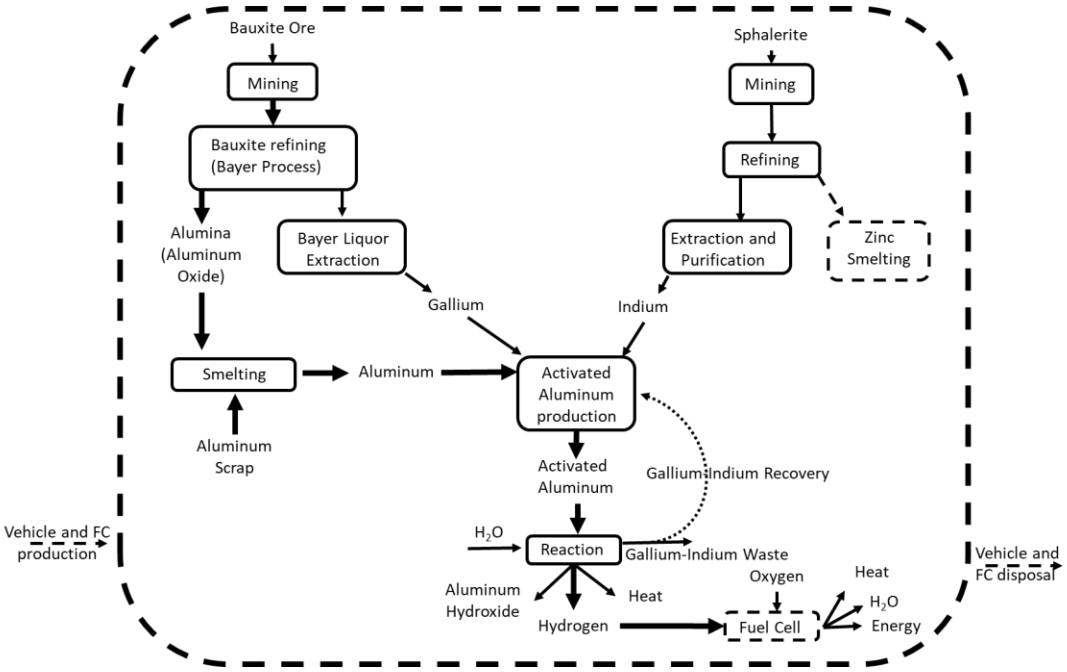

Figure 9: Activated Aluminum System Boundary

As previously stated, the functional unit is 1 kWh. This allows for comparison between the energy produced from a hydrogen fuel cell and a diesel engine despite being very different methods of energy conversion. Additionally, as either fuel can be used to power a vehicle or generator, it allows for a more versatile comparison, outside of the LRUSV.

The following discusses transportation assumptions that were used to develop the life cycle models in GaBi. With Australia containing a significant portion of global

bauxite reserves, proximity to the theater of interest, and current national relationship, it was assumed that aluminum and gallium would be produced and procured from within Australia ((Department of State), 2022). While gallium is not produced at commercial quantities in Australia, it has the potential for 416 kt of reserves due to its bauxite deposits (Yellishetty et al., 2017). The developed model has bauxite produced in the Alcoa bauxite mine in Western Australia, converted to alumina, and transported 3,500 km via rail to the Portland aluminum smelter. The aluminum is then transported 3,700 km via rail to Darwin. Gallium is transported 3,700 km via rail from Alcoa to Darwin. As indium is produced in Canada, with deposits in the US, it was assumed that indium was shipped from the United States to Darwin, a distance of 13,000 km (USGS, 2020). Railroad distances were calculated using a combination of railroad map data and Google Earth (Google, 2021; *Made with Natural Earth*, 2021; Reichert, 2021).

With the assumption of operations in the Western Pacific, it was assumed that the activated aluminum was produced in Darwin then shipped where necessary. The distance between Darwin and Okinawa, 4,500 km, was used as a surrogate for different distribution points as the predicted operational areas are unknown and Okinawa has a significant US military presence. All shipping distances were calculated using a combination of shipping lane data and Google Earth (Clark et al., 2021; Google, 2021).

With approximately “42 percent of Japan’s maritime trade” passing through the South China Sea and Japan’s reliance on oil from the Middle East, a potential conflict with China would make sourcing fuel from Western Pacific countries unlikely ((PE International AG), 2012; China Power Team, 2021). Additionally, considering that the

US is currently an oil exporter, it was assumed that diesel would be shipped from California to Okinawa, a distance of 10,300 km ((U.S. EIA), 2021).

GaBi's databases and user interface allow for an intuitive development of the inventory analysis. Each process, such as aluminum smelting, has its own inputs and require attaching the appropriate flows, or inputs. For example, aluminum smelting requires alumina, an anode, electricity, and various other fuels for powering the process; which in turn have their own inputs ((PE International AG), 2012). However, due to the education license obtained for GaBi and the unique combination of materials to activate aluminum, several processes were not available and had to be manually created. Gallium and indium production were two such processes. These were manually created with data from the Ecoinvent database. Table 16 shows all the manually created processes, where the data was obtained, and specific notes.

Table 16: GaBi Model User Created Processes

Process	**Data Origin**	**Notes**
Activated Aluminum Production	(Davidson, 2016; Slocum, 2018)	Content of metals 96.5% Al and 3.55% eutectic. Energy required to heat to 120ºC for 120 minutes is based on specific heat of the metals and 56% efficient oven.
Activated Aluminum Reaction	(Godart et al., 2021)	430 kJ/mol-Al of excess heat produced during the reaction
Aluminum Recycle Mix	(Graedal et al., 2011)	Placeholder that allows for varying the recycled content of aluminum
Electricity from Diesel Generator	Ecoinvent	Directly from Ecoinvent database (Menard, 2021)
Fuel Cell Reaction	Author calculations	Fuel cell produces 8.9 kg of water per kg of fuel (Montero-Sousa et al., 2020)
Gallium	Ecoinvent	Directly from Ecoinvent database (Tuchschmid, 2021)
Gallium Recycle Mix	(Graedal et al., 2011)	Placeholder that allows for varying the recovered content of gallium
Indium	Ecoinvent	Directly from Ecoinvent database

		(Classen, 2021)
Indium Recycle Mix	(Graedal et al., 2011)	Placeholder that allows for varying the recovered content of indium
Recycled Gallium	(Slocum, 2018; Szepessy & Thorwid, 2018)	Centrifuge the activated aluminum to recover excess eutectic. Energy requirements for centrifuge use is 1.4 kWh/m^3.
Recycled Indium	(Slocum, 2018; Szepessy & Thorwid, 2018)	

Additionally, flows have different emissions based on specific regions. This allowed for developing the model with regional considerations. Specifically, the crude oil mix for diesel generation in the US and electricity generation mix for power in Australia. The model uses 2016 data for diesel generation with the US producing 53% of its own crude oil; importing 19.3% from Canada, 19% from OPEC countries, and the remainder from various non-OPEC countries ((PE International AG), 2012; (U.S. EIA), 2021). The model also uses 2016 data for Australia's electricity generation mix with 44.6% coal, 19% lignite, 19.7% natural gas, and the remainder a mix of hydro, wind, photovoltaic, heavy fuel oil, biomass, and biogas, in descending order of contribution ((PE International AG), 2012).

The LCIA methodology selected was TRACI 2.1. It was selected because the intended audience is US government employees, the program was developed with US specific considerations, and it was current and available on both GaBi and Simapro (Bare, 2012; PE International AG, 2012; Pré, 2021). Using the provided Monte Carlo analysis tool in GaBi, each scenario ran for 2,000 iterations with the recycled content for aluminum, gallium, and indium as the variables. Each environmental impact category generated by GaBi, as shown in Table 1, was then monetized to provide a straightforward comparison between diesel and the scenarios. The monetary value used for each category is listed in Table 17. Most values were obtained from the European Union Environmental

Prices Handbook and adjusted for currency conversion and inflation. With values in 2015 Euros, they were converted to 2015 US dollars (USD), by the average 2015 conversion rate of 1.108 USD to 1 Euro, and adjusted to 2021 USD using 18% inflation ((US Bureau of Labor), 2021; Reserve, 2021; Turner et al., 2019).

Due to differences in units, some values were not available in the Environmental Prices Handbook, specifically the human health cancerous, human health noncancerous, ecotoxicity, resource depletion, and smog categories. Based on the literature, CTUh is equivalent to 11.5 disability-adjusted life years (DALY) for cancerous and 2.7 DALY for noncancerous (Fantke et al., 2017). These multipliers were applied to the DALY monetary range in the Environmental Prices Handbook to obtain the cancerous and noncancerous human health values.

Resource depletion values were taken from an environmental impact monetization review that evaluated and converted values from several monetization methods to 2019 Euros. The lowest and highest values stated were used for the respective lower and upper values with the overall average taken as the central (Arendt et al., 2020). These values were converted to 2019 USD, by the average 2019 currency exchange rate of 1.12 USD to 1 Euro, and adjusted to 2021 USD using 8% inflation ((US Bureau of Labor), 2021; Reserve, 2021). The same reference and method were used for the ecotoxicity unit, CTUe.

Smog formation in the Environmental Prices Handbook has the unit of kg NMVOC-eq, which is not equitable to the TRACI 2.1 unit. A document from Canada's Victoria Transport Policy Institute references the impacts of ground level ozone as a combination of deleterious effects on human health, agricultural crops, and building

materials. These impacts accrue for a total cost of $1.739 per kg of O_3 in 2005 Canadian dollars (Litman & Doherty, 2011). This price was converted to 2005 USD, by the average 2005 currency exchange rate of 1 USD to 1.216 Canadian dollar, and adjusted to 2021 USD using 43% inflation ((US Bureau of Labor), 2021; Reserve, 2021).

Table 17: Environmental Category Prices

Category	Unit	Lower	Central	Upper	Source
Global Warming	$/kg CO_2-eq	$0.029	$0.075	$0.123	(de Bruyn et al., 2018)
Acidification	$/kg SO_2-eq	$10.854	$15.039	$23.409	(de Bruyn et al., 2018)
Ecotoxicity	$/CTUe	$0.0001	$0.007	$0.015	(Arendt et al., 2020)
Eutrophication	$/kg N-eq	$13.08	$22.89	$32.96	(de Bruyn et al., 2018)
Human Health Particulate Matter	$/kg $PM_{2.5}$-eq	$36.23	$50.61	$77.81	(de Bruyn et al., 2018)
Human Health Cancerous	$/CTUh	$751,964	$1,052,749	$1,654,320	(de Bruyn et al., 2018; Fantke et al., 2017)
Human Health Noncancerous	$/CTUh	$176,548	$247,167	$388,406	(de Bruyn et al., 2018; Fantke et al., 2017)
Ozone Depletion	$/kg CFC-11 eq	$170	$400	$659	(de Bruyn et al., 2018)
Resource Depletion (fossil fuel)	$/MJ	$0.0001	$0.010	$0.027	(Arendt et al., 2020)
Smog Formation	$/kg O_3-eq	$1.099	$2.045	$2.406	(de Bruyn et al., 2018; Litman & Doherty, 2011)

Due to the lower, central, and upper monetary values of each category, besides the point value of smog formation, a triangular distribution was assumed. To combine this distribution with the normal distribution of the environmental impact results, a Monte Carlo simulation with 5,000 iterations was used to determine the mean and standard deviation surrounding each monetized result. Like previously discussed Monte Carlo

simulations, the logic used Equation 7 with a, m, b, and y equating to the lower, central, upper, and random values, respectively. The random result of the triangular distribution was then multiplied by a randomly generated number based on the normal distribution of the associated environmental impact category. Convergence was qualitatively determined by plotting a running average against a log n-axis for several categories. Each monetary value was then combined to provide a total environmental cost per scenario.

Summary

The methodology used for this thesis required developing a LCA model on GaBi, applying monetary values to the LCIA methodology results, and determining the market value for each fuel. These steps required determining the consumption rates of each fuel and the amount of hydrogen obtained from the activated aluminum reaction. Chapter Four will discuss the results of each step.

IV. Analysis and Results

Chapter Overview

This chapter discloses and analyzes the results of the research. First, the efficiency and price of diesel is discussed, followed by the diesel LCA and LCIA. Next, the efficiency for hydrogen fuel cells is discussed, which leads into determining the amount of hydrogen obtained from the reaction of activated aluminum with water. Then the results from the LCA and LCIA for activated aluminum are revealed. From there, the prices for aluminum, gallium, and indium are used to determine the economic cost for activated aluminum. The LCIA and economic results are combined to compare how each scenario economically and environmentally compares to each other and diesel. This is followed by a brief discussion on logistical considerations. Finally, areas of potential improvement to lessen activated aluminum's environmental and economic impacts are introduced.

Diesel Results

Using the Monte Carlo simulation for diesel fuel efficiency, as described in the previous chapter, the mean was determined to be 0.232 kg/kWh. Additional statistical results are in Table 18. Using Equation 6, the LHV for diesel, and converting this quantity to percentage, it equates to 36.4% efficiency. While on the high side of the efficiencies found in the literature, shown in Table 10, it is a reasonable result. Particularly as most of the literature tested actual engines and this data was pulled from the manufacturer's power charts, which report ideal results.

Figure 10 shows a histogram of the simulation, which when compared to Figure 11, highlights the fuel injection limit that was modeled as a point value for the sprint or full throttle profile of the LRUSV. Also apparent is the triangular distribution as the rpm decreases towards idle, with increasing kg/kWh. After several thousand iterations the simulation appears to converge to the mean, shown in Appendix E. The mean and standard deviation were used as inputs for the diesel model in GaBi and to determine the $/kWh.

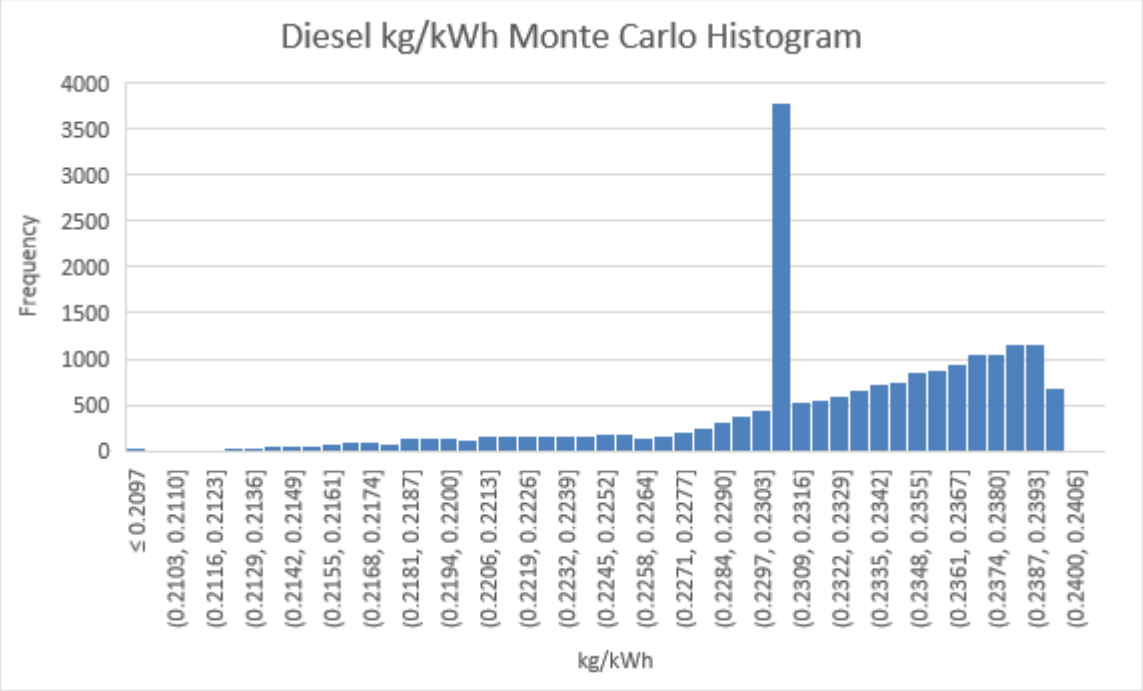

Figure 10: Diesel kg/kWh Histogram

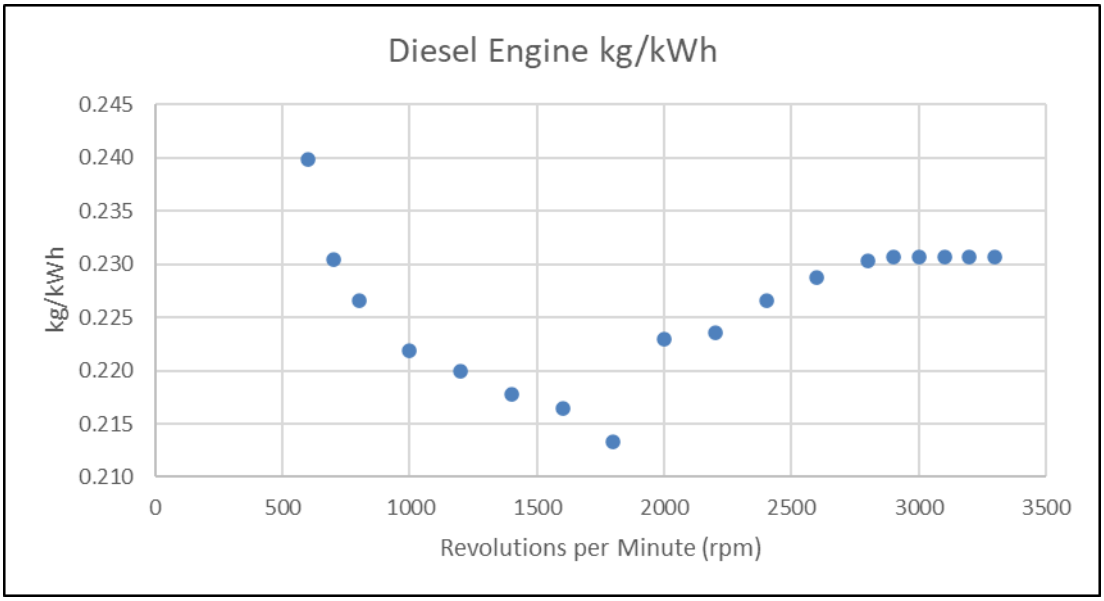

Figure 11: Diesel Engine kg/kWh versus rpm

(Data obtained from (Cummins, 2013))

After determining the average price per gallon for diesel and converting gallons to kg, Equation 9 was used to determine the standard deviation and cost of energy for diesel fuel. The results are also shown in Table 18.

Table 18: Diesel kg/kWh and $/kWh Results

Statistic	kg / kWh	$ / gal	$ / kg	$ / kWh
Mean	0.232	3.07	0.958	0.222
Standard Deviation	0.006	0.58	0.181	0.042
Median	0.233	2.91	0.908	0.212
Minimum	0.200	2.18	0.681	0.136
Maximum	0.247	4.07	1.272	0.314

The environmental category impact results from the GaBi LCA model are shown in Table 19. When comparing the results to Table 11, the value for global warming matches the literature. Breaking the results down further, 0.74 kg CO_2-eq or 85% of the total 0.873 kg CO_2-eq is from combustion, which also matches the literature. For further comparison, a model was developed in SimaPro with the results giving a GWP of 0.863

kg CO_2-eq. Further SimaPro results are shown in Appendix F. Of note, the GWP category is prioritized because it is the most discussed in the literature and has the most consistent calculation methods that result in the unit of CO_2-eq. The other environmental impact criteria are not discussed as all the different environmental evaluation processes use varying types of units and calculation methods. Also shown in Table 19 are the results of using a Monte Carlo simulation, as previously discussed, to monetize the categories with the values in Table 17. To confirm there were sufficient iterations, an evaluation for convergence was conducted and, shown in Appendix E, 5,000 iterations appear sufficient.

Table 19: Diesel LCA and LCIA Results

		TRACI 2.1		**Monetized Values (USD 2021) / kWh**	
Category	**Unit / kWh**	Mean Values	Standard Deviation	Mean Values	Standard Deviation
Global Warming	kg CO_2-eq	0.873	0.026	0.066	0.017
Acidification	kg SO_2-eq	4.19E-03	1.27E-04	0.069	0.011
Ecotoxicity	CTUe	0.129	3.88E-03	9.58E-04	3.84E-04
Eutrophication	kg N-eq	3.92E-04	1.18E-05	9.01E-03	1.61E-03
Human Health Particulate Matter	kg $PM_{2.5}$-eq	3.02E-04	9.18E-06	0.017	2.63E-03
Human Health Cancerous	CTUh	1.16E-09	3.49E-11	1.34E-03	2.20E-04
Human Health Noncancerous	CTUh	4.55E-08	1.37E-09	0.012	2.03E-03
Ozone Depletion	kg CFC-11 eq	9.03E-17	2.72E-18	3.71E-14	9.05E-15
Resource Depletion (fossil fuel)	MJ	1.600	0.047	0.019	0.009
Smog Formation	kg O_3-eq	0.141	4.26E-03	0.261	0.040
			Total	**0.456**	**0.022**

(Data obtained from ((PE International AG), 2012))

Hydrogen Fuel Cell Results

Using the Monte Carlo simulation to determine the efficiency of the fuel cell, as described in the previous chapter, the mean was 0.0548 kg/kWh. Additional statistical

results are in Table 20. Using Equation 6, the LHV for hydrogen, and converting this quantity to percentage, it equates to 54.8% efficiency. This is well within the efficiencies found in the literature, shown in Table 4, if a little on the high side. The higher average efficiency is due to the predominance of time spent at idle, the most efficient profile for a fuel cell (Lohse-Busch et al., 2018). This is apparent when comparing Figure 12, a histogram of the simulation, to Figure 6, the Mirai fuel cell efficiency graph, as the fuel burned per kWh increases as the load increases and the histogram shows the distinct increase in frequency at each kg/kWh for the idle, cruise, and sprint ranges, in descending order. After several thousand iterations the simulation appears to converge to the mean, shown in Appendix E. The mean and standard deviation were used as inputs for determining how much activated aluminum is needed to produce 1 kWh and as an input into the model in GaBi.

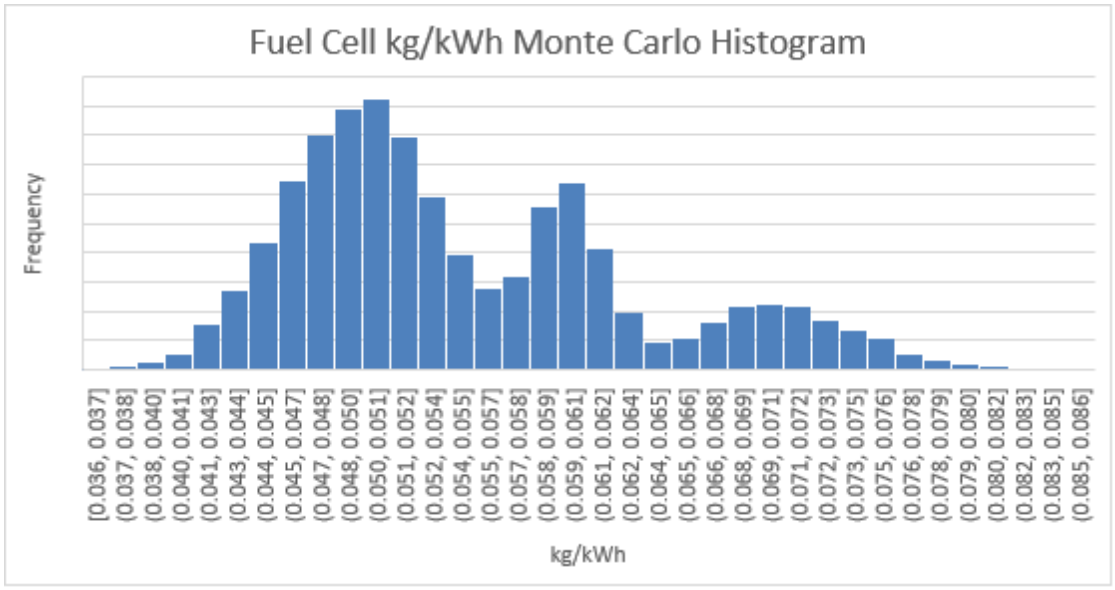

Figure 12: Fuel Cell kg/kWh Histogram

Activated Aluminum Results

Using the Monte Carlo simulation for activated aluminum as previously discussed, the mean price per mass of activated aluminum was $17.99/kg-ActAl, the mean mass of activated aluminum per energy unit was 0.571kg-ActAl /kWh, and the price per kWh from activated aluminum was $10.38/kWh. Additional statistics, as well as the average prices of each metal, are available in Table 20. Comparing these results to a different study, the amount of aluminum needed to create 1 kWh was assumed as 0.454 kg-Al/kWh (Godart & Hart, 2020). Assuming 3.55% eutectic by weight, this equates to 0.471 kg-ActAl/kWh, which is within two standard deviations of the mean in this report. For the cost estimates in Table 20, they reflect the market price of the materials, they do not consider recovering any of the eutectic once the reaction is complete or substituting scrap aluminum, obtained at a lower price, for primary aluminum. A separate study using 2019 values of metals determined the cost of activated aluminum as $11.90/kg, which is within one standard deviation of this thesis' mean (Godart et al., 2021). Then, the mean and standard deviation for mass of activated aluminum per kWh was used as an input for the LCA model in GaBi.

Table 20: Hydrogen and Activated Aluminum kg/kWh and $/kWh Results

Statistic	**kg-H_2 / kWh**	**USD_{2021} / kg-Al**	**USD_{2021} / kg-Ga**	**USD_{2021} / kg-In**	**USD_{2021}/kg-ActAl**	**kg-ActAl / kWh**	**USD_{2021} / kWh**
Mean	0.0548	1.92	474.93	389.25	17.99	0.571	10.30
Standard Deviation	0.0087	0.41	184.31	253.34	6.92	0.091	4.38
Median	0.0524	-	-	-	16.85	0.571	9.55
Minimum	0.0356	-	-	-	4.05	0.277	2.02
Maximum	0.0852	-	-	-	75.24	0.942	49.79

Evaluating the histogram for the price per kWh, shown in Figure 13, the log-normal influence of the metal values is readily apparent. Conversely, and as expected, the histogram for the mass of activated aluminum needed to generate 1 kWh, shown in Figure 14, shows a normal distribution. When each characteristic was evaluated for convergence, it was apparent that several thousand iterations were sufficient. These convergence charts are available in Appendix E.

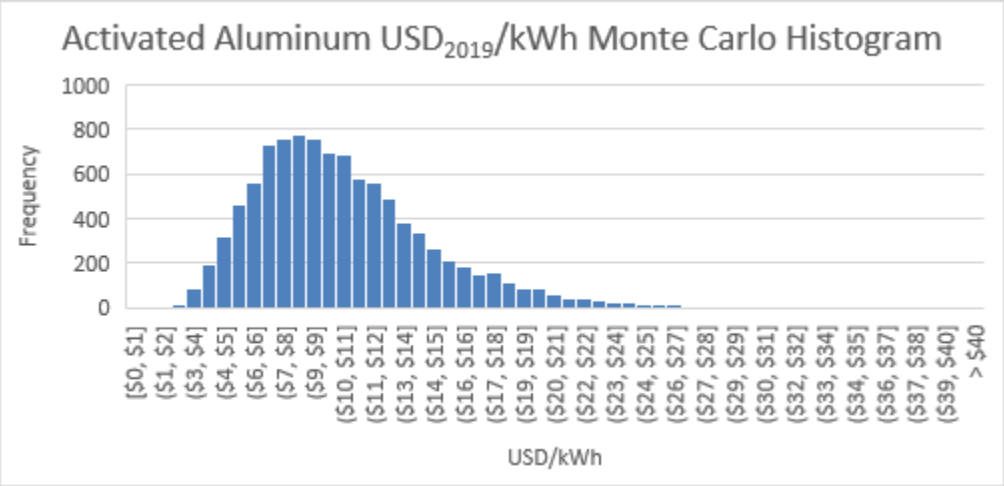

Figure 13: Activated Aluminum USD/kWh Histogram

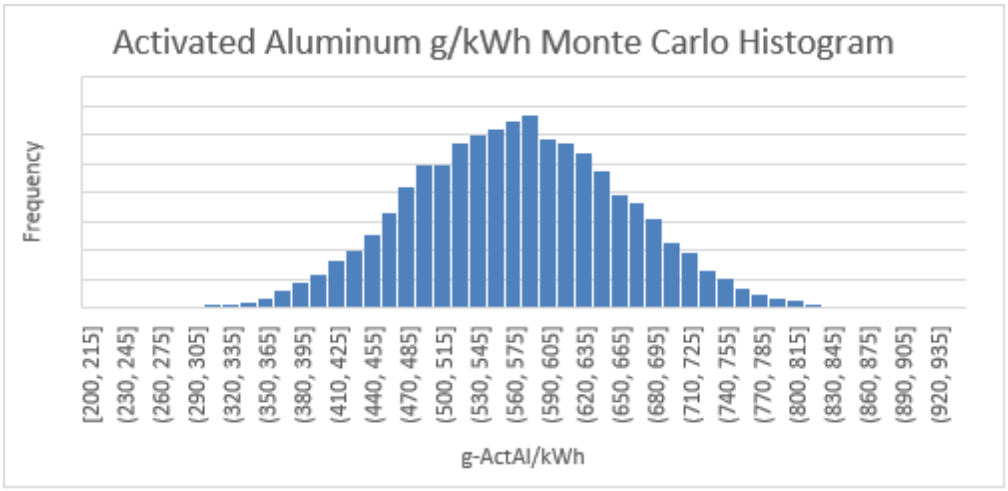

Figure 14: Activated Aluminum g/kWh Histogram

The environmental category impact results from the GaBi LCA model are shown for each scenario in Table 21. When comparing the results of Scenario 1, the author's assumed most likely, to Table 7 and the CO_2-eq impacts of gallium and indium, the value for global warming, 9.28 kg CO_2-eq, equates with the literature. Breaking the results down further, approximately 75% of the total GWP of activated aluminum is from primary aluminum production. Then, 74% of primary aluminum production's GWP is from electricity generation, which also matches the literature. For further comparison, a model was developed in SimaPro with the results giving a global warming potential of 12.6 kg CO_2-eq. The higher amount is due to issues with applying regional characteristics in SimaPro, leading to differences in power generation mixes and the resulting emissions. However, 74% of the total GWP is from primary aluminum production, which matches the literature. Further SimaPro results are shown in Appendix F. Table 21 shows the results of using a Monte Carlo simulation, as previously discussed, to monetize the categories. An evaluation for convergence, shown in Appendix E, was conducted on Scenario 1's GWP category and 5,000 iterations appear sufficient.

Table 21: Activated Aluminum LCA and LCIA Results

		TRACI 2.1									
		Scenario 1		Scenario 2		Scenario 3		Scenario 4		Scenario 5	
Category	Unit/kWh	Mean	Monetized	Mean	Monetized	Mean	Monetized	Mean	Monetized	Mean	Monetized
Global Warming	kg CO_2-eq	9.280	0.700	1.780	0.135	12.400	0.936	7.060	0.533	8.610	0.650
Acidification	kg SO_2-eq	0.043	0.700	0.008	0.136	0.058	0.948	0.033	0.541	0.041	0.681
Ecotoxicity	CTUe	0.400	0.003	0.058	0.000	0.504	0.004	0.289	0.002	0.285	0.002
Eutrophication	kg N-eq	0.001	0.026	0.0003	0.006	0.002	0.035	0.001	0.020	0.001	0.025
Human Health Particulate Matter	kg $PM_{2.5}$-eq	0.004	0.195	0.001	0.036	0.005	0.265	0.003	0.150	0.003	0.191
Human Health Cancerous	CTUh	3.7E-09	0.004316	5.0E-10	0.000576	4.7E-09	0.005455	2.7E-09	0.003112	2.7E-09	0.003105
Human Health Noncancerous	CTUh	3.2E-07	0.087	4.6E-08	0.012	4.0E-07	0.109	2.3E-07	0.063	2.2E-07	0.061
Ozone Depletion	kg CFC-11 eq	4.8E-10	1.96E-07	7.6E-11	3.13E-08	6.6E-10	2.72E-07	3.7E-10	1.5E-07	4.8E-10	1.97E-07
Resource Depletion	MJ	18.300	0.222	2.960	0.035	23.400	0.285	13.500	0.165	14.100	0.171
Smog Formation	kg O_3-eq	0.510	0.944	0.119	0.221	0.680	1.263	0.399	0.739	0.493	0.913
Total (USD_{2021}/kWh)			2.88		0.58		3.85		2.22		2.70
Standard Deviation			0.24		0.09		0.32		0.18		0.22

Data obtained from ((PE International AG), 2012))

Observing the difference between Scenario 1 and 5 in the table above, where the aluminum recycled rate remained constant and gallium and indium recovery rates changed from 1% to 95%, it is clear the amount of recycled aluminum content has the greatest impact on the environmental categories, which is intuitive as it has the greatest mass.

Economic Analysis and Comparison

To obtain a price for each scenario, the scenario specific aluminum recycling and eutectic recovery percentages were applied to the mean cost of the respective metal quantities needed to produce 1 kWh. For this, eutectic recovery was assumed to have negligible cost while aluminum recycling rates were assumed to bear the cost of scrap aluminum at $1.01/kg (Godart et al., 2021). For example, in Scenario 1, 65% of the aluminum is priced at the market mean and the remaining 35% costs the scrap price. The

eutectic price, with a 1% recovery rate, costs 99% of the market mean. This was applied for all the scenarios with the prices for the respective metals and total cost per kWh shown in Table 22. Observing the economic totals for each scenario, diesel is the cheapest option. From there, eutectic recovery has the biggest impact between the scenarios. A similar reduction in cost with eutectic recovery was also observed in the literature with a 95% recovery rate of eutectic reducing the cost from $11.90/kg to $2.88/kg, or $1.64/kWh (Godart et al., 2021).

Table 22: Economic and Environmental Impact Summation

	Economic Analysis (USD_{2021}/kWh)					
	Scenario 1	**Scenario 2**	**Scenario 3**	**Scenario 4**	**Scenario 5**	**Diesel**
Aluminum	0.88	0.61	1.01	0.81	0.88	-
Gallium	7.69	0.39	7.69	3.88	0.39	-
Indium	1.56	0.08	1.56	0.79	0.08	-
Economic Total	10.13	1.07	10.25	5.48	1.35	0.22
Environmental Impact Total	2.88	0.58	3.85	2.22	2.70	0.46
Economic and Environmental Sum	12.95	1.65	14.04	7.67	4.05	0.68
Standard Deviation	3.136	0.018	3.147	1.581	0.303	0.047

For a more complete comparison between the activated aluminum scenarios and diesel, the monetized sum of each environmental category was combined with the economic sum. Table 22 shows the resulting means and standard deviations. Diesel has the least total impact with the best-case activated aluminum scenario, Scenario 2, still having more than double the total cost. For another perspective on Scenario 2, in comparison to Table 3, which compares different hydrogen generation methods, to

produce 1 kg-H_2 with activated aluminum, it costs $19.56 and produces 32.2 kg CO_2-eq, which is well above any other method in price and CO_2-eq production.

Figure 15, the graphical representation of Table 22, with error bars indicating one standard deviation, shows the impacts from activated aluminum are sensitive to the amount of recycled aluminum used and the amount of eutectic recovered. Specifically, comparing the environmental results of scenarios two and five, where aluminum recycled content is decreased from 90% to 35%, there is a 26% increase in cost and a 365% increase in environmental impacts. Conversely, when comparing scenarios one and five, where eutectic recovery is increased from 1% to 95%, there is an 87% reduction in cost and a 6% decrease in environmental impacts. This represents that the environmental impact is highly sensitive to the percentage of aluminum recycled content while the economic impact is highly sensitive to eutectic recovery rates.

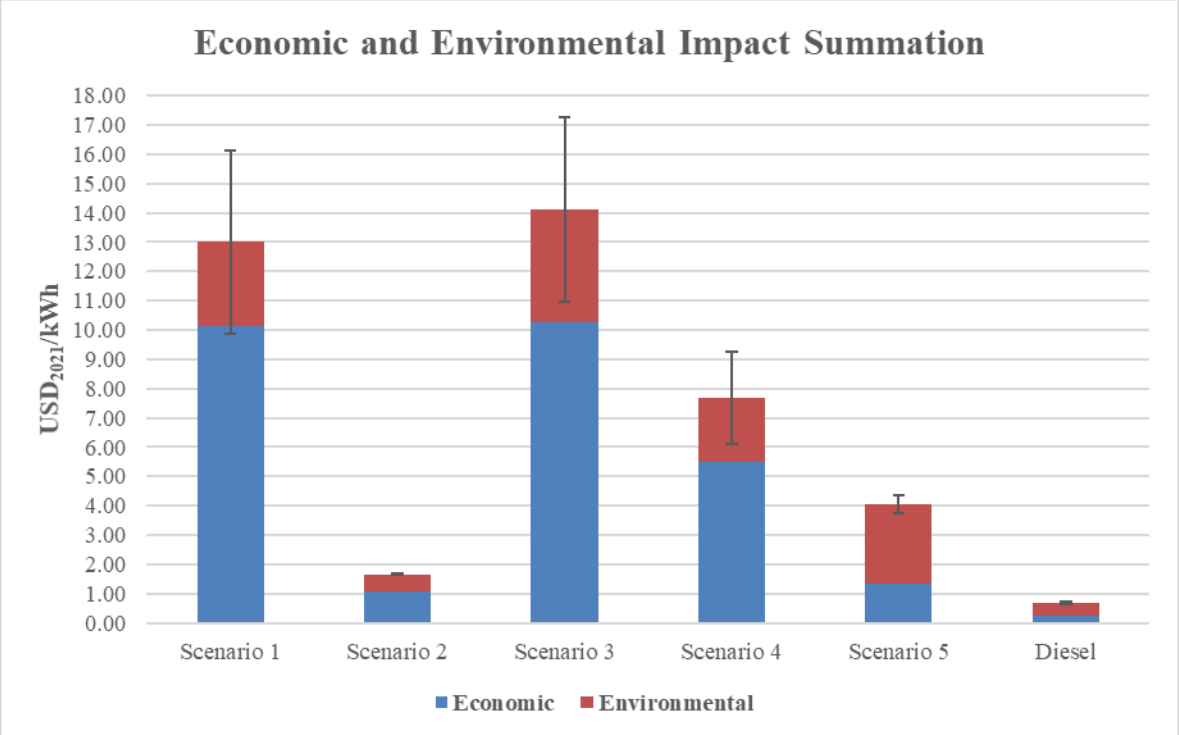

Figure 15: Economic and Environmental Impact Summation

Logistical Comparison

An energy source that can alleviate the logistical issues with DMO, needs advantageous volumetric and gravimetric power densities, survivability when attacked, and capable of being cached for long periods of time. While diesel has convenient properties with gravimetric and volumetric energy densities at 9.7 kWh/kg and 10.8 kWh/L, respectively, it also has disadvantages (Slocum, 2018). Specifically, it is flammable, has negative health effects, negatively affects the environment if spilled, and has a shelf-life. Conversely, aluminum does not burn and is essentially inert for health, environmental, and storage considerations. However, it is dense and, if activated, is reactive with water.

Diesel's flashpoint is at 52°C with an auto-ignition temperature range of 254-285°C (INCHEM, 2004). The National Fire Protection Association (NFPA) flammability hazard rating is a two: ignites if moderately heated (Global, 2019). This decreases the survivability of both the fuel and the fuel carrier in case of an attack or improper handling. In contrast, aluminum is not flammable, but has a melting point at 660°C and several alloys are able to withstand temperatures up to 982°C before melting, not burning. However, if aluminum is in powdered form and oxidized it will burn (Lemmon & Weritz, 2020). Additionally, activated aluminum becomes reactive to water and produces heat and hydrogen (Slocum, 2018). If transported on a ship this could be a considerable hazard as normal firefighting efforts with water would enhance the reaction. Gallium and indium are not fire hazards, but if burned could result in hazardous vapors (Strem Chemicals, 2011; Teck Metals Ltd, 2015).

For human health considerations diesel is a possible carcinogen, corrodes skin, can be toxic if absorbed repeatedly, and the vapor has negative health effects. The NFPA health hazard rating is a two: can cause injury and requires prompt treatment (ExxonMobil, 2020). Aluminum, gallium, and indium, unless inhaling dust or fumes, do not have any particular health impacts ((Kaiser Aluminum), 2017; Strem Chemicals, 2011; Teck Metals Ltd, 2015).

For environmental impacts, diesel is both acutely and chronically toxic to aquatic organisms (NOAA, 2006). Spills or leaks on land can migrate into drinking water and cause health impacts, such as underground storage tanks leaking into well reservoirs on Camp Lejeune (ATSDR, 2017). Aluminum, gallium, and indium have no determined ecotoxicological impacts ((Kaiser Aluminum), 2017; Strem Chemicals, 2011; Teck Metals Ltd, 2015). Additionally, as a solid, activated aluminum would be more robust against damage during transportation and could even be air dropped.

Depending on storage conditions and the quality of fuel, diesel can last for about six months without additives and special storage conditions before being detrimental to machinery. However, there are cases where fuel was stored in specially prepared conditions and lasted for years without significant deterioration. In this situation, the fuel was kept cold and moisture mitigation was employed (Whisman et al., 1991). Neither condition is likely in the Western Pacific or South China Sea. Alternatively, aluminum, gallium, and indium do not have any particular storage limits, other than surface corrosion from water with aluminum (Alumeco, 2021; Strem Chemicals, 2011; Teck Metals Ltd, 2015). However, activated aluminum cannot have contact with moisture or it

will start reacting. This leads the author to believe that exposure to humid air would eventually degrade the fuel and limit its shelf-life.

Comparing the density of diesel to activated aluminum, diesel's density, depending on temperature, is 845 kg/m^3. Alternatively, activated aluminum is 2,727 kg/m^3. This was calculated by applying a weighted average of each constituent metal's mass to the respective densities of each metal; 96.5% aluminum at 2,600 kg/m^3, etc. (Engineer's Edge, 2022; Viornery-Portillo et al., 2020). However, that is considering a solid mass. If, as was used in the literature, the activated aluminum is in congruent spheres, to provide sufficient surface area for the reaction, then the density of packing will never exceed 74% of the solid (Hales, 1998). This reduces the density of transported activated aluminum to 2,017 kg/m^3. Comparing the two, using the respective kg/kWh determined in this study, diesel provides 3,642 kWh/m^3 and aluminum spheres provide 3,532 kWh/m^3. If, however, the activated aluminum is a solid block, then it would provide 4,772 kWh/m^3. Consequently, activated aluminum likely provides similar or less energy by volume than diesel while requiring nearly 2.5 times the weight to provide the same amount of energy.

The last consideration is availability of the fuel. As previously discussed, in a contest against China, diesel would likely have to come from the US to support operations in the Western Pacific. While not ideal, there is a historical precedent of supporting a Pacific Campaign with petroleum-based fuels and petroleum is still widely available around the globe (US EIA, 2021). Based on the minimum 300 gallons a day requirement for a forward operating base (FOB) in Afghanistan, for a six month deployment that is 54,000 gallons (E2O, 2011). At 3.22 kg/gal and 0.232 kg/kWh, the

total power requirement is almost 750 thousand kWh. Fulfilling that power requirement with activated aluminum and no eutectic recovery, at 0.571 kg-AAl/kWh, would require 413 tonnes of aluminum, 12 tonnes of gallium, and 3 tonnes of indium. Removing China's production of gallium, with 96% of the 2020 total production, in 2020 the rest of the world produced 10 tonnes of gallium with Russia producing 4 tonnes of that (Jaskula, 2021). Consequently, obtaining enough gallium to meet one FOB's energy requirements would be difficult.

Potential Areas of Improvement

Activated aluminum is a new technology that could become viable if portions of the life cycle improved. The main areas for improvement are the energy mix used in aluminum production, an integrated eutectic recovery and storage mechanism, and making use of the reaction's waste heat.

With the electrolysis stage of aluminum production and its energy usage producing at least 70% of the aluminum production's GWP, any shift to cleaner energy mixes would result in significant dividends to the overall environmental impact. This includes reductions in GWP, acidification, particulate matter, and other pollution categories (EPA, 2019). Table 7 highlights the stark difference in GWP emissions with the global average producing 10.2 kg CO_2-eq per kg of aluminum and the GWP from the BAT producing 0.01 kg CO_2-eq per kg of aluminum.

As the economic analysis is highly sensitive to eutectic recovery rates and the majority of gallium and indium are produced in China, recovering and reusing eutectic is necessary to make this fuel viable. Consequently, while developing the technology to

commercialize the use of activated aluminum, an efficient method of separating the eutectic from the byproducts would substantially increase the economic viability of this fuel.

The aluminum and water reaction results in around half of the potential energy in aluminum releasing as heat. This waste heat, combined with waste heat from fuel cell operations, could be repurposed with waste heat recovery methods to increase the overall efficiency of the system.

Summary

Throughout the study it was determined that, within the confines of the model, diesel is cheaper and, during the course of their respective life cycles, is a less environmentally impactful fuel source than activated aluminum. Even the best case activated aluminum scenario, Scenario 2, had double the combined economic and social cost of diesel with $1.79/kWh compared to $0.84/kWh. Additionally, while activated aluminum provides certain logistical advantages, such as non-inflammability and low human and ecological toxicity, it does not provide volumetric power density savings, has negative gravimetric power density impacts, and severe production limitations. However, with adjustments in aluminum production, effective eutectic recovery methods, and waste heat recovery, activated aluminum could be a viable alternative.

V. Conclusions and Recommendations

Overview

Initially, this chapter summarizes the results of the study and the purpose for this research. Then the assumptions made, and limitations found during the course of the study are discussed. This chapter also identifies potential follow-on research topics. Finally, the chapter examines the significance of the research.

Summary of Research Question

The primary objective of this research was to determine if using activated aluminum to produce hydrogen is viable as a fuel source when compared to diesel. The primary metrics used to evaluate this question were economic cost, which fuel costs the least money, and environmental cost, which fuel has the least environmental impact over its entire life cycle. An additional consideration was how difficult or hazardous is it to procure and transport either fuel to support operations in the Western Pacific.

Based on the estimated best case scenario's result of $1.79/kWh compared to diesel's $0.84/kWh, as the technology stands activated aluminum cannot compete with diesel economically or environmentally. Logistically, activated aluminum has some benefits, but in the author's opinion those benefits are outweighed by the supply chain's vulnerability to our primary competitors and poor gravimetric power density. Consequently, without making aluminum production more environmentally friendly, high eutectic recovery and reuse rates, and using heat recovery methods to increase the reaction efficiency, activated aluminum is not recommended as a fuel source.

Limitations and Assumptions

This research used historical market data to develop market price estimates for materials and a conglomeration of ranges for monetizing environmental impact categories. With market variability, there are unknown circumstances that can significantly impact commodity prices, such as the COVID-19 pandemic. For the LCA and LCIA, there are many variables that can change depending on regional differences, technological advances, or even government policy changes. Additionally, using activated aluminum as a source of hydrogen fuel is an immature technology that could have a breakthrough that makes it a viable alternative. Based on the multitude of variables and assumptions that were made, the results are not exact.

A significant assumption that overlies this thesis is using activated aluminum in contested military operations against China. This makes saving and returning aluminum hydroxide and eutectic seem unwieldy and unlikely. Also, shifting to a fuel source where our antagonist controls the majority of the production seems inadvisable. An uncontested scenario without political supply constraints, where scrap aluminum is readily available and infrastructure allows for byproduct processing, would make activated aluminum use more reasonable.

Another assumption for the study was considering the heat produced from aluminum reacting with water as wasted. Using the heat byproduct productively would increase the overall efficiency of the process and dilute the negative aspects of the fuel. Related to this, as the LRUSV is a maritime craft, the water needed for the reaction was assumed to be pulled from the surrounding water with no impact on the study. If this energy system was used in an area where water is not abundant, then the added weight

and energy needed to provide water to the system, anywhere from 1.9 to 16 kg of water per kg of activated aluminum, would significantly impact the usefulness of this energy system. This range results from a perfect reaction, calculated from Equation 1, where a kg of activated aluminum requires at least 1.9 kg of water and, based on the literature, 5 mL of water was needed to complete the reaction of the activated aluminum spheres (Slocum, 2018). This equates to 16 kg of water per kg of activated aluminum. Comparing the functional unit, this study shows 0.232 kg/kWh is needed for diesel while activated aluminum needs 0.571 kg/kWh of just activated aluminum. A minimum of an additional 1.14 kg/kWh of water is needed for an ideal reaction. This results in a lower limit of 1.69 kg/kWh for activated aluminum, a substantial decrease in gravimetric energy density.

The LCA databases used for this analysis are based on data that is at best five years old, if not older. With increasing focus on global warming and the resulting changes in policies, the aluminum industry continues to search for methods of decreasing their carbon and environmental footprint (Wang, 2022). Coupled with this is the growth of cleaner power generation. Consequently, depending on where aluminum is sourced and the age of the data used, the environmental impacts are drastically different. Table 7 is an excellent example of this.

The above assumptions and limitations create uncertainty in the final result. However, they were applied equally to all the scenarios and the results provide sufficient evidence to make a comparison between the two fuels.

Future Research

While the LCA attempted to be exhaustive, there are aspects of the study that bear further examination. Specifically, the impacts of the engine compared to fuel cells, comparison of activated aluminum to batteries, and including packaging necessary for activated aluminum.

Examining the impacts of the engine and fuel cell life cycles would provide clarification on the impact of switching to hydrogen fuel. This would also require exploring transportation methods for hydrogen and mapping the number of resupply trips needed to provide energy quantities equivalent to diesel. Related to this topic, examining the impacts of spills, from accidents or military action, could affect the results.

As batteries are heavy and contain precious metals, activated aluminum power sources could save weight, space, and be more environmentally friendly. Consequently, using this study to compare battery recharging with diesel to activated aluminum power sources could result in a different recommendation.

Significance of Research

The USMC, and DoD as a whole, is looking for alternative energy sources to ease its logistical, economic, and environmental energy burdens. In that search, some methods, while initially sound promising, may not provide any advantages to conventional power or have characteristics compatible for military operations. Consequently, technological improvements, a change in circumstances, or a change in the use of the technology would have to happen before further research or funding could be justified.

Based on this study and current military systems, activated aluminum falls firmly into that category. If the military was using hydrogen as an energy source, activated aluminum could be used as an emergency cache to support local hydrogen production if hydrogen shipments were delayed. However, without changes in the life cycle of its constituents, high rates of eutectic recovery, waste heat recovery, or other means of improving the environmental impacts of the lifecycle or economic constraints, the characteristics of activated aluminum do not currently support using it as an alternative energy source to petroleum fuels. The barriers to adopting activated aluminum as a fuel source are surmountable with existing technology but would require substantial research and development and a water-rich environment.

Appendix A: DLA Diesel Price Compilation

	Diesel ($/gal)	
Year	DS1	DS2
2009	4.07	3.92
2010	2.78	2.68
2011	3.03	2.92
2012	3.95	3.81
2013	3.73	3.6
2014	3.62	3.49
2015	3.77	3.57
2016	2.33	2.18
2017	2.83	2.67
2018	3.05	2.88
2019	3.06	2.86
2020	2.43	2.28
2021	2.44	2.29
2022	2.89	2.73
	Average	3.07
	Stdev	0.58

(Compiled from (DLA, 2021))

Appendix B: Metal Prices

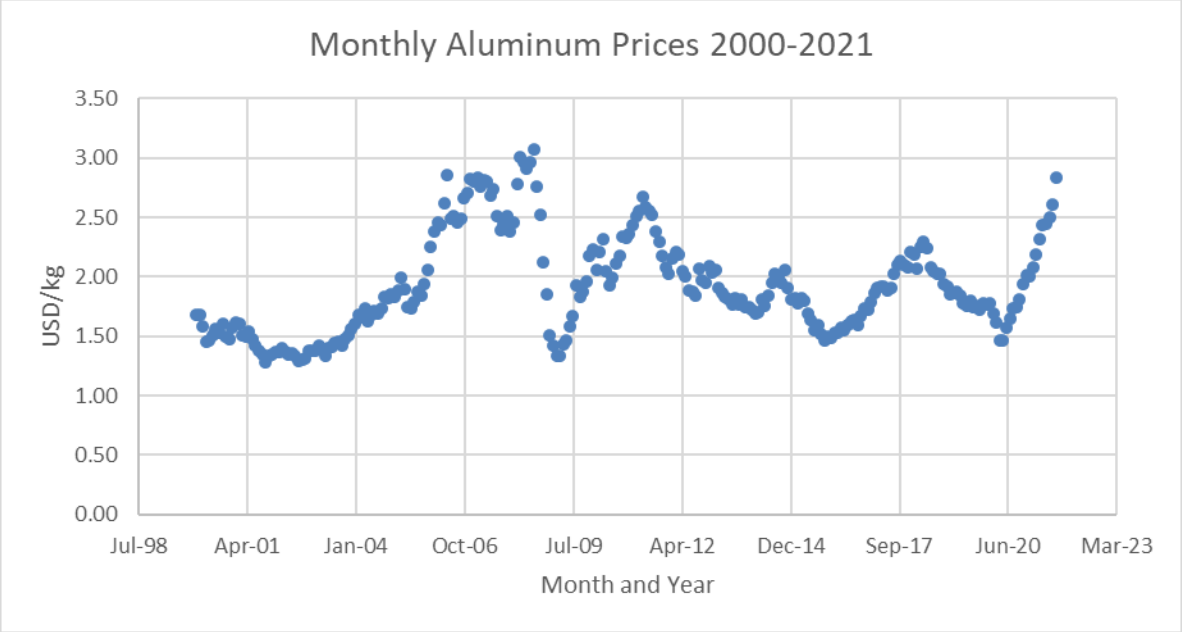

(Data obtained from (FRED, 2021))

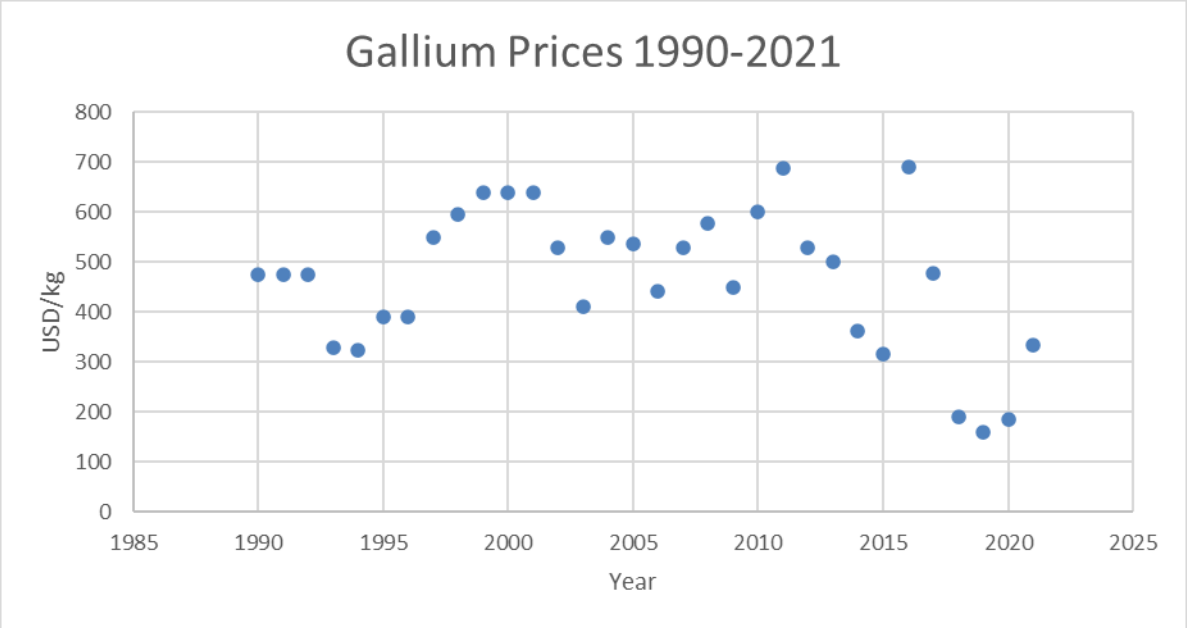

(Data obtained from (*Trading Econ.*, 2021; USGS et al., 2017))

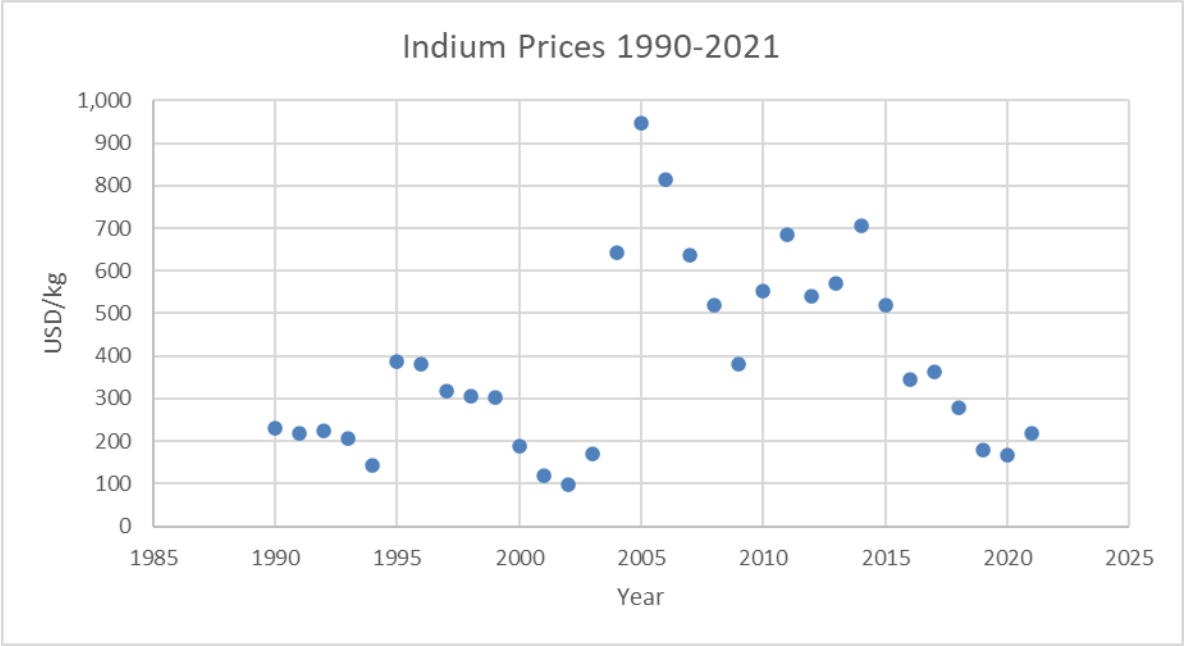

(Data obtained from (*Trading Econ.*, 2021; USGS et al., 2017))

Appendix C: GaBi Activated Aluminum Plan

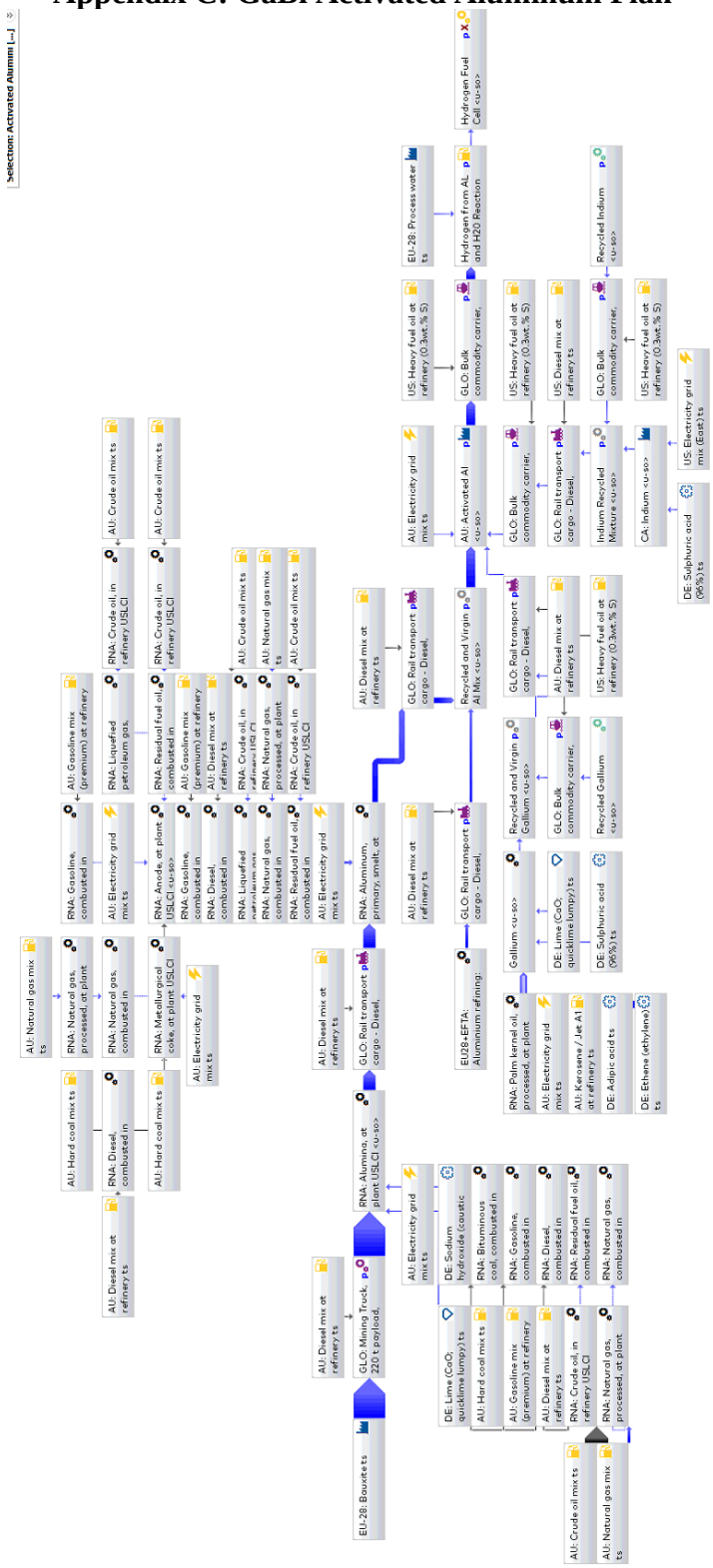

((PE International AG), 2012)

Appendix D: GaBi Diesel Plan

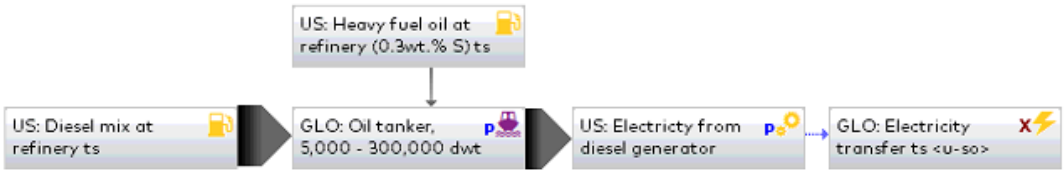

((PE International AG), 2012)

Appendix E: Monte Carlo Convergence Analyses

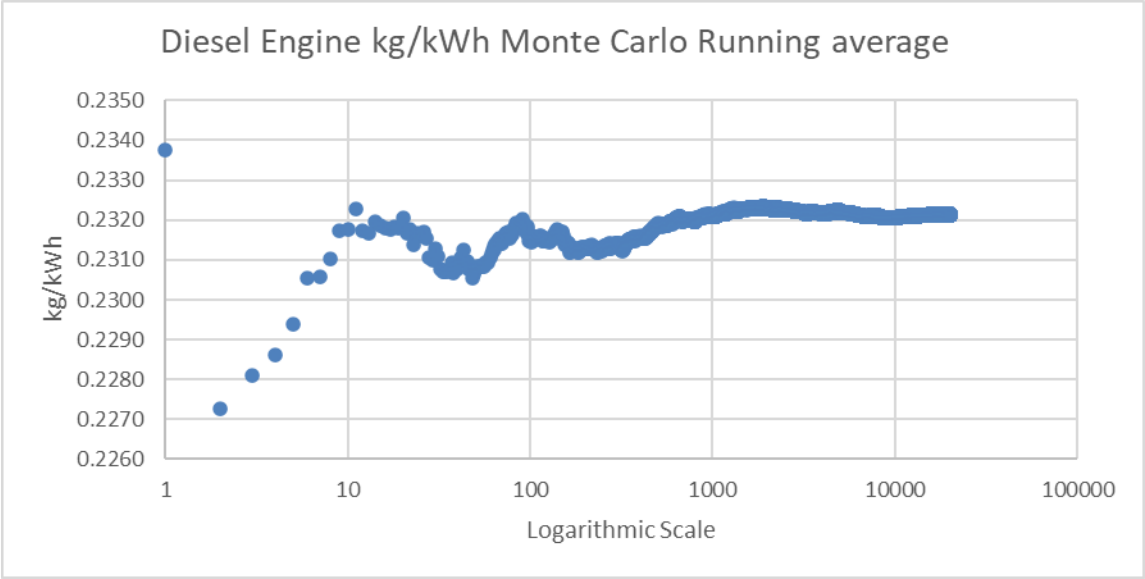

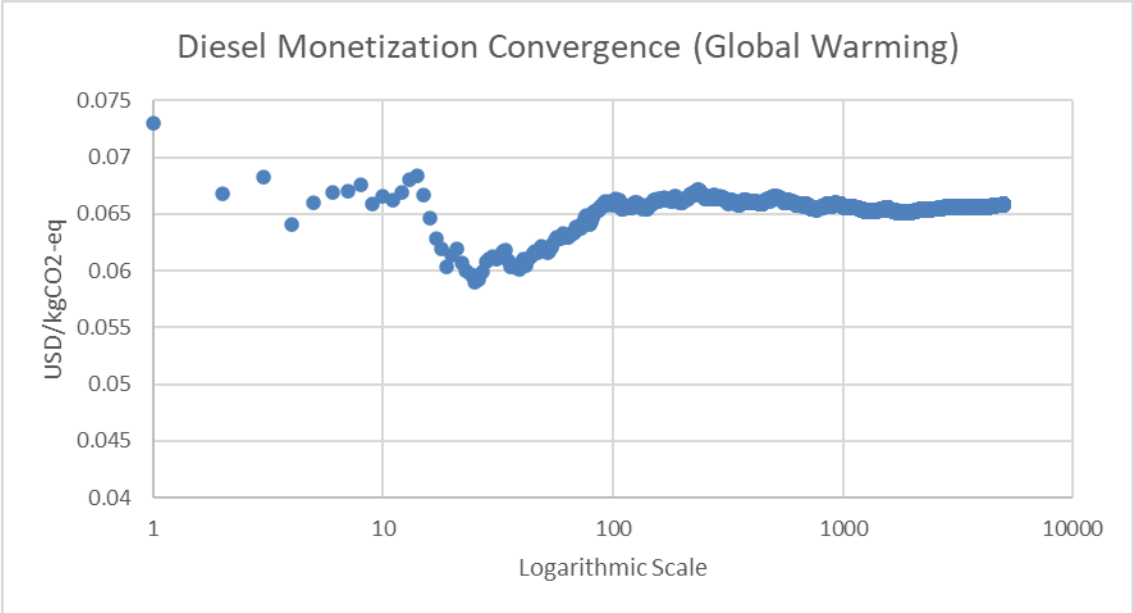

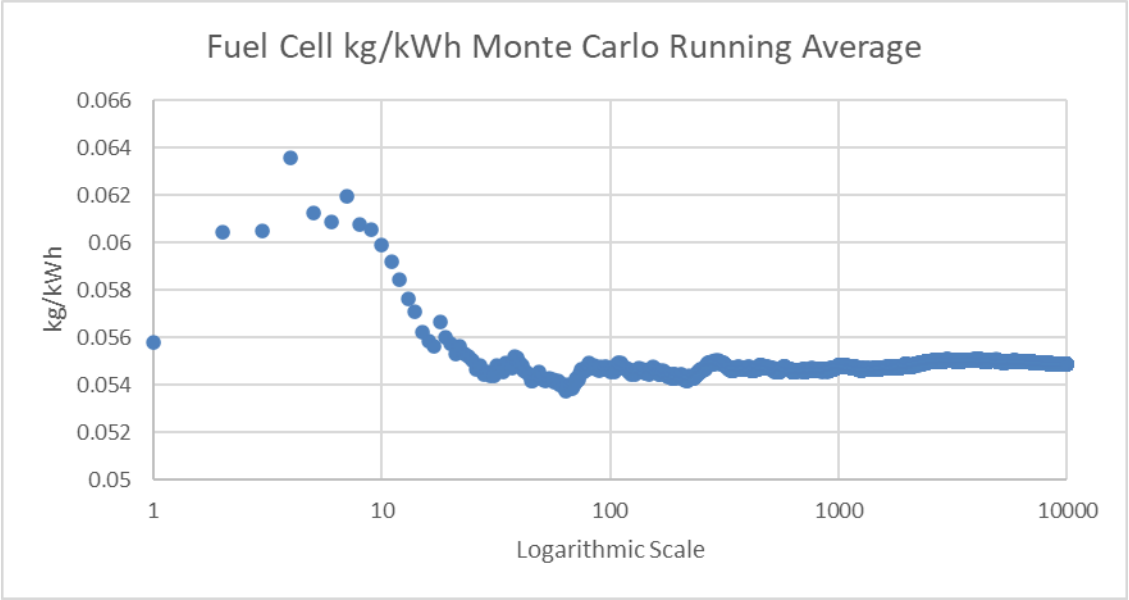
Fuel Cell kg/kWh Monte Carlo Running Average
kg/kWh
0.066
0.064
0.062
0.06
0.058
0.056
0.054
0.052
0.05
1
10
100
1000
10000
Logarithmic Scale

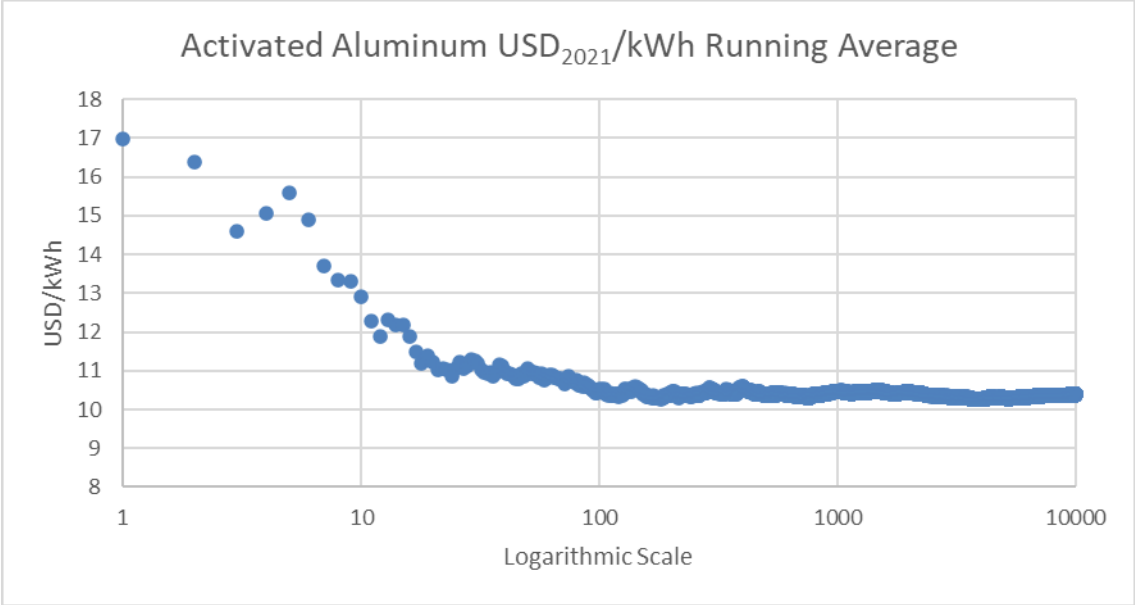
Activated Aluminum USD2021/kWh Running Average
USD/kWh
18
17
16
15
14
13
12
11
10
9
8
1
10
100
1000
10000
Logarithmic Scale

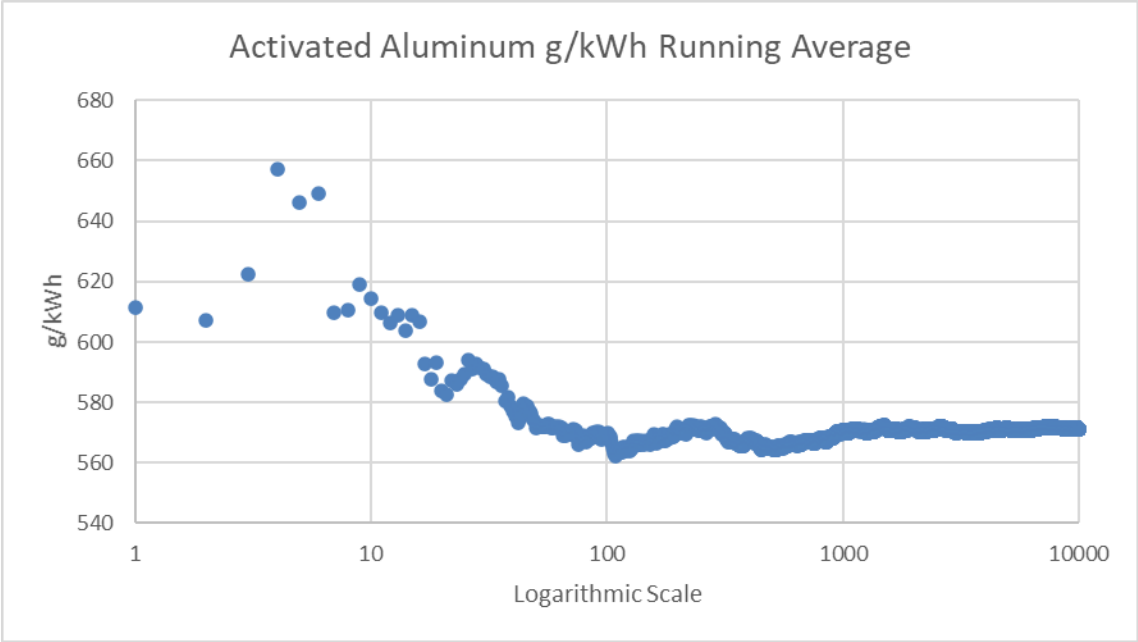
Activated Aluminum g/kWh Running Average
680
660
640
620
600
580
560
540
g/kWh
1
10
100
1000
10000
Logarithmic Scale

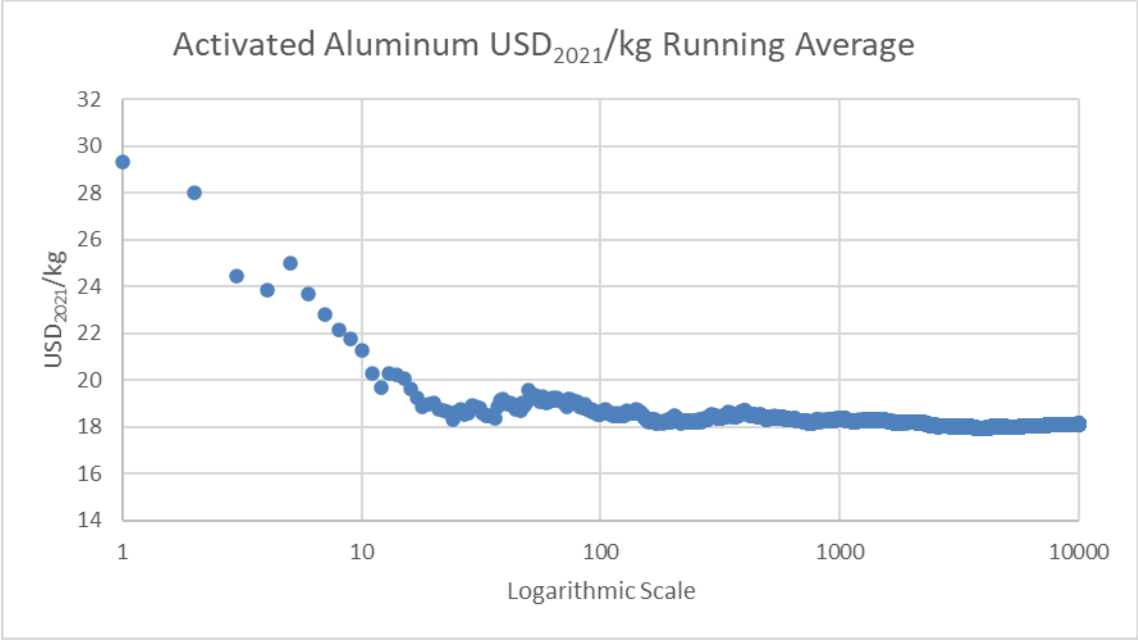
Activated Aluminum USD2021/kg Running Average
32
30
28
26
24
22
20
18
16
14
USD2021/kg
1
10
100
1000
10000
Logarithmic Scale

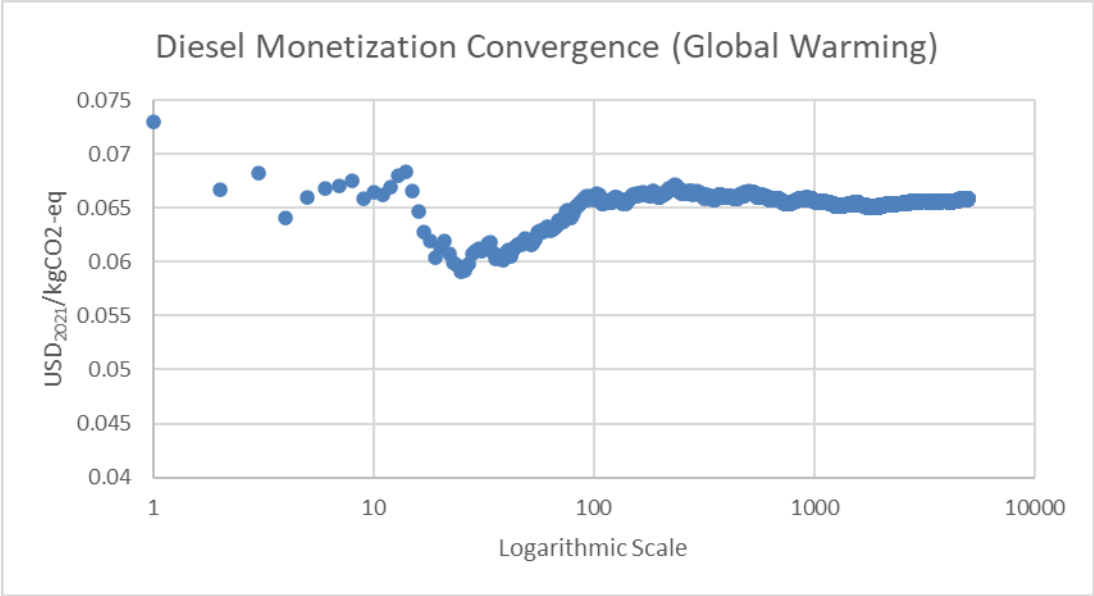
Diesel Monetization Convergence (Global Warming)
0.075
0.07
0.065
0.06
0.055
0.05
0.045
0.04
USD2021/kgCO2-eq
1
10
100
1000
10000
Logarithmic Scale

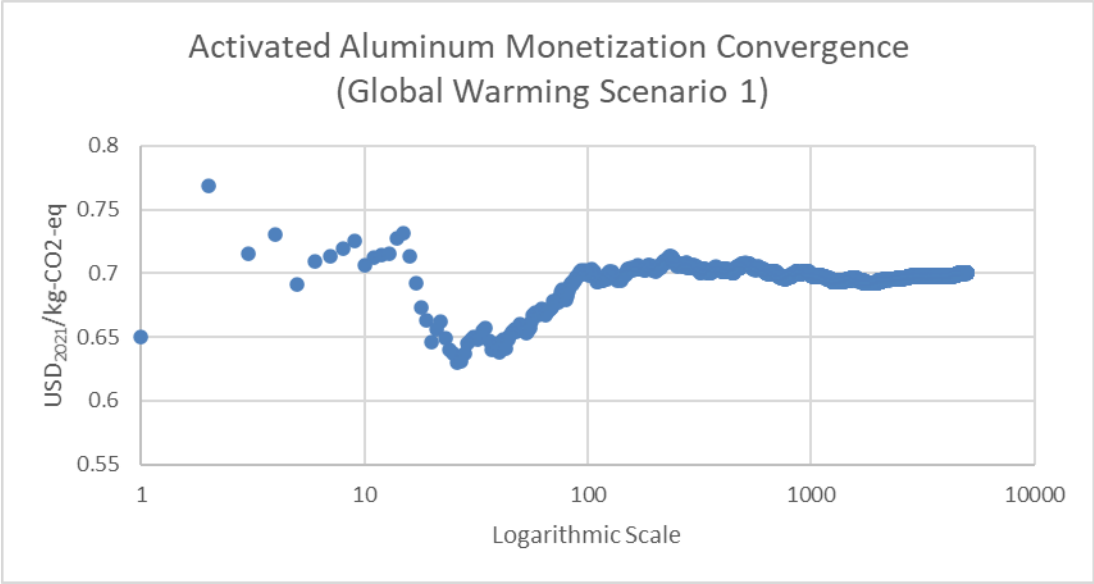
Activated Aluminum Monetization Convergence
(Global Warming Scenario 1)
0.8
0.75
0.7
0.65
0.6
0.55
USD2021/kg-CO2-eq
1
10
100
1000
10000
Logarithmic Scale

Appendix F: SimaPro Results

		TRACI 2.1 Diesel		TRACI 2.1 Scenario 1	
Category	**Unit**	Mean Values	Monetized Values	Mean Values	Monetized Values
Global Warming	kg CO_2-eq	0.863	0.06	12.6	0.94
Acidification	kg SO_2-eq	6.73E-03	0.10	0.070	1.05
Ecotoxicity	CTUe	1.2	0.01	12.2	0.09
Eutrophication	kg N-eq	8.58E-04	0.02	0.013	0.29
Human Health Particulate Matter	kg $PM_{2.5}$-eq	1.25E-03	0.06	0.012	0.60
Human Health Cancerous	CTUh	1.86E-08	0.02	3.34E-07	0.35
Human Health Noncancerous	CTUh	1.75E-06	0.43	7.29E-06	1.80
Ozone Depletion	kg CFC-11 eq	1.18E-07	4.72E-05	8.84E-07	3.54E-04
Resource Depletion (fossil fuel)	MJ	2.730	0.03	9.42	0.09
Smog Formation	kg O_3-eq	0.115	0.35	0.68	2.06
		Total	**1.08**	**Total**	**7.27**

(Data obtained from (Pré, 2021))

Bibliography

(Department of State). (2022). *Our Relationship*. U.S. Embassy and Consulates in Australia. https://au.usembassy.gov/our-relationship/

(EERE), O. of E. E. and R. E. (2020). *Hydrogen Production Processes*. Energy.Gov. https://www.energy.gov/eere/fuelcells/hydrogen-production-processes

(International Energy Agency). (2021). *Global Hydrogen Review 2021*. www.iea.org

(Kaiser Aluminum). (2017). Aluminum and Aluminum Alloys SDS. *Material Safety Data Sheet*.

(PE International AG). (2012). *GaBi: Software and database contents for Life Cycle Engineering*.

(U.S. EIA). (2021). *Oil and petroleum products explained: Oil imports and exports*. U.S. Energy Information Administration. https://www.eia.gov/energyexplained/oil-and-petroleum-products/imports-and-exports.php

(US Bureau of Labor). (2021). *CPI Inflation Calculator*. US Bureau of Labor Statistics. https://www.bls.gov/data/inflation_calculator.htm

40 Defiant. (2020). Metal Shark. https://www.metalsharkboats.com/40defiant/

Abdelkareem, M. A., Elsaid, K., Wilberforce, T., Kamil, M., Sayed, E. T., & Olabi, A. (2021). Environmental aspects of fuel cells: A review. *Science of the Total Environment*, *752*, 141803. https://doi.org/10.1016/j.scitotenv.2020.141803

Al-Qahtani, A., Parkinson, B., Hellgardt, K., Shah, N., & Guillen-Gosalbez, G. (2021). Uncovering the true cost of hydrogen production routes using life cycle monetisation. *Applied Energy*, *281*, 115958. https://doi.org/10.1016/j.apenergy.2020.115958

Alumeco. (2021). *Proper handling and storage of aluminium*. https://www.alumeco.com/knowledge-technique/storage-handling/proper-handling-and-storage-of-aluminium

Anderson, C. S. (2021). Indium. In *Mineral Commodity Summaries*.

Arendt, R., Bachmann, T. M., Motoshita, M., Bach, V., & Finkbeiner, M. (2020). Comparison of different monetization methods in LCA: A review. *Sustainability (Switzerland)*, *12*(24), 1–39. https://doi.org/10.3390/su122410493

ATSDR. (2017). CAMP LEJEUNE DRINKING WATER. *US Department of Health and Human Services: Agency for Toxic Substances and Disease Registry*, *January*.

Bagshaw, A. N. (2017). *The Aluminum Story: Bauxite to Alumina: The Bayer Process*.

Balli, O., Ozbek, E., Ekici, S., Midilli, A., & Hikmet Karakoc, T. (2021). Thermodynamic comparison of TF33 turbofan engine fueled by hydrogen in benchmark with kerosene. *Fuel*, *306*(May), 121686. https://doi.org/10.1016/j.fuel.2021.121686

Ballio, F., & Guadagnini, A. (2004). Convergence assessment of numerical Monte Carlo simulations in groundwater hydrology. *Water Resources Research*, *40*(4), 1–5. https://doi.org/10.1029/2003WR002876

Bare, J. (2012). Tool for the Reduction and Assessment of Chemical and Other Environmental Impacts (TRACI) version 2.1. *U.S. Environmental Protection Agency*, *600/R-12/5*(August), 24.

Berger, D. H. (2020). *Force Design 2030*. *March*, 1–15. https://www.hqmc.marines.mil/Portals/142/Docs/CMC38 Force Design 2030 Report

Phase I and II.pdf?ver=2020-03-26-121328-460
Caldwell, J., & Vahidsafa, A. (2020). *Propagation of Error*. Chemistry LibreTexts. https://chem.libretexts.org/@go/page/353
China Power Team. (2021). *How Much Trade Transits the South China Sea?* China Power. https://chinapower.csis.org/much-trade-transits-south-china-sea/
Clark, D., Houston, R., Schaumeier, J., & Smith, T. (2021). *Shipping Map*. Kiln. https://www.shipmap.org/
Classen, M. (2021). Indium Production. *Ecoinvent Database Version 3.8*.
Collins, L. (2021, July 29). World's first international liquid-hydrogen shipment delayed again by up to eight months. *Recharge: Global News and Intelligence for the Energy Transition*. https://www.rechargenews.com/energy-transition/world-s-first-international-liquid-hydrogen-shipment-delayed-again-by-up-to-eight-months/2-1-1046004
Comer, B., & Osipova, L. (2021). Accounting for well-to-wake carbon dioxide equivalent emissions in maritime transportation climate policies. *International Council on Clean Transportation*.
Costa, M., Marchitto, L., Piazzullo, D., & Prati, M. V. (2021). Comparison between the energetic and environmental performance of a combined heat and power unit fueled with diesel and waste vegetable oil: An experimental and numerical study. *Renewable Energy*, *168*, 791–805. https://doi.org/10.1016/j.renene.2020.12.099
Crawford, N. C. (2019). Pentagon Fuel Use, Climate Change, and the Costs of War. In *Costs of War*. Boston University.
Cummins. (2013). *Marine Performance Curves QSB 6.7*. https://mart.cummins.com/imagelibrary/data/assetfiles/0055797.pdf
Davidson, I. (2016). Oven Efficiency. *Biscuit Baking Technology*, 253–267. https://doi.org/10.1016/b978-0-12-804211-3.00016-9
de Bruyn, S., Bijleveld, M., de Graaff, L., Schep, E., Schroten, A., Vergeer, R., & Ahdour, S. (2018). Environmental Prices Handbook. *Committed to the Environment Delft*, *18.7N54.12*. https://cedelft.eu/publications/environmental-prices-handbook-eu28-version/
de Oliveira, R. P., Benvenuti, J., & Espinosa, D. C. R. (2021). A review of the current progress in recycling technologies for gallium and rare earth elements from light-emitting diodes. *Renewable and Sustainable Energy Reviews*, *145*(January), 111090. https://doi.org/10.1016/j.rser.2021.111090
Department of Defense Office of the Undersecretary of Defense (Acquisition and Sustainment). (2021). *Department of Defense Draft Climate Adaptation Plan: Report Submitted to National Climate Task Force and Federal Chief Sustainability Officer*. https://media.defense.gov/2021/Oct/07/2002869699/-1/-1/0/DEPARTMENT-OF-DEFENSE-CLIMATE-ADAPTATION-PLAN-2.PDF
Department of Energy. (2020). 2019 Annual Progress Report: DOE Hydrogen and Fuel Cells Program. *DOE Hydrogen and Fuel Cells Program: 2019 Annual Progress Report*, *April*, 993.
DLA. (2021). *DLA Standard Prices for Petroleum*. Defense Logistics Agency. https://www.dla.mil/Energy/Business/Standard-Prices/
DOE. (2009). DOE Hydrogen and Fuel Cells Program: Hydrogen Storage. *U.S*

Department Of Energy, *25*, 6. http://www.hydrogen.energy.gov/storage.html
E2O. (2011). *United States Marine Corps Expeditionary Energy Strategy and Implementation Plan*. https://www.hqmc.marines.mil/Portals/160/Docs/USMC Expeditionary Energy Strategy Implementation Planning Guidance.pdf
Engineer's Edge. (2022). *Densities of Metals and Elements Table*. https://www.engineersedge.com/materials/densities_of_metals_and_elements_table_13976.htm
EPA. (2004). Risk assessment guidance for superfund (RAGS). Volume I. Human health evaluation manual (HHEM). Part E. Supplemental guidance for dermal risk assessment. *U.S. Environmental Protection Agency*, *1*(540/R/99/005). https://doi.org/EPA/540/1-89/002
EPA. (2016). Social Cost of Carbon. *EPA Fact Sheet*, *December*, 1–5. https://www.epa.gov/sites/default/files/2016-12/documents/social_cost_of_carbon_fact_sheet.pdf
EPA. (2019). *Public Health Benefits per kWh of Energy Efficiency and Renewable Energy in the United States: A Technical Report*. *July*.
Eser, S. (2020). *Chemistry of Catalytic Reforming*. Penn State College of Earth and Mineral Sciences: FSC 432 Petroleum Processing. https://doi.org/10.3775/jie.67.11_972
ESSOM Co. LTD. (2019). *Heating Values of Hydrogen and Fuels*. 1. https://chemeng.queensu.ca/courses/CHEE332/files/ethanol_heating-values.pdf
ExxonMobil. (2020). No. 2 Diesel Fuel. *Safety Data Sheet*.
Fantke, P., Bijster, M., Guignard, C., Hauschild, M. Z., Huijbregts, M. A. J., Jolliet, O., Kounina, A., Magaud, V., Margni, M., McKone, T. E., Posthuma, L., Rosenbaum, R. K., van de Meent, D., & van Zelm, R. (2017). *USEtox 2.0 Documentation (Version 1)*. https://doi.org/10.11581/DTU:00000011
FRED. (2021). *Global Price of Aluminum*. Federal Reserve Bank of St. Louis. https://fred.stlouisfed.org/series/PALUMUSDM
Frischknecht, R., & Rebitzer, G. (2005). The ecoinvent database system: A comprehensive web-based LCA database. *Journal of Cleaner Production*, *13*(13–14), 1337–1343. https://doi.org/10.1016/j.jclepro.2005.05.002
Fthenakis, V., Wang, W., & Kim, H. C. (2009). Life cycle inventory analysis of the production of metals used in photovoltaics. *Renewable and Sustainable Energy Reviews*, *13*(3), 493–517. https://doi.org/10.1016/j.rser.2007.11.012
Global. (2019). *SAFETY DATA SHEET Diesel Fuel*. *June*, 1–11.
Godart, P., Fischman, J., & Hart, D. (2021). Kilowatt-Scale Fuel Cell Systems Powered by Recycled Aluminum. *Journal of Electrochemical Energy Conversion and Storage*, *18*(1), 1–9. https://doi.org/10.1115/1.4046660
Godart, P., & Hart, D. (2020). Aluminum-powered climate change resiliency: From aluminum debris to electricity and clean water. *Applied Energy*, *275*(March), 115316. https://doi.org/10.1016/j.apenergy.2020.115316
Goedkoop, M., Oele, M., Vieira, M., Leijting, J., Ponsioen, T., & Meijer, E. (2016). SimaPro Tutorial. *SimaPro*, *May*.
Google. (2021). Distance Calculator. *Google Earth*. 15 Nove
Graedal, T. E., Allwood, J., Birat, J.-P., Reck, B. K., Sibley, S. F., Sonnermann, G.,

Buchert, M., & Hageluken, C. (2011). UNEP (2011) Recycling Rates of Metals - A Status Report. A Report of the Working Group on the Global Metla Flows tot he International Resource Panel. In *United Nations Environment Program*.

Hales, T. C. (1998). *An overview of the Kepler conjecture*. http://arxiv.org/abs/math/9811071

Harrison, K. W., Remick, R., Martin, G. D., & Hoskin, A. (2010). Hydrogen Production: Fundamentals and Case Study Summaries. *National Renewable Energy Laboratory*.

Herrmann, I. T., & Moltesen, A. (2015). Does it matter which Life Cycle Assessment (LCA) tool you choose? - A comparative assessment of SimaPro and GaBi. *Journal of Cleaner Production*, *86*, 163–169. https://doi.org/10.1016/j.jclepro.2014.08.004

Hosseinzadeh-Bandbafha, H., Rafiee, S., Mohammadi, P., Ghobadian, B., Lam, S. S., Tabatabaei, M., & Aghbashlo, M. (2021). Exergetic, economic, and environmental life cycle assessment analyses of a heavy-duty tractor diesel engine fueled with diesel–biodiesel-bioethanol blends. *Energy Conversion and Management*, *241*(May), 114300. https://doi.org/10.1016/j.enconman.2021.114300

Huijbregts, M. A. J., Steinmann, Z. J. N., Elshout, P. M. F., Stam, G., Verones, F., Vieira, M., Zijp, M., Hollander, A., & van Zelm, R. (2017). ReCiPe2016: a harmonised life cycle impact assessment method at midpoint and endpoint level. *International Journal of Life Cycle Assessment*, *22*(2), 138–147. https://doi.org/10.1007/s11367-016-1246-y

INCHEM. (2004). *Diesel Fuel No. 2*. https://inchem.org/documents/icsc/icsc/eics1561.htm

ISO. (2006a). ISO 14040: Environmental management–life cycle assessment—Principles and framework. *International Organization for Standardization*, *2006*.

ISO. (2006b). *ISO 14044 Environmental management - Life cycle assessment - Requirements and guidelines*.

Jaskula, B. W. (2021). Gallium. In *Mineral Commodity Summaries*.

Kim, J., & Kim, T. (2015). Compact PEM fuel cell system combined with all-in-one hydrogen generator using chemical hydride as a hydrogen source. *Applied Energy*, *160*, 945–953. https://doi.org/10.1016/j.apenergy.2015.03.084

Kinsel, W. C. (2010). *Environmental LCA of Coal-Biomass to Liquid Jet Fuel Compared to Petroleum-Derived JP-8 Jet Fuel* (Issue March) [Air Force Institute of Technology]. https://apps.dtic.mil/sti/pdfs/ADA522304.pdf

Koroneos, C., Dompros, A., Roumbas, G., & Moussiopoulos, N. (2005). Advantages of the use of hydrogen fuel as compared to kerosene. *Resources, Conservation and Recycling*, *44*(2), 99–113. https://doi.org/10.1016/j.resconrec.2004.09.004

Kotz, S., & Rene van Dorp, J. (2004). *Beyond Beta: Other Continuous Families of Distributions with Bounded Support and Applications*. https://doi.org/https://doi.org/10.1142/5720

Kragelund, S., Dobrokhodov, V., Monarrez, A., Hurban, M., & Khol, C. (2013). Adaptive speed control for autonomous surface vessels. *OCEANS 2013 MTS/IEEE - San Diego: An Ocean in Common*, *March*.

Lemmon, A., & Weritz, J. (2020). Fire Safety of Aluminum & Its Alloys. *The Aluminum Association*.

Litman, T. A., & Doherty, E. (2011). Transportation Cost and Benefit Analysis II - Air

Pollution Costs. *Victoria Transport Policy Institute*. https://www.vtpi.org/tca/
Lohse-Busch, H., Duoba, M., Stutenberg, K., Lliev, S., Kern, M., Richards, B., Christenson, M., & Loiselle-Lapointe, A. (2018). *Technology Assessment of a Fuel Cell Vehicle: 2017 Toyota Mirai*.
Lototskyy, M. V., Tolj, I., Pickering, L., Sita, C., Barbir, F., & Yartys, V. (2017). The use of metal hydrides in fuel cell applications. *Progress in Natural Science: Materials International*, *27*(1), 3–20. https://doi.org/10.1016/j.pnsc.2017.01.008
Made with Natural Earth. (2021). Natural Earth. https://www.naturalearthdata.com/
Menard, J.-F. (2021). Machine operation, diesel, >= 74.57 kW, generators, GLO. *Ecoinvent Database Version 3.8*.
Meroueh, L., Eagar, T. W., & Hart, D. P. (2020). Effects of Mg and Si Doping on Hydrogen Generation via Reduction of Aluminum Alloys in Water. *ACS Applied Energy Materials*, *3*(2), 1860–1868. https://doi.org/10.1021/acsaem.9b02300
Montero-Sousa, J. A., Aláiz-Moretón, H., Quintián, H., González-Ayuso, T., Novais, P., & Calvo-Rolle, J. L. (2020). Hydrogen consumption prediction of a fuel cell based system with a hybrid intelligent approach. *Energy*, *205*. https://doi.org/10.1016/j.energy.2020.117986
Nicholas, J. M., & Steyn, H. (2017). *Project Management for Engineering Business and Techology* (5th ed.). Routledge.
NOAA. (2006). Small Diesel Spills (500-5,000 gallons). *National Oceanic and Atmospheric Administration National Ocean Service*, 2. https://response.restoration.noaa.gov/sites/default/files/Small-Diesel-Spills.pdf
Nuss, P., & Eckelman, M. J. (2014). Life cycle assessment of metals: A scientific synthesis. *PLoS ONE*, *9*(7), 1–12. https://doi.org/10.1371/journal.pone.0101298
Öberg, S., Odenberger, M., & Johnsson, F. (2022). Exploring the competitiveness of hydrogen-fueled gas turbines in future energy systems. *International Journal of Hydrogen Energy*, *47*(1), 624–644. https://doi.org/10.1016/j.ijhydene.2021.10.035
OECD. (1993). Commodity Price Variability: Its Nature and Causes. *Organization For Economic Co-Operation and Development*.
Özçelep, Y., Sevgen, S., & Samli, R. (2020). A study on the hydrogen consumption calculation of proton exchange membrane fuel cells for linearly increasing loads: Artificial Neural Networks vs Multiple Linear Regression. *Renewable Energy*, *156*, 570–578. https://doi.org/10.1016/j.renene.2020.04.085
PE International AG. (2012). *GaBi Manual*. 388.
Peng, T., Ou, X., Yan, X., & Wang, G. (2019). Life-cycle analysis of energy consumption and GHG emissions of aluminium production in China. *Energy Procedia*, *158*, 3937–3943. https://doi.org/10.1016/j.egypro.2019.01.849
Pré. (2021). *Simapro Database Manual*. 3–48. http://www.pre-sustainability.com/download/DatabaseManualMethods.pdf
Ratnakar, R. R., Gupta, N., Zhang, K., van Doorne, C., Fesmire, J., Dindoruk, B., & Balakotaiah, V. (2021). Hydrogen supply chain and challenges in large-scale LH2 storage and transportation. *International Journal of Hydrogen Energy*, *46*(47), 24149–24168. https://doi.org/10.1016/j.ijhydene.2021.05.025
Reichert, M. (2021). *OpenRailwayMap*. OpenStreetMap Foundation. https://www.openrailwaymap.org/

Reserve, F. (2021). *Foreign Exchange Rates*. Board of Governors of the Federal Reserve System. https://www.federalreserve.gov/releases/h10/current/

Reuter, M., Hudson, C., van Schaik, A., Heiskanen, K., Meskers, C., & Hagelücken, C. (2013). *UNEP (2013) Metal Recycling: Opportunities, Limits, Infrastructure, A Report of the Working Group on the Global Metal Flows to the International Resource Panel*. United Nations Environment Program.

Rusman, N. A. A., & Dahari, M. (2016). A review on the current progress of metal hydrides material for solid-state hydrogen storage applications. *International Journal of Hydrogen Energy*, *41*(28), 12108–12126. https://doi.org/10.1016/j.ijhydene.2016.05.244

Saevarsdottir, G., Kvande, H., & Welch, B. J. (2020). Aluminum Production in the Times of Climate Change: The Global Challenge to Reduce the Carbon Footprint and Prevent Carbon Leakage. *JOM*, *72*(1), 296–308. https://doi.org/10.1007/s11837-019-03918-6

Samaras, C., Nuttall, W. J., & Bazilian, M. (2019). Energy and the military: Convergence of security, economic, and environmental decision-making. *Energy Strategy Reviews*, *26*(September), 100409. https://doi.org/10.1016/j.esr.2019.100409

Schulte, R. F., & Foley, N. K. (2014). Compilation of gallium resource data for bauxite deposits. *United States Geological Survey*, 21. http://pubs.er.usgs.gov/publication/ofr20131272

Shi, W., Stapersma, D., & Grimmelius, H. T. (2009). Analysis of energy conversion in ship propulsion system in off-design operation conditions. *WIT Transactions on Ecology and the Environment*, *121*, 449–460. https://doi.org/10.2495/ESU090411

Shih, T., & Yu, H.-C. (2010). Probability Distribution of Return and Volatility in Crude Oil Market. *The Journal of Global Business Management*. http://www.jgbm.org/page/21 Tung-Li Shih .pdf

Shinde, B. J., & K., K. (2021). Recent progress in hydrogen fuelled internal combustion engine (H2ICE) – A comprehensive outlook. *Materials Today: Proceedings*, *xxxx*. https://doi.org/10.1016/j.matpr.2021.10.378

Slocum, J. T. (2018). *Characterization and science of an aluminum fuel treatment process* (Issue February) [Massachusetts Institute of Technology]. https://dspace.mit.edu/handle/1721.1/115674

Slocum, J. T., Eagar, T. W., Taylor, R., & Hart, D. P. (2020). Activation of bulk aluminum and its application in a hydrogen generator. *Applied Energy*, *279*(August), 115712. https://doi.org/10.1016/j.apenergy.2020.115712

Smith, C., Burrows, J., Scheier, E., Young, A., Smith, J., Young, T., & Gheewala, S. H. (2015). Comparative Life Cycle Assessment of a Thai Island's diesel/PV/wind hybrid microgrid. *Renewable Energy*, *80*, 85–100. https://doi.org/10.1016/j.renene.2015.01.003

Strem Chemicals. (2011). Gallium metal MSDS. *Material Safety Data Sheet*.

Szepessy, S., & Thorwid, P. (2018). Low Energy Consumption of High-Speed Centrifuges. *Chemical Engineering and Technology*, *41*(12), 2375–2384. https://doi.org/10.1002/ceat.201800292

Tabatabaei, M., Aghbashlo, M., Najafi, B., Hosseinzadeh-Bandbafha, H., Faizollahzadeh Ardabili, S., Akbarian, E., Khalife, E., Mohammadi, P., Rastegari, H., &

Ghaziaskar, H. S. (2019). Environmental impact assessment of the mechanical shaft work produced in a diesel engine running on diesel/biodiesel blends containing glycerol-derived triacetin. *Journal of Cleaner Production*, *223*, 466–486. https://doi.org/10.1016/j.jclepro.2019.03.106

Taylor, B. (2021, May). Aluminum scrap sector faces demanding future. *Recycling Today*. https://www.recyclingtoday.com/article/aluminum-recycling-scrap-demand-global-ing-article/

Teck Metals Ltd. (2015). Indium Metal Safety Data Sheet. *Material Safety Data Sheet*.

Tekade, S. P., Pednekar, A. S., Jadhav, G. R., Kalekar, S. E., Shende, D. Z., & Wasewar, K. L. (2020). Hydrogen generation through water splitting reaction using waste aluminum in presence of gallium. *International Journal of Hydrogen Energy*, *45*(44), 23954–23965. https://doi.org/10.1016/j.ijhydene.2019.09.026

Trading Economics. (2021). Trading Economics. https://tradingeconomics.com/commodity/

Tuchschmid, M. (2021). Gallium production, semiconductor-grade. In *ecoinvent database version 3.8*.

Turner, H. C., Lauer, J. A., Tran, B. X., Teerawattananon, Y., & Jit, M. (2019). Adjusting for Inflation and Currency Changes Within Health Economic Studies. *Value in Health*, *22*(9), 1026–1032. https://doi.org/10.1016/j.jval.2019.03.021

US EIA. (2021). *Does the world have enough oil to meet our future needs*. Frequently Asked Questions. https://www.eia.gov/tools/faqs/faq.php?id=38&t=6

US EPA. (2005). Emission Facts: Average Carbon Dioxide Emissions Resulting from Gasoline and Diesel. *Office of Transportation and Air Quality*, *February*.

USGS. (2020). 2017 Minerals Yearbook: Indium. *U.S. Geological Survey*, *April*, 1–9. https://www.usgs.gov/centers/nmic/indium-statistics-and-information

USGS. (2021a). Aluminum. *US Geological Survey Mineral Commodity Summaries*. https://pubs.usgs.gov/periodicals/mcs2021/mcs2021-aluminum.pdf

USGS. (2021b). Bauxite and alumina statistics and information: 2021 mineral commodity summaries annual publication. *US Geological Survey Mineral Commodity Summaries*. https://pubs.usgs.gov/periodicals/mcs2021/mcs2021-bauxite-alumina.pdf

USGS, Kelly, T. D., Matos, G. R., Buckingham, D. A., DiFrancesco, C. A., & Porter, K. E. (2017). *Historical Statistics for Mineral and Material Commodities in the United States*. National Mineral Information Center. https://www.usgs.gov/centers/national-minerals-information-center/historical-statistics-mineral-and-material-commodities

USMC. (2021). *TENTATIVE MANUAL FOR EXPEDITIONARY ADVANCED BASE OPERATIONS* (Issue February).

Viornery-Portillo, E. A., Bravo-Díaz, B., & Mena-Cervantes, V. Y. (2020). Life cycle assessment and emission analysis of waste cooking oil biodiesel blend and fossil diesel used in a power generator. *Fuel*, *281*(March), 118739. https://doi.org/10.1016/j.fuel.2020.118739

Volkswagen. (2019). Hydrogen or battery? A clear case, until further notice. *Volkswagen Aktiengesellschaft*. https://www.volkswagenag.com/en/news/stories/2019/08/hydrogen-or-battery--that-is-the-question.html#

Wakim, E. (2019, January). Sealift is America's Achilles Heel in the Age of Great Power Competition. *War on the Rocks*. https://warontherocks.com/2019/01/sealift-is-americas-achilles-heel-in-the-age-of-great-power-competition/

Wang, J. (2022). The Environmental Footprint of Semi-Fabricated Aluminum Products in North America: A Life Cycle Assessment Report. *The Aluminum Association*. https://www.aluminum.org/sites/default/files/2022-01/2022_Semi-Fab_LCA_Report.pdf

Whisman, M. L., Anderson, R. P., Giles, H. N., & Woodward, P. W. (1991). Crude oil and finished fuel storage stability: an annotated review. *National Institute for Petroleum and Energy Research*. https://www.osti.gov/servlets/purl/6199765

Yellishetty, M., Huston, D., Graedel, T. E., Werner, T. T., Reck, B. K., & Mudd, G. M. (2017). Quantifying the potential for recoverable resources of gallium, germanium and antimony as companion metals in Australia. *Ore Geology Reviews*, *82*, 148–159. https://doi.org/10.1016/j.oregeorev.2016.11.020

Yesilyurt, M. K. (2020). The examination of a compression-ignition engine powered by peanut oil biodiesel and diesel fuel in terms of energetic and exergetic performance parameters. *Fuel*, *278*(June), 118319. https://doi.org/10.1016/j.fuel.2020.118319

REPORT DOCUMENTATION PAGE

Form Approved
OMB No. 074-0188

1. REPORT DATE *(DD-MM-YYYY)*	**2. REPORT TYPE**	
24-03-2022	Master's Thesis	June 2022 – June 2022

TITLE AND SUBTITLE

Life Cycle Analysis of Hydrogen Fuel Derived from Aluminum versus Diesel

5a. CONTRACT NUMBER

5b. GRANT NUMBER

5c. PROGRAM ELEMENT NUMBER

6. AUTHOR(S)

Metlen, Tyson S., Major, USMC

5d. PROJECT NUMBER

5e. TASK NUMBER

5f. WORK UNIT NUMBER

7. PERFORMING ORGANIZATION NAMES(S) AND ADDRESS(S)
Air Force Institute of Technology
Graduate School of Engineering and Management (AFIT/EN)
2950 Hobson Way, Building 640
WPAFB OH 45433-7765

8. PERFORMING ORGANIZATION REPORT NUMBER

AFIT-ENV-MS-22-M-236

9. SPONSORING/MONITORING AGENCY NAME(S) AND ADDRESS(ES)
Major Aaron Stone
USMC Expeditionary Energy Office (E2O)
3300 Russell Road, Quantico, VA 22134

10. SPONSOR/MONITOR'S ACRONYM(S)

11. SPONSOR/MONITOR'S REPORT NUMBER(S)

12. DISTRIBUTION/AVAILABILITY STATEMENT
DISTRUBTION STATEMENT A. APPROVED FOR PUBLIC RELEASE; DISTRIBUTION UNLIMITED.

13. SUPPLEMENTARY NOTES
This material is declared a work of the U.S. Government and is not subject to copyright protection in the United States.

14. ABSTRACT
The Department of Defense needs energy sources beyond petroleum products to effectively combat area denial strategies employed by its adversaries. Petroleum fuels are expensive, they have deleterious environmental impacts, and most of the world's oil reservoirs are in volatile countries. A proposed alternative energy carrier is reacting aluminum with water to produce hydrogen and using the hydrogen as a fuel source. Normally aluminum forms a protective oxide layer that prevents continuous reaction but if aluminum is mixed with a 3.5% by weight gallium-indium eutectic, the oxide layer cannot form, and the reaction is sustainable. This study conducts a life cycle assessment, economic analysis, and discusses logistical considerations to compare using diesel to hydrogen derived from the aluminum-water reaction in a Western Pacific theater. The life cycle assessment uses Sphera's GaBi software and life cycle impact assessment tool TRACI 2.1, to characterize and compare the environmental impacts of diesel and aluminum. Every category of environmental impact is monetized and combined with the economic analysis to provide a single score for comparison. The result is that aluminum, even with the best-case scenario of 90% scrap aluminum and 95% eutectic recovery, is more environmentally harmful and economically expensive than diesel.

15. SUBJECT TERMS
Life Cycle Analysis, Activated Aluminum, Diesel, Economic Analysis, TRACI 2.1 Monetized

16. SECURITY CLASSIFICATION OF:			**17. LIMITATION OF ABSTRACT**	**18. NUMBER OF PAGES**	**19a. NAME OF RESPONSIBLE PERSON**
a. REPORT	**b. ABSTRACT**	**c. THIS PAGE**			Dr. Eric Mbonimpa, AFIT/ENV
U	**U**	**U**	**UU**	118	**19b. TELEPHONE NUMBER** *(Include area code)* (937) 255-3636, ext 7405 (eric.mbonimpa@afit.edu)

Standard Form 298 (Rev. 8-98)
Prescribed by ANSI Std. Z39-18